PROTECTION FROM OXIDATIVE STRESS IN THE CARDIAC

H9C2-CELL LINE BY THE TRANSCRIPTION FACTOR NRF2

Except where reference is made to the work of others, the work described in this dissertation is my own or was done in collaboration with my advisory committee. This dissertation does not include proprietary or classified information.

_____
Heather Gray Edwards

Certificate of Approval:

_____   _____
James L. Sartin   Dean D. Schwartz, Chair
Professor   Associate Professor
Anatomy, Physiology and   Anatomy, Physiology and
Pharmacology   Pharmacology

_____   _____
Robert L. Judd   Robert J. Kemppainen
Associate Professor   Professor
Anatomy, Physiology and   Anatomy, Physiology and
Pharmacology   Pharmacology

_____   _____
Holly R. Ellis   Joe F. Pittman
Associate Professor   Interim Dean
Chemistry   Graduate School

PROTECTION FROM OXIDATIVE STRESS IN THE CARDIAC

H9C2-CELL LINE BY THE TRANSCRIPTION FACTOR NRF2

Heather Gray Edwards

A Dissertation

Submitted to

the Graduate Faculty of

Auburn University

in Partial Fulfillment of the

Requirement for the

Degree of

Doctor of Philosophy.

Auburn, Alabama
August 4, 2007

PROTECTION FROM OXIDATIVE STRESS IN THE CARDIAC

H9C2-CELL LINE BY THE TRANSCRIPTION FACTOR NRF2

Heather Gray Edwards

_____
Signature of Author

_____
Date of Graduation

VITA

Heather Gray Edwards, daughter of Timothy Shawn Gray and Jennifer Anne Gray, was born December 7th, 1980 in Phoenix, Arizona. She graduated from the University of Arizona, in Tucson, Arizona with a Bachelor of Science in Microbiology in August, 2003. In the spring of 2003, she was awarded the BRAVO fellowship and studied in Madrid, Spain at the Consejo Superior de Investigaciones Científicas under the guidance of Dr. Sebastián Cerdán. In the fall of 2003, she was granted a fellowship as a graduate student in the Department of Cellular and Molecular Biology in the College of Science and Math at Auburn University, Auburn, Alabama. In fall 2004 she joined the Department of Anatomy, Physiology and Pharmacology in the College of Veterinary Medicine as a graduate teaching assistant under the guidance of her mentor, Dr. Dean Schwartz. She is married to Michael Edwards, son of Robert Patrick Edwards and Jacklyn Barrett Edwards.

DISSERTATION ABSTRACT

PROTECTION FROM OXIDATIVE STRESS IN THE CARDIAC

H9C2-CELL LINE BY THE TRANSCRIPTION FACTOR NRF2

Heather Gray Edwards

Doctor of Philosophy, August 4th, 2007
(B.S., University of Arizona, Tucson, AZ, 2003)

158 Typed Pages

Directed by Dean D. Schwartz

Cardiovascular disease (CVD) is the leading cause of death in the United States, and its prevalence is increasing in all populations and age groups worldwide (71). In 2002 alone, more than 927,000 Americans died from heart disease-related conditions. Oxidative stress, or the generation of reactive oxygen species (ROS), is a contributing factor to the progression of many cardiovascular diseases. One approach to combat the detrimental effects of oxidative stress in cardiac disease is to use the cell's inherent ability to increase the expression of various stress-related proteins to eliminate the oxidative stress. NF-E2 related factor 2 (Nrf2) is the transcriptional activator of the antioxidant response element (ARE) found in the promoter region of antioxidant and phase II detoxifying genes. In this study, we examined the role of Nrf2 in protecting the H9c2 cardiac-like cell line against oxidative stress. Nrf2 was induced using the known Nrf2 activator *tert*-butyl hydroquinone (tBHQ). We measured heme oxygenase-1 (HO1)

and NAD(P)H:quinone oxidoreductase 1 (NQO1) gene and protein expression as markers of ARE-driven gene activation in response to tBHQ. We also determined ROS generation using the fluorescent probe carboxy-H_2DCFDA, and cell viability in response to the prooxidants *tert*-butyl hydroperoxide (tBHP) and H_2O_2 in the presence and absence of activated Nrf2. To directly evaluate the roles of Nrf2 and its inhibitory protein Keap1, we utilized Nrf2 and Keap1 siRNAs to knockdown Nrf2 and Keap1 expression. H9c2 cells overexpressing Nrf2 tagged with either green fluorescent protein (GFP) were also generated to examine Nrf2 localization using fluorescent microscopy and gene expression of ARE-containing genes.

In H9c2 cells tBHQ activated Nrf2 resulting in the translocation of Nrf2 into the nucleus and increased the transcription and translation of the ARE-driven genes HO1 and NQO1. The prooxidant, tBHP increased ROS generation and cell death in H9c2 cells and pretreatment with tBHQ abrogated both these effects. Nrf2 knockdown experiments resulted in a blunted induction of tBHQ-induced HO1 and NQO1 expression and a loss in the protective effect of tBHQ on tBHP-induced ROS generation. Cell death in response to tBHP and H_2O_2 was augmented in cells treated with Nrf2 siRNAs, but rescued by Keap1 knockdown. H9c2 cells overexpressing Nrf2-GFP displayed fluorescence that was sequestered in the cytoplasm and translocated to the nucleus upon treatment with tBHQ. Along similar lines, HO1 and NQO1 gene expression remained at basal levels, despite Nrf2 overexpression and cytoplasmic localization. HO1 and NQO1 gene expression was enhanced in Nrf2 overexpressing cells after tBHQ treatment. From these studies, we conclude that Nrf2 protects the cardiac-like H9c2 cells from oxidative stress.

ACKNOWLEDGEMENTS

I would like to express my gratitude to those in Auburn University's College of Veterinary Medicine, its Dean Boosinger, the Associate Dean of research Dr. Pinkert, as well as those in the Department of Anatomy, Physiology and Pharmacology and its Department Head Dr. Morrison for the opportunity to attend graduate school at Auburn University. I would also like to thank the Molecular and Cellular Biosciences Program and Kathy Feminella and Dr. Bartol for support throughout my graduate career. I would like to express my deepest appreciation to my mentor and major advisor, Dr. Schwartz, for his support and guidance. Without him, none of this would have been possible. I would also like to thank the members of my committee, Dr. Ellis, Dr. Judd, Dr. Kemppainen and Dr. Sartin for all their help planning and executing this project. For their assistance in the laboratory and friendship during this work, I would like to thank Colin Rogers, Dr. Chancey, Dr. Clarke, Dr. Bedi, Dr. Brunson, Zhechuan Fan, Dr. Ahluwalia, Kathy O'Donnell and Barbara Steele. I would also like to thank Debbie Allgood, Hattie Alvis, Diane Smith, Dorothy Spain, Bobby Meadows and Mary Lloyd for all their help and support. I would also like to express my profound appreciation to my family, Timothy Gray, Tyler Gray, Jennifer Gray and Sharon Graham for their love and support. Most of all, I would like to thank my husband, Mike Edwards, for his level-headedness and endless support during this process.

Style manual or journal used: <u>American Journal of Physiology</u>

Computer software used: <u>Microsoft Word, Endnote, Microsoft Excel, Minitab,</u>

<u>and Adobe Photoshop.</u>

TABLE OF CONTENTS

LIST OF TABLES

LIST OF FIGURES

INTRODUCTION

Cardiovascular disease is the number one killer in the United States. Four to five million Americans currently have heart failure, and it is estimated that the number of heart failure patients will reach 10 million in 2007. This number is expected to further skyrocket as the US population ages and risk factors such as obesity, smoking and sedentary lifestyle increase. In 2002, more than 927,000 Americans died from heart disease-related conditions, such as heart attack, high blood pressure, stroke and heart failure. Despite advances in cardiovascular medicine, congestive heart failure death rates are still on the rise (57, 106). Attempts to improve cardiac function in the late phases of heart failure continue to be ineffective (1), and many believe the solution lies in prevention of underlying heart disease (138). Increasing evidence suggests that the progression of many cardiovascular diseases including hypertension, atherosclerosis, congestive heart failure and diabetes-associated vascular complications are attributed to increases in cellular oxidative stress (94, 95, 112, 143). Animal and human studies support a role for reactive oxygen species (ROS) in the onset and progression of cardiovascular disease (153, 154) and, while it has been thought that antioxidant therapy delays the onset of heart failure (253, 285, 286), recent clinical trials have yielded mixed results (12, 155, 206, 254, 276).

Oxidative stress is thought to be a contributing factor to the progression of complications of many cardiovascular diseases. Oxidative stress is a general term used to

describe the steady state level of oxidative damage in a cell or tissue caused by reactive oxygen species (ROS). ROS have been associated with the progression of cardiovascular disease, insulin resistance, β-cell dysfunction, impaired glucose tolerance and diabetes mellitus (13, 34-36, 77, 161, 240). In fact, clinical studies confirm that the incidence of heart disease is much greater among diabetics and is the leading cause of death in this population (97). An increasing body of literature supports the hypothesis that oxidative stress is a common pathogenic mechanism in these disease states and may explain why they often appear together or consecutively (13, 34-36, 77, 161, 240).

Another approach to combat the deleterious effects of ROS generation in the progression of cardiovascular disease is to use the cell's inherent ability to increase the expression of various stress-related proteins to eliminate the oxidative stress. The induction of a cell's endogenous defense mechanisms is, at least in part, due to the activation of the *cis*-acting regulatory element appropriately termed the antioxidant response element (ARE). The ARE is located in the 5' region of many genes involved in detoxifying the cell as well as maintaining the cellular redox potential. The ARE is conserved between species and genes and is activated in response to a variety of drugs and antioxidants including heavy metals, flavoniods, heme complexes, phenolic antioxidants and xenobiotics (223). The ARE was first discovered as an element that activated phase II detoxifiers and drug metabolizing enzymes and was distinguished from another *cis*-acting element, the xenobiotic response element (XRE), because it was not associated with a receptor mediated activation, but rather an intracellular event (257).

In response to oxidative stress, a cluster of genes commonly known as antioxidants and phase II enzymes can be transcriptionally regulated through the

activation of the NF-E2 related factor 2 (Nrf2) transcription factor (209), a member of the Cap 'N Collar (CNC) family of bZIP proteins (223). Nrf2 activation begins with oxidative stress, which either directly or through a signaling cascade leads to the activation of Nrf2 causing it to dissociate from the inhibitor protein Kelch like-ECH-associated protein 1 (Keap1) (120). The disruption of the Keap1-Nrf2 complex is mediated by either the direct release of Keap1 from Nrf2 by reaction of the oxidant with cysteines on the Neh (binding) domain of the Keap1 molecule (133); or through the phosphorylation of Nrf2 by some unknown second messenger and phosphorylation cascade. Various signaling cascades have been shown to promote the dissociation of Nrf2, including the MAPK kinase cascades of ERK, JNK and p38 (3, 56, 268, 304-306, 315, 316); the PI3 kinase cascade (128, 130, 165, 175, 252) and the PKC cascade (53, 103, 111, 163).

Once Nrf2 is activated, it translocates to the nucleus and binds a small Maf protein forming a heterodimer that binds to the regulatory element appropriately termed the antioxidant response element (ARE) (113). The Nrf2 protein recognizes the conserved core sequence TGACnnnGC on the ARE, (209). Many genes are known to have an ARE element, including heme oxygenase-1 (HO1), NAD(P)H quinone oxidoreductase 1 (NQO1), glutathione reductase, glutathione peroxidase, glutathione S-transferase, superoxide dismustase 2, and catalase. These genes have been shown to be upregulated or have increased activity after oxidative stress in cardiac cells (28-30, 54, 83, 108, 199, 260, 302, 303), brain (125, 174-176, 264, 266), as well as in other tissues such as the lung (8, 47-49, 51, 187, 198, 232, 269, 291), liver (39), vascular endothelium (26) and heart (31, 217, 248).

Based on reports in the literature, Nrf2 appears to be a universal activator of antioxidant genes, however evidence directly linking Nrf2 activation to protection in cardiac cells against oxidative stress is lacking. Therefore, we hypothesize that in the cardiac cell, oxidative preconditioning occurs through the Nrf2/ARE pathway and constitutive activation of this Nrf2 pathway will leave the cardiac cell in an oxidative stress-resistant state. The specific aims of this study were to characterize the gene expression and translation of the ARE-containing genes HO1 and NQO1 in the H9c2 cardiac-like cell line after oxidative stress and determine the effect of oxidative preconditioning on cell survival. Furthermore, it was determined whether 1) activation of ARE-containing genes (HO1 and NQO1) in response to oxidative stress was mediated by NF-E2-related factor 2 (Nrf2); and 2) whether constitutively expressing ARE-containing genes by blocking transcription of Kelch-like-E2 associated protein (Keap1), the Nrf2 inhibitory protein, would mimic the effect of oxidative stress preconditioning.

These studies target an important issue relating alterations in cardiomyocyte redox potentials to the development of functional abnormalities in such diseases as diabetic cardiomyopathy and atherosclerosis. An understanding of the pathways involved in oxidative stress on the heart is an important step in the development of strategies to reduce the incidence of heart disease and increase the overall life expectancy and quality of life for cardiovascular disease patients.

LITERATURE REVIEW

The antioxidant response element (ARE) was first discovered in the 1970's. The ARE is a *cis*-acting regulatory element located in the 5' region of many genes encoding detoxifying enzymes and antioxidants. Transactivation by the transcription factor Nrf2 results in increased gene expression of ARE-containing genes such as heme oxygenase 1 (HO1), NADPH:quinone oxidoreductase 1 (NQO1), glutathione reductase, glutathione peroxidase, glutathione S-transferase, superoxide dismustase 2, and catalase. Activation of the ARE by Nrf2 has recently been implicated as a protective mechanism in cardiovascular disease and has been shown to protect against oxidative stress in the brain after stroke and in neurological disorders such as Alzheimer's and Parkinson's disease. Due to its apparent role in protection against oxidative stressors in various organs, Nrf2 has earned the title of the multi-organ protector (166).

I. DISCOVERY OF THE ANTIOXIDANT RESPONSE ELEMENT

Phase I and II enzymes were originally thought to be induced by the well-characterized ayrl-hydrocarbon receptor (AhR) mechanism. The AhR activates enzyme transcription with the direct binding of a xenobiotic to the ayrl-hydrocarbon receptor (AhR). The active AhR dimerizes with the AhR-nuclear translocator protein, then translocates into the nucleus, and binds to the xenobiotic response element (XRE), a

DNA enhancer sequence. Xenobiotics can activate phase I or phase II enzyme transcription separately or simultaneously, depending on their chemical properties (87, 88, 156, 195, 230). Phenolic antioxidants, for example, are capable of selectively activating phase II enzymes, whereas β-naphthoflavone is capable of activating both phase I and II enzymes (59, 127, 257). The AhR was thought to be responsible for the activation of both phase I and II enzymes, despite the ability of different compounds to selectively activate phase I and II enzyme transcription.

In 1985, a separate mechanism was proposed to be responsible for phase II enzyme induction based on the observation that azo dyes induce phase I and II enzymes differentially. It was suggested that phase I enzymes were induced by the previously-accepted AhR mechanism whereas phase II enzyme induction was thought to involve cytochrome P-450 (C^{P450}). It was further suggested that metabolism of azo dyes by C^{P450} resulted in the generation of reactive species that were responsible for phase II enzyme activation (246). Similar observations were reported in other laboratories supporting a role for C^{P450} in mediating phase II enzyme activation. In one study, the administration of benzo[a]pyrene in cultured embryonic hamster cells resulted in the production of several redox-sensitive and toxic quinones. These compounds initially activated phase I enzymes, and only after an increase in C^{P450} activity did the levels of the phase II enzymes increase (156, 193, 230). As further support of C^{P450}-mediated phase II activation, the administration of SKF 525, a C^{P450} inhibitor, prevented the activation of phase II enzymes (107). Interestingly, a study by Denison found that the C^{P450} gene, *CYP 1A1*, contains an XRE (60), suggesting that xenobiotics are able to increase their own metabolism by C^{P450} activating phase II enzymes. These data suggest that C^{P450} could be

6

involved in phase II enzyme induction by a different mechanism from that of phase I enzymes.

To determine whether the selective activation of phase II enzymes worked though the AhR pathway, cell lines expressing AhRs with low affinities for xenobiotics were generated. In these cells, β-naphthoflavone, a compound that activates both phase I and II enzymes, exhibited impaired phase II activation. However, the phenolic antioxidant *tert*-butyl hydroquinone was able to activate expression of phase II enzymes. These data suggested that phase II activation by phenolic antioxidants utilized a pathway separate from the AhR (257). Therefore, compounds that could induce both phase I and II enzymes through an AhR-dependent mechanism were termed bifunctional inducers, while those that regulate the expression of only phase II enzymes in a AhR-independent mechanism were termed monofunctional inducers (247).

In 1990, a novel *cis*-acting regulatory element was discovered in the 5'-flanking region of the glutathione S-Transferase Ya subunit that was responsive to the bifunctional inducer β-naphthoflavone (β-NF). To analyze the nature of this element, a reporter construct was generated containing the chloramphenicol acetyltransferase (CAT) gene fused with the cloned DNA element. Treatment with β-NF resulted in increased transactivation suggesting that the responsive element was activated by planar aromatic compounds like β-NF. Further analysis of the promoter element revealed distinct sequence differences from the xenobiotic response element (XRE). The new element was termed the β-naphthoflavone-response (β-NF) element (255, 283). The same element located in the promoter region of the rat glutathione S-transferase Ya A2 subunit gene was also identified by another group and was termed the electrophile response

element or EpRE (86). The two elements were later reclassified following data showing that phenolic antioxidants, like *tert*-butyl hydroquinone, increased transactivation of the DNA element through a C^{P450} and the AhR independent pathway. The *cis*-acting DNA was renamed the antioxidant response element (ARE) (257).

II.   XENOBIOTICS THAT ACTIVATE THE ANTIOXIDANT RESPONSE ELEMENT

A structurally diverse group of compounds has been shown to activate transcription of antioxidant response element (ARE)-containing genes, including phenolic antioxidants, synthetic antioxidants (256), 3-hydroxycoumarin (139), isothiocyanates (22, 279, 280), GSH depleting agents (136), phorbol esters (111), flavoniods (256, 257) and 1,2-dithiole-3-thiones (157, 158) (table 1). These ARE-driven gene activators can be further subdivided into the monofunctional and bifunctional inducers. The monofunctional inducers, which activate gene expression through a mechanism separate from the AhR, have similar chemical properties in that they all react with sulfhydryl groups. The bifunctional inducers must be oxidatively metabolized by C^{P450} prior to obtaining ARE-activating properties (69). For a complete list of ARE-inducing compounds, please see appendix A.

Table 1: Compounds that induce ARE-mediated transcription
Modified from Nguyen *et al.*, 2003.

Class	Structure	Compound	Nature of compound
Synthetic phenolic antioxidant		Butylated hydroxyanisole (BHA)	Food preservative; Antioxidant in dermatological creams
Synthetic phenolic antioxidant		*tert*-butyl hydroquinone	Food preservative; Metabolite of BHA
Synthetic antioxidant		Ethoxyquin	Pesticide/insecticide; Pet food preservative
Synthetic antioxidant		Pyrrolidin-edithiocarbamate	Blocks NF-κB and activates iNOS
3-hydroxycoumarin		Coumarin	Chemopreventative agent in legumes
Isothiocyanate		Sulforaphane Oxidizes cysteines mimics oxidative stress	Chemopreventative agent in cruciferous vegetable
GSH depleting agent		Diethyl maleate Oxidizes cysteines mimicking oxidative stress	Synthetic compound inducing agent of drug metabolizing enzymes
Phorbol Ester		Phorbol 12-myristate (PMA)	Tumor promoting agent; PKC activator; Increases expression iNOS and COX-2
Flavonoid		β-naphthoflavone	Synthetic compound used as a model inducer of drug-metabolizing enzymes
1,2-dithiole-3-thione		Oltipraz	Cancer preventive agent Antischistosomal drug

III. DISCOVERY OF Nrf2

As previously mentioned, the antioxidant response element was discovered by two separate groups simultaneously (257, 283). The EpRE and the β-naphthoflavone-response element *cis*-acting DNA elements were changed to the antioxidant response element (ARE) after it was reported to be responsive to phenolic antioxidants, namely *tert*-butyl hydroquinone (257). In 1991 the consensus sequence of the ARE 5'-TGACnnnGC-3', was discovered through the use of deletion mutants of the original
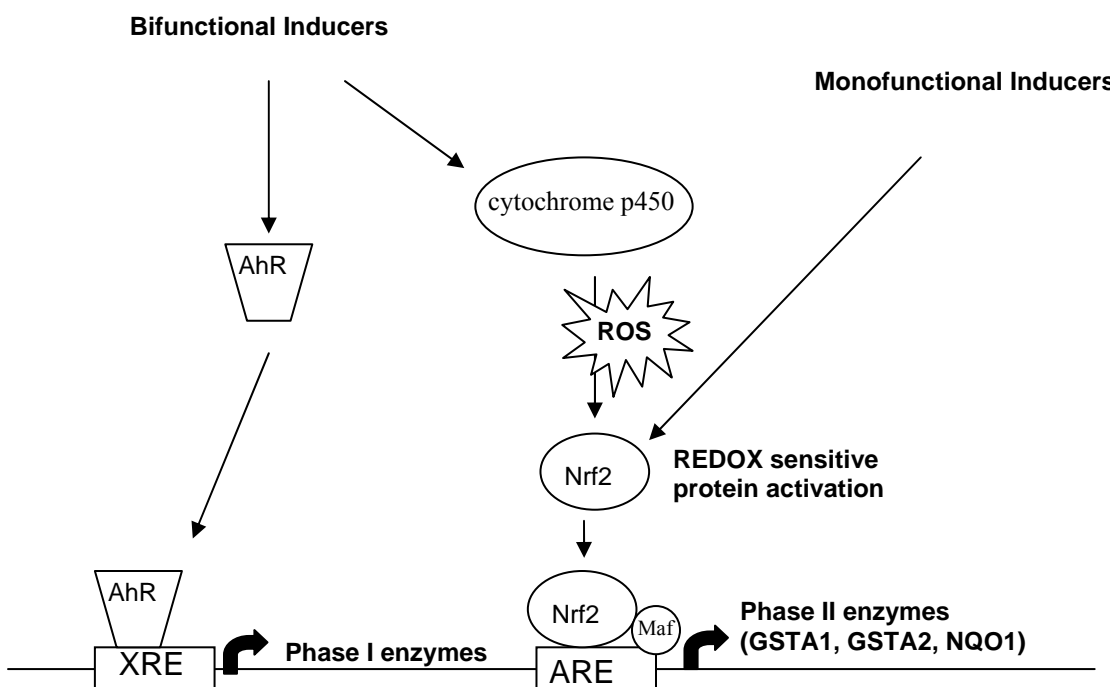
Figure 1: Phase II enzyme induction distinct from the AhR pathway.
The pathway states that bifunctional inducers activate the ARE through the generation of reactive oxygen species (ROS) from reactions with cytochrome p450. These ROS then react with a redox sensitive protein, later discovered to be Nrf2, and its interaction with the ARE results in the activation of transcription phase II enzymes. Modified from Nguyen *et al.*, 2003.

ARE/CAT reporter construct. In the same study, it was also reported that ARE/CAT transactivity was mediated directly through generation of reactive oxygen species (256). The ARE was later reported to be in the promoter regions of the mouse glutathione S-

transferase Ya A1 subunit gene (86) and the rat and human NADPH:quinone oxidoreductase 1 genes (NQO1) (Figure 1) (78, 79, 184). This supports the theory that increased transactivation of the ARE is responsible for phase II enzyme induction.

The observation that reactive oxygen species resulted in the activation of this element gave rise to the hypothesis that a redox-sensitive transcription factor recognizes the DNA sequence of the ARE; furthermore, this protein-DNA interaction could be responsible for increased transcription of phase II enzymes (255).

The NF-E2 related factor 2 (Nrf2) protein was discovered while looking for proteins closely related to erythroid transcription factor NF-E2, a dimeric protein involved in the regulation of the globin gene in hematopoietic cells (6, 209, 219). Utilizing the Activator Protein 1 (AP1)-NF-E2 sequence as a probe to screen a cDNA expression library, two DNA binding proteins were discovered. One was identical to the recently discovered Nrf1 (NF-E2 related factor 1) and the second protein was named NF-E2 related factor 2 (Nrf2). Both Nrf1 and Nrf2 were also found to be ubiquitously expressed (38, 41). After the Nrf2 protein was cloned, several studies analyzed its sequence and predicted that it would have an activation domain, a cap'N'collar region (CNC), a DNA binding domain and a leucine zipper domain (37, 201, 209, 210) (Figure 2). The structural elements of the Nrf2 protein are present in other transcription factors that recognize AP1-like elements as well; therefore Nrf2 was proposed to recognize an AP1-like element.

Nrf2

Figure 2. The structure of Nrf2. Nrf2 contains a hydrophilic N-terminus region followed by an acidic activation domain, a cap 'n' collar domain, a basic DNA binding domain and a leucine zipper. Figure modified from Moi *et al.* 1994.

The Nrf1 and Nrf2 proteins were identified in the context of studies aimed at identifying a redox-sensitive transcription factor that recognized the DNA sequence of the ARE. Nrf1 and Nrf2 have very similar tissue distribution to that of the ARE-driven gene, NADPH:quinone oxidoreductase 1 (NQO1) (293), and the similarity of the ARE and Nrf1/Nrf2 binding motifs implicated them as possible regulators of the ARE. To determine which protein was responsible for ARE-driven transcription, Venugopal *et al.* transfected HepG2 cells with Nrf1 or Nrf2 along with the ARE/CAT reporter construct. Cells transfected with Nrf1 and Nrf2, separately or combined, showed transactivation of the ARE/CAT reporter construct (293), implying both could be responsible for ARE-mediated gene transcription. Nrf1 and Nrf2 both recognized the ARE, increasing its transactivation and activating phase II enzyme transcription.

Both Nrf1 and Nrf2 were believed to be responsible for ARE-driven gene transcription until the Nrf2 knockout mouse was generated. This development led to the identification of Nrf2 as the major activator of ARE-driven gene transcription (41). Nrf2 was also shown to control the transcriptional activation of human γ-glutamyl cysteine synthase heavy and light subunits (γ-GCS$_{h\&l}$)(297), mouse heme oxygenase 1 (HO1) (2),

12

and rat NQO1 and GSTA2 subunits (220). Nrf2 was also shown to control both induced and basal levels of GSTA1 and NQO1 gene expression in Nrf2 knockout mice. Butylated hydroxyanisole (BHA), a phenolic antioxidant, was unable to stimulate ARE activity in the Nrf2 knockout mice (119), supporting the theory that phase II enzyme activation is dependent upon the Nrf2 protein. Further experiments using Nrf2 knockout mice also showed decreased NQO1, GST and γ-GCS enzyme activities (42, 201). For a complete list of Nrf2-regulated genes see appendix B. Following the development of the Nrf2 knockout mouse, ARE transactivation and phase II enzyme induction was attributed to the Nrf2 transcription factor.

IV. NRF2 ACTIVATION
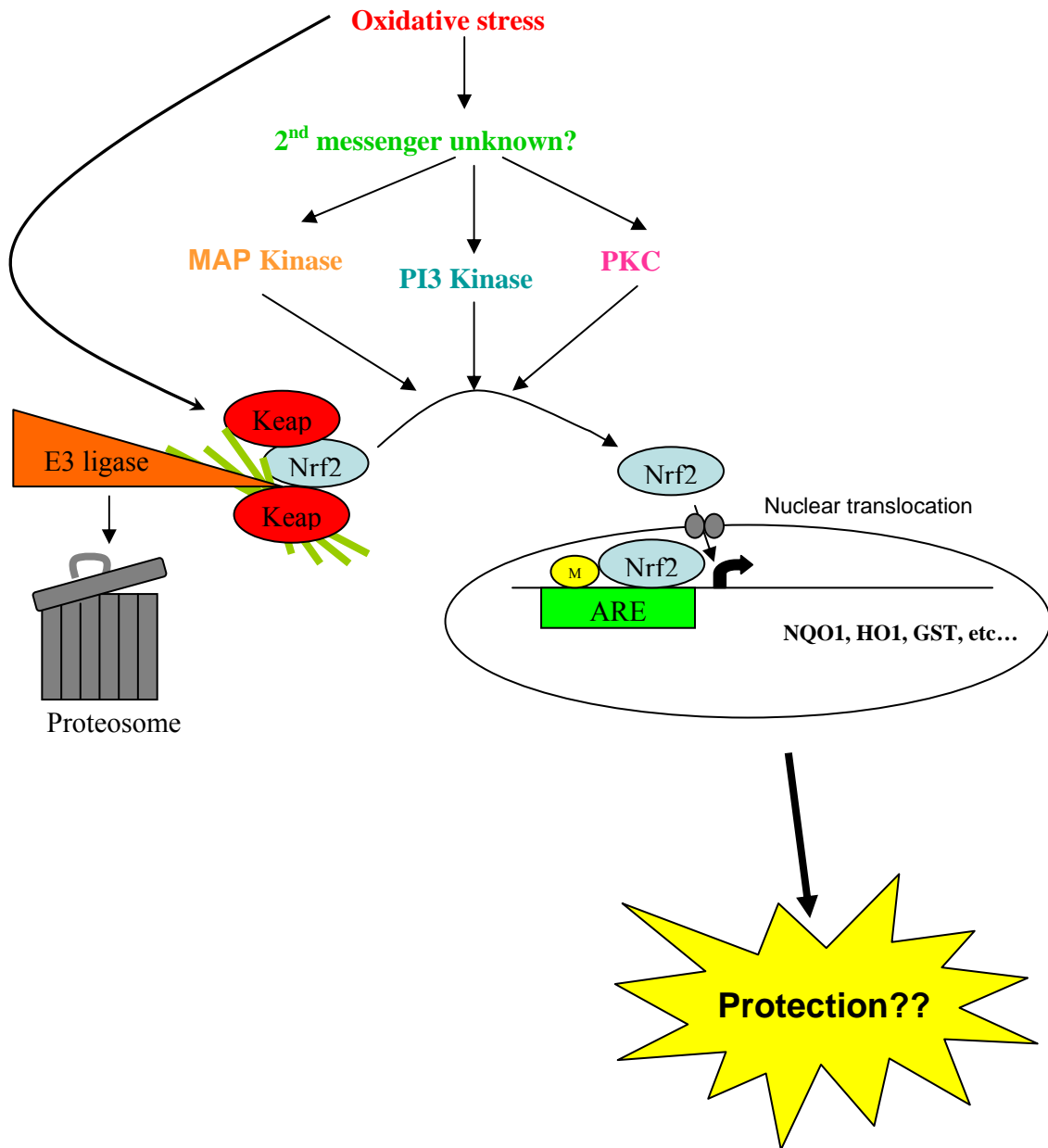
Figure 3. <u>Nrf2 activation</u> The activation of Nrf2 can occur directly by oxidative stress or through a second messenger (MAPK, PI3 K or PKC) signaling the dissociation of Nrf2 (blue) from Keap1 (red). Upon separation, Nrf2 translocates into the nucleus and binds the ARE along with a co-transcription factor, thought to be small Maf protein (yellow). Upon binding Nrf2-Maf results in increased transcription of ARE-containing genes. Schematic is a modified version from Nguyen et al 2002 (223).

Transactivation of the antioxidant response element occurs when Nrf2 binds to the ARE. Nrf2 mediated activation was shown by transactivation of the ARE-CAT reporter construct and by studies using the Nrf2 knockout mouse. The proposed cascade for ARE activation (Figure 3) begins with a xenobiotic, which can activate Nrf2 directly through a redox reaction or indirectly through a signaling cascade (209). Nrf2 is present in an inactive form bound to Keap1 in the cytoplasm. Once activated, Nrf2 dissociates from Kelch like-ECH-associated protein 1 (Keap1) and translocates into the nucleus, where it binds to a co-transcription factor, the small Maf protein, forming a heterodimer. The Nrf2-Maf heterodimer recognizes and binds to the ARE and initiates the transcription of phase II enzymes.

Different signaling cascades have been reported to cause the dissociation of Nrf2, including the MAPK kinase cascades of ERK, JNK and p38 (3, 56, 268, 304-306, 315, 316); the PI3 kinase cascade (128, 130, 165, 175, 252) and the PKC cascade (53, 103, 111, 163). Current research indicates that the signaling cascade involved in the activation of Nrf2 is both gene- and tissue-specific.

MAPK SIGNALING PATHWAY The mitogen-activated protein kinase (MAPK) signaling pathway was the first investigated in Nrf2 activation. Extracellular signal regulated kinase 2 (ERK2) was shown to increase NQO1 transcription after tBHQ and sulforaphane treatment in mouse hepatoma cell lines. Using a dominant negative mutant of ERK2, ARE induction was blocked. These data suggest that ERK2 may be involved in signaling Nrf2 activation as well (305).

In contrast, the p38 MAPK pathway was shown to inactivate Nrf2. Treatment with tBHQ or β-naphthoflavone activated the p38 MAPK pathway in mouse hepatoma cell lines, but resulted in decreased Nrf2 activation. In addition, the p38 MAPK inhibitor SB 203580 and use of a dominant negative mutant of p38 resulted in Nrf2 activation and the increased transcription of NQO1. Thus, the activation of the p38 pathway resulted in a down-regulation of both basal and inducible ARE transactivation (306). The inhibitory role of p38 was later challenged when different findings resulted from treatment with the ARE inducer pyrrolidin-edithiocarbamate (PDTC) in human hepatoma cells. PDTC was reported to activate transcription of γ-glutamylcysteine synthetase heavy and light subunits (γ-GCS$_{h\&l}$) through p38 and ERK in a synergistic manner. Complete inhibition of transcription of GCS$_{h\&l}$ subunit genes was obtained only when both pathways were inhibited by the use of the pharmacological inhibitors DP 98059 and SB 202190. In this study, p38 was implicated as an activator of ARE-driven transcription. Thus, p38 MAPK has been implicated as both a negative and positive regulator of ARE-driven genes. The different reports on the role of p38 can be explained in part by the use of different xenobiotics and different ARE-driven genes as an index of ARE transactivation. Thus the role of p38 is likely to be tissue-, gene-, and inducer-specific.

c-Jun N-terminal kinase (JNK), has also been implicated in Nrf2 activation. JNK was reported to activate Nrf2 after sodium arsenite and mercury chloride (304). This activation had a positive effect on NQO1 transcription, suggesting that JNK activates Nrf2- and ARE-driven transcription (304). These data support the JNK pathway as a possible mechanism in Nrf2 activation.

To date, the MAPK pathways have been reported to have both negative and positive effects on ARE transactivation. These studies have utilized different xenobiotics to activate the three major MAPK pathways and have yielded different results. Taken together, these studies show that the MAPK signaling pathway affects Nrf2 and ARE transactivation, but the role of p38 appears to be tissue-, gene-, and inducer-specific.

PI3K SIGNALING PATHWAY The phosphatidylinositol 3-kinase (PI3K) pathway has also been shown to be involved in Nrf2-ARE activation. Studies in the IMR-32 neuroblastoma cell line show that PI3K activates transactivation of a reporter construct containing the ARE from the NQO1 promoter. Using the pharmacological inhibitor of PI3K, LY 294002, there was an observed decrease in the transactivation of the ARE. In the same study it was also shown that ERK was not important for transactivation of the ARE. The pharmacological ERK inhibitor, PD 98059, had no effect on ARE transactivation (165), suggesting that ERK does not play a role in activating Nrf2 in neuroblastoma cells. Using microarray analysis, tBHQ was found to increase transcription of 63 genes in the IMR-32 cells. Of those, the transcription of 43 was blocked by LY 294002. The same group later showed that PI3K was involved in ARE-driven gene expression in primary cortical cultures derived from human placental alkaline phosphatase (hPAP) ARE reporter mice. Decreased hPAP activity was observed in cultures treated with LY 294002 (125, 152), supporting PI3K as an important second messenger in Nrf2 activation. These studies implicate PI3K as an important signaling pathway of ARE transactivation in neuronal cell lines and primary cultures.

PKC SIGNALING PATHWAYS In all of the studies elucidating the signaling pathway responsible for Nrf2 activation, PKC is the only second messenger shown to phosphorylate Nrf2 directly. Nrf2 is directly activated through phosphorylation by PKC at Ser[40] in the rat hepatoma cell line H4IIE (110, 111). To first evaluate the role of the PKC pathway in Nrf2 signaling, Huang *et al.* made reporter constructs containing the ARE from both NQO1 and GSTA2 promoter regions were generated. Decreased ARE transactivation was reported using broad spectrum PKC inhibitors (staurosporine and RO-32-0432) in response to tBHQ, TPA and β-naphthoflavone. Phosphorylation of Nrf2 was shown by radiolabeling experiments that indicated Nrf2 protein as being phosphorylated at Ser[40] by PKC. In addition, phosphorylation of Nrf2 by PKC resulted in Nrf2 translocation into the nucleus. To confirm these results, Ser[40] was mutated to an Ala and no detectable phosophorlyation was observed compared to wild-type. Keap1 sequesters Nrf2 in the cytoplasm. Therefore the disruption of the Nrf2/Keap1 complex by phosphorylation was tested. Keap1 was labeled with ^{35}S, co-immunoprecipitated (coIP) with Nrf2, followed by SDS page, and free Nrf2 was determined by autoradiography. Thus, PKC phosphorylates Nrf2 at Ser[40] and causes both disruption of the Nrf2-Keap1 complex and Nrf2 translocation into the nucleus (110, 111). These experiments were the first to show a direct interaction by a signaling kinase and Nrf2, providing conclusive evidence that Nrf2 is activated by the second messenger PKC.

The signaling pathways of MAPK, PI3K and PKC have all been shown to be involved in Nrf2 signaling. It appears that MAPK signaling is important in hepatoma cell lines, whereas PI3K seems to regulate ARE-driven transcription in neuroblasoma cells and primary cortical astrocytes. The only signaling molecule shown to phosphorylate

Nrf2 directly is PKC, providing conclusive evidence that PKC acts as a regulator of Nrf2 activation. It is also possible that all three pathways are involved in Nrf2 activation and that the second messenger is dependent upon 1) the xenobiotic, 2) the gene measured and 3) the tissue or cell line used.

NRF2 TRANSLOCATION The import of Nrf2 into the nucleus is regulated by the nuclear localization signal (NLS), located in the C-terminus of the Nrf2 protein (122). Deletion of the NLS renders Nrf2 unable to enter the nucleus in response to the Nrf2 activating compound *tert*-butyl hydroquinone (tBHQ) (122). Once translocated into the nucleus, another mechanism prevents extended nuclear localization. The Nrf2 protein contains a redox-insensitive nuclear export signal (NES) (122, 182), which regulates its export from the nucleus. Deletion of the NES resulted in increased nuclear localization of Nrf2 after treatment with tBHQ (122). Nuclear export of Nrf2 occurs by the phosphorylation of tyrosine[568] on the Nrf2 molecule by the nuclear localized protein Fyn kinase, a member of the Src family. Crm1, a nuclear factor vital in deciphering nuclear export signals and exporting proteins from the nucleus (84, 229, 275), then recognizes the phosphorylated Nrf2, binds it and facilitates Nrf2 exportation (123). Together, the NLS and the NES tightly control nuclear localization of Nrf2.

V. DIFFERENTIAL REGULATION OF THE ARE

The ARE is controlled by a number of factors that initiate or prevent ARE-driven transcription. The major positive regulator of the ARE is the Nrf2 protein, however NF-E2 related factor 1 (Nrf1) has also been shown to activate ARE-driven transcription.

Activating Transcription Factor 4 (ATF-4) and Nuclear Receptor-Associated Coactivator-3 (RAC3) have also been reported to increase ARE transactivation indirectly. Other proteins have been shown to negatively regulate the ARE including Keap1, Fos proteins, and Nrf3. All of these factors have been shown to bind the ARE, blocking the transcription of ARE-containing genes. The family of Maf proteins has also been shown to negatively and positively regulate the ARE depending on the dimer formed. A dimer consisting of two Maf proteins negatively regulates the ARE, whereas a heterodimer of Maf with Nrf2 results in activation. Maf, Fos and Jun all contain a DNA binding domain, but do not have a transactivation domain and, therefore, are unable to initiate transcription alone. The observation that multiple proteins can differentially regulate ARE activation suggests that they may play a role in the observed differential expression of ARE-containing genes.

SEQUENCE OF THE ARE Differential regulation of ARE containing genes can also be explained by the differences in ARE sequences. DNA footprinting and gel mobility shift assays have shown that the promoter regions differ between the rat GSTA2 and NQO1 genes, and these sequence differences are responsible for differential expression of GSTA2 and NQO1. In this study, exogenous Nrf2 coupled to the MafK co-transcription factor increased binding affinity for rat NQO1 when compared to GSTA2 (220). These data suggest that the gene-specific sequence of the ARE affects the binding of a specific Nrf2:Maf heterodimer.

SMALL MAF PROTEIN Binding of Nrf2 to the ARE requires the formation of a Nrf2 heterodimer with a co-transcription factor. The structurally similar NF-E2 protein heterodimerizes with a small Maf protein (113); suggesting that Nrf2 could also dimerizes with a member of the Maf family (119). The small Maf family consists of three known members: MafF, MafG and MafK. Their structures consist of a DNA binding domain and a leucine zipper. They lack a transactivation domain making them function strictly as co-transcription factors (214). Within their DNA binding component, the small Maf proteins have a cap'N'collar (CNC) homology, facilitating the recognition of the AP1-like binding motif, as seen in the ARE (140). Small Maf proteins localize in the nucleus, binding to various transcription factors including Bach (231), NF-E2 (21, 113, 151, 197), AP1 (134) and Nrf2 (93, 197, 211, 220, 257, 297).

The small Maf proteins have also been shown to bind Nrf2 and to aid in the transcription of ARE-driven genes, although the isotype involved appears to be gene- and tissue- specific (197, 220). Studies have also shown a role for MafK (93, 211, 216, 220), MafG (211, 297) and MafF (211) in increased ARE transactivation. Transcription of the small Maf proteins can be induced by pyrrolidinedithiocarbamate (PDTC) and phenylethyl isothiocyanate (PEITC), but not tBHQ, suggesting that increased transcription of the small Maf protein is not necessary for ARE-driven transcription (211). The small Maf protein is vital for Nrf2 binding to its target (197, 220), because Nrf2 cannot form a homodimer to activate the ARE(209).

The small Maf proteins appear to act as molecular switches with respect to ARE gene transcription. In transfection studies using ARE/CAT fusion constructs generated from rat GSTA2 and NQO1 promoter regions, increased levels of MafK plasmid resulted

21

in decreased levels of transcription of Nrf2; and it appears that a concentration-dependent relationship between Nrf2 and MafK exists(65, 220). On the other hand, Nrf2 co-transfected at a 10-fold higher level than MafG resulted in an increase in transcription of γ-glutamylcysteine synthetase in both the heavy and light subunits. When the levels of MafG were increased, transcriptional inhibition was observed (297). The small Maf proteins have also been shown to form heterodimeric (134) and homodimeric transcriptional repressors (214) in response to increased ARE-driven transcription.

In all, the small Maf proteins act as transcriptional activators when bound to Nrf2, as well as a transcriptional inhibitors when bound to itself or other proteins. It has also been suggested that the small Maf proteins can act as either heterodimeric partners with transcription factors or as homo- or heterodimeric transcriptional repressors, as they lack the transactivation domain but still recognize the DNA sequence of the ARE (214).

OTHER PROTEINS Nrf2 has been reported to interact with other proteins, changing the transactivity of Nrf2. The cAMP Responsive Element Binding protein (CREB) binds to the Neh4 and Neh5 domains of Nrf2, increasing transcription of ARE-containing genes. This increase in ARE-driven gene synthesis is thought to occur due to the attraction of DNA polymerase by CREB (135). BTB and CNC homology 1 (Bach1) has been described as an negative regulator of Nrf2. Bach1 has also been reported to form a heterodimer with small Maf proteins, competing with Nrf2 for the ARE binding site(63). Nuclear receptor-associated coactivator-3 (RAC3) has been shown to activate ARE-driven transcription. RAC3 increased transactivation of Nrf2 when co-transfected with Nrf2 (186). Activating Transcription Factor 4 (ATF-4) has been reported to directly

22

increase HO1 transcription by dimerizing with Nrf2. A dominant negative mutant of the ATF-4 gene decreased Nrf2 transactivation, suggesting that ATF-4 is a positive regulator of Nrf2 and the HO1 gene (102). The Jun and Fos families of proteins have also been implicated as Nrf2 interacting proteins. The Fos family of proteins has repeatedly been reported as a negative regulator of the ARE (134, 140, 184, 191, 221, 293), whereas the Jun family of proteins has been shown to positively regulate the ARE (294). The interaction of other proteins with Nrf2 and the ARE effect the expression of ARE-driven genes in a gene-specific manner. These data suggest that other Nrf2 effector proteins differentially regulate ARE-driven genes and may be responsible for deciphering the intracellular signal as to which gene needs to be activated.

NRF1 NF-E2 related factor 1 (Nrf1) was cloned in 1993 (37). It activates the ARE through direct binding and, when overexpressed alone or in conjunction with Nrf2, results in increased transactivity of the ARE (293, 294). Nrf1 is protective against oxidative stress in fibroblasts (160), lesioned hippocampus (104) and in liver cells against tert-butyl hydroperoxide-induced cell death (43). Unlike its family member Nrf2, Nrf1 gene disruption results in anemia and embryonic lethality in mice, suggesting that it plays a large role in development (38). Nrf1 has also been reported to crossover and interact with promoters other than the ARE. Nrf1, along with FosB, c-Jun, JunD and ATF2, has been reported to interact with the AP1 site of tumor necrosis factor α (TNFα), stimulating its transcription (224, 245). Nrf1 is negatively regulated through a different mechanism than that of Nrf2. Nrf1 is targeted to the endoplasmic reticulum (ER) membrane by its N-terminus, and upon endoplasmic reticulum stress, Nrf1 nuclear

23

localization is increased (296). These data suggest that while Nrf1 is able to modulate

ARE-driven transcription, it may also play a role in ER stress.

NRF3   Another member of the Nrf family, NF-E2 related factor 3 (Nrf3) was cloned in

1999. In this report, Nrf3 dimerization with MafK and binding of the heterodimer to the

Maf recognition elements (MARE) within the β-globulin enhancer were observed (145).

Nrf3 has been reported to negatively regulate the ARE when overexpressed in Hep-G2

cells through the formation of a heterodimer with a small Maf protein, competing with

Nrf2 for the ARE.   These results suggest that Nrf3 is a negative regulator of ARE-

mediated gene transcription (259).   A Nrf3 knockout mouse, generated in 2004, showed

no apparent problems, even as a double mutant with the Nrf2 knockout. Nrf3 was found

to be predominantly expressed in the placenta, B cells and monocytes (61). Upon closer

analysis of Nrf3 in the placenta, it was determined that Nrf3 shows potent transactivation

when forming a heterodimer with MafG on the NF-E2/Maf enhancer sequence. Nrf3 was

present in placental chronic villi from 12 weeks of gestation until term and, interestingly,

Nrf3 transcription and translation was reported to be activated by TNF α (46). These

data suggest that Nrf3 also plays a role in placental development.

A number of factors have been shown to influence ARE activation by Nrf2. The

observed interaction of various proteins on Nrf2 and the ARE may explain the

differential regulation of ARE-driven genes. Negative regulation is mediated not only by

the Nrf2 inhibitory protein Keap1, but also by Nrf3 and the families of Maf and Fos

proteins. Positive regulators include Nrf1, ATF-4, RAC3 and the families of Maf and

Jun proteins. These studies suggest that differential regulation of ARE-driven synthesis

is due, at least in part, to the interactions of other regulatory proteins within the ARE system.

VI. DISCOVERY OF KEAP1

In 1999, an inhibitory protein for Nrf2 was discovered (120). It was reported that the Neh2 hydrophilic domain of Nrf2 was not involved in transactivation. Upon deletion of the Neh2 domain and transfection of the mutant Nrf2 protein plus an ARE/LUC reporter construct, high levels of transactivation were discovered. It was concluded that this portion of the protein was somehow involved in negative regulation. In an effort to find an inhibitory protein, the Neh2 domain was used as bait in the yeast 2-hybrid system. Screening of 80 clones revealed that the majority encoded a single novel protein. Upon structural analysis of the novel protein, two characterized interaction domains (the BTB domain (14) and a double glycine repeat (DGR) domain (4)) were found. Bioinformatic database searches further revealed that the protein was very similar to the Drosophila cytoskeleton binding protein Kelch (298). The new protein was named Kelch-like associated protein-1 (Keap1) (120).

Keap1 was found to be expressed in a variety of mouse cell lines, with its highest expression in fibroblasts. Mutational analysis determined that the interaction between the Neh2 domain of Nrf2 and the DGR domain of Keap1 were responsible for Nrf2 inhibition. In the absence of the Neh2 domain of Nrf2, inhibition by Keap1 was lost. It was also reported that administration of electrophilic agents, namely diethylmalate (DEM) and catechol, caused the dissociation of the Nrf2-Keap1 complex, suggesting the interaction between Nrf2 and Keap1 was redox-sensitive (120). Given that Keap1 is

25

closely related to the cytoskeleton binding protein Kelch, it was hypothesized that Keap1 could also interact with the cytoskeleton, retaining Nrf2 in the cytoplasm. In QT6 cells transfected with fluorescently-tagged Keap1-green fluorescent protein (GFP), expression of Keap1 was localized in the cytoplasm. Cytoplasmic localization was confirmed in cells transfected with unlabelled Keap1 and fluorescently-labeled Neh2 domain of Nrf2 (120). Subsequently, it was shown that Keap1 binds to actin via the DGR domain, sequestering Nrf2 in the cytoplasm (131). Similar results were reported by Dhakshinamoorthy *et al.* (64). These studies showed that the newly discovered Keap1 protein is responsible for negative regulation of Nrf2 through binding of the DGR domain on Keap1 and the Neh domain on Nrf2. In addition, Keap1 negative regulation of Nrf2 was shown to occur by cytoplasmic retention through an interaction between Keap1 and actin filaments.

The cellular sensor within the Nrf2-Keap1 complex responsible for separation of Nrf2 from Keap1 was discovered in 2002 (68). It was proposed that there must be a cellular sensor within the Nrf2-Keap1 complex, either by alkylation or oxidation, that induces the dissociation of Nrf2. Nrf2 activation was shown in response to treatment with nine structurally-dissimilar classes of compounds, the only similarity being their ability to react with thiol groups. Due to the fact that Keap1 is cysteine rich and Nrf2 has relatively few cysteine residues, it was proposed that the thiol reaction occurs within the Keap1 protein. Through competition binding studies and kinetic measurements of the thiol reaction on Keap1 with dipyridyl disulfides it was determined that there were four reactive cysteines. Confirmation of these results with radiometric, UV spectroscopic and mass spectrophotometric techniques showed four especially reactive cysteines, including

26

Cys^{257}, Cys^{273}, Cys^{288} and Cys^{297} on Keap1 (68). It was concluded that these cysteines were responsible for the dissociation of Nrf2 from Keap1 by a direct thiol reaction with the Nrf2 activating compounds. Conversely, it was reported that modification of these cysteines by a variety of known ARE inducers was insufficient to disrupt the Nrf2/Keap1 complex (72), although this study used lower concentrations of the ARE inducers. Overall, evidence supports the idea of reactive cysteines serving as redox sensors within the Keap1-Nrf2 complex which, upon reaction with an inducer, results in Nrf2 activation. This thiol reaction is dependent upon xenobiotic concentrations.

The first study to suggest that Nrf2 could be a substrate for proteosomal degradation reported that inhibition of the 26S subunit of the proteosome induced expression of the catalytic subunit of gamma-glutamylcysteine synthase, a Nrf2-regulated gene. This report was followed by a series of studies further implicating the proteosomal pathway in Nrf2 degradation showing that Nrf2 is an extremely labile protein and is rapidly identified and degraded by the proteosomal system (277). A month later it was reported that, upon activation, Nrf2 was stabilized and not degraded by the 26S proteosome (222). However, Nrf2 activation by antioxidants or overexpression resulted in increased expression of proteosome 20, suggesting that Nrf2 might increase proteosome levels as a negative feedback mechanism (159). It is thought that Nrf2 is constitutively ubiquitinated and degraded by the proteosome through the Nrf2:Keap1 interaction, and that Nrf2 is stabilized by oxidative stress through the antagonism of this interaction (202). These results suggest that proteosomal degradation of Nrf2 is dependent upon Keap1. The role of Keap1 as the regulator of Nrf2 translocation and degradation was later confirmed and found to be slowly degraded in the nucleus (121).

27

This interaction between the proteosome and Keap1 was reported to involve two cysteine residues on Keap1, Cys^{273} and Cys^{288}. It was also determined that these cysteines are required for Keap1-dependent ubiquitination of Nrf2 (308). These studies outlined the proteosomal degradation of Nrf2 by the proteosome. Proteosomal degradation of Nrf2 requires interaction with Keap1. Upon dissociation from Keap1, Nrf2 is stabilized and not targeted for degradation by the proteosome.

The role of cullin 3-ROC1 in mediating Nrf2 degradation was reported by two different groups the following year (67, 146). Both studies reported that Keap1 functions as an adaptor protein for the cullin 3-ROC1 complex acting as an E3 ligase in the ubiquitin-dependent proteosomal system. Ubiquitin conjugation requires the action of three enzymes: the ubiquitin-activating enzyme (E1), the ubiquitin conjugating enzyme (E2) and the ubiquitin ligase (E3). The E3 ligases both recognize the substrate protein and catalyze the isopeptide bond between the substrate and the ubiquitin. These studies showed that Keap1 interacts with the cullin 3-ROC1 E3 ligase facilitating the degradation of Nrf2 by ubiquitin-dependent proteosomal system (67, 146). A study by Kobayashi *et al.* (147) showed that the cullin 3-Roc E3 ligase complex requires Cys^{273} and Cys^{288} on Keap1 in order to ubiquitinate and subsequently degrade Nrf2. In the presence of an oxidant, Cys^{273} and Cys^{288} are oxidized and subsequently inactivate the cullin 3-ROC1 E3 ligase complex resulting in the release and stabilization of Nrf2 (147). This same group proposed a "fixed ends model" which suggests that a single Nrf2 protein is bound in two sites to two separate Keap1 monomers. The double-binding of Nrf2 to Keap1 facilitates an opening of the Neh domain of Nrf2 for the cullin-3-ROC1-E3 ligase complex to ubiquitinate Nrf2 and target it for degradation (Figure 5) (203, 287, 288).

These studies established the role of the proteosome in Nrf2 degradation, concluding that through two cysteines on the Keap1 molecule, the proteosome actively degrades Nrf2 and when the two cysteine residues are oxidized the proteosome is inactivated.

The Keap1 protein prevents Nrf2 activation by a direct binding to the Nrf2 protein and the actin skeleton. This interaction was reported to occur by the binding of the DGR domain of the Keap1 molecule to the Neh domain of the Nrf2 protein. The binding is redox sensitive, with four reactive cysteines on Keap1 that can react with known Nrf2 activators, resulting in the dissociation of Nrf2. Keap1 not only inactivates Nrf2, but also actively recruits Nrf2 for degradation by the proteosomal system. Each Keap1 molecule binds two Nrf2 proteins and facilitates their degradation by the cullin 3-ROC1 E3 ligase, a member of the proteosome. Taken together, These studies show that Keap1 is the major regulator of Nrf2 activation through direct binding action, as a redox sensor and recruitment of Nrf2 for proteosomal degradation.

VIII. Nrf2 as a multi-organ protector.

The Nrf2/ARE system has been shown to be protective in many tissues and disease states. Nrf2-mediated protection is attributed to its unique ability to induce the transcription of phase II antioxidants and detoxifying proteins that neutralize reactive oxygen species and thereby balance the cells redox state. Since the discovery of Nrf2, its protective effects have been demonstrated in the lung, brain, endothelium, epithelium, kidney, pancreas and cardiovascular system and it has been shown to protect against many forms of cancer. The widespread reach of the protective effects of the Nrf2 protein has earned it the title of "the multi-organ protector" (166).

NRF2 IN THE LUNG Nrf2 protection in the lung was at first attributed to the proteins controlled therein. In 1996, a review article was published on the protective effects of the inducible protein heme oxygenase 1 (HO1). The authors concluded that HO1 induction was caused by a wide array of chemically diverse compounds and protects against oxidant-mediated lung injury, thus maintaining cellular homeostasis (51). The protective effects of ARE-containing genes, such as HO1, against oxidative stress was attributed to ARE-mediated transcription (58). Nrf2 has been found to protect the lung against a host of pulmonary diseases, including pulmonary fibrosis (50), hydroxytouene-mediated pulmonary dysfunction (40), acute pulmonary injury (40, 198), asthma (180), hyperoxic lung injury (47, 234, 235) and emphysema (115, 117, 251). Somatic mutations within the Keap1 molecule have been implicated in the pathogenesis of lung cancer (68, 232, 269). Deletion, insertion and missense mutations of Keap1 have been detected in cancer cell lines as well as in samples from patients with non-small cell lung cancer at frequencies of 50% and 19%, respectively. These mutations appear to be localized in the DGR domain of the Keap1 molecule, decreasing or abolishing the affinity of Keap1 for Nrf2 (232, 269). While Nrf2 protects the lung against many pathologies, increased free Nrf2 caused by non-functional Keap1 has been implicated in the development of non-small cell lung cancer. Nrf2 in the lung has been extensively reviewed (48, 49, 291).

NRF2 IN THE SKIN A role for Nrf2 in skin biology was recently defined. The skin is constantly bombarded with UV radiation, inducing the formation of reactive oxygen species (ROS). Additionally, skin wounds attract inflammatory cells which release large

quantities of ROS. The first report that Nrf2 was present in skin was its induction by keratinocyte growth factor, a compound released in response to injury (24). Since then, a role for Nrf2 in wound healing has emerged. Increased levels of Nrf2 have been found in wounded tissues (20, 237) while Nrf2 has been reported to be activated by lipopolysaccaride (LPS) (242, 258, 274, 284). In addition, Nrf2 has been shown to be activated by the inflammatory molecule, 15-deoxy-delta (12,14)-prostaglandin J(2) (15dPGJ2), in epithelial cells (137). Nrf2 induction in keratinocytes has also been reported using various inducers and insults. First, treatment with Keap1 siRNAs results in an increase in ARE-containing gene expression (62). ARE-driven gene induction has been reported in response to electrophiles, tBHQ, hyperoxia, H_2O_2, glucose oxidase (70), arsenic (238), and low to moderate doses of UV radiation (132, 238). These studies, suggest that Nrf2 plays a large role in maintaining a redox balance in the skin through the regulation of wound healing and protection against daily attacks of reactive oxygen species on the skin (20).

The role of Nrf2 in the skin is further revealed by the phenotype of the Keap1 knockout mouse. The Keap1 knockout is a lethal mutation and Keap1 knockout mice die in the first three weeks after birth from food obstruction and ulceration caused by hyperkeratosis in the esophagus and stomach. Furthermore, the Keap1 knockout mouse also has hyperthickening of the epidermis. Upon closer analysis, increased expression of keratin 1 and 6 in the keratinocytes was found (213, 295), suggesting that keratin genes in epithelia are hypersensitive to Nrf2.

Nrf2 may also play a role in the prevention of skin cancer. Nrf2 knockout mice exhibit skin papillomas in response to carcinogens at an earlier age and at a higher

quantity than that of wild-type. Upon closer analysis of the Nrf2 knockout mouse papillomas, decreased levels of γ-GCS and NQO1 were observed. Interestingly, ARE reporter mice treated with the same carcinogen showed no detectable increase in ARE induction. This suggests that basal Nrf2-driven gene expression is responsible for the anti-tumorigenic properties of Nrf2 (10).

Nrf2 has been implicated as a regulator of the redox status of the wound and has been shown to be activated by electrophiles, tBHQ, hyperoxia, H_2O_2, glucose oxidase, arsenic and low to moderate doses of UV radiation. Nrf2 appears to play a role in skin biology, as it responds to keratinocyte growth factor. Excessive free Nrf2, as seen in the Keap1 knockout mouse, increases expression of keratins 1 and 6 and results in hyperkeratosis and hyperthickening of the epidermis. Mice deficient in Nrf2 also have decreased expression of ARE-driven genes, causing increased skin papillomas. In all, while Nrf2 is an important protective protein in skin biology, free Nrf2 levels must be regulated by Keap1 to prevent deleterious effects.

NRF2 IN THE VASCULATURE The significance of reactive oxygen species in the vasculature is very complicated in that they not only act as signaling molecules, but can also be harmful substances (282). In the endothelium, shear stress stimulates ARE-driven gene transcription through the generation of reactive oxygen species (126), whereas the type of blood flow (laminar vs. oscillatory) can also affect Nrf2 activation (45, 109). The activation of Nrf2 in response to shear stress in the endothelium is thought to be mediated by the activation of the inflammatory factors cyclooxygenase-2 (Cox-2) and 15-deoxy-Delta-(12,14)-prostaglandin J12 (109). Vasodilation is a mechanism to relieve shear

stress (76). The vasodilator effect of dopamine in kidney endothelial cells is also mediated by Nrf2 (17).

One of the major tools that the vascular system utilizes to combat atherosclerosis is nitric oxide (NO). The actions of NO in the vascular system include vasodilation, interactions with proteins involved in prevention of platelet aggregation, inhibition of leukocyte adhesion, DNA synthesis, mitogenesis and proliferation of vascular smooth muscle cells. NO has also been implicated in preventing thrombosis and plaque formation. The role of NO in the vasculature has been extensively reviewed (85, 281, 314)). Activation of Nrf2 by NO has been documented in both endothelial and smooth muscle cells, suggesting a possible role for Nrf2 in NO signaling. Nitric oxide (NO) has been reported to activate Nrf2 in endothelial cells, resulting in Nrf2 translocation and protection of the endothelial cell from oxidative injury and subarachnoid hemorrhage (44, 90). In smooth muscle, Nrf2 is also activated by NO and protects the cell from nitrosative stress (189). Studies have shown that activation of antioxidant genes by Nrf2 through NO (189, 217) and from the more harmful peroxynitrate ion (129, 178, 236) protects vascular smooth muscle against cell death. The reports of Nrf2 activation by NO in both layers of the vasculature suggests that it might be acting as a signaling molecule between the cellular layers of blood vessels. No evidence of a direct interaction between nitric oxide synthase (NOS) and Nrf2 has been reported. Therefore, Nrf2 is likely a downstream target of NO.

Other ROS in the vasculature have been reported to activate Nrf2. Nrf2 is both activated in response to, and is protective against H_2O_2 in both smooth muscle (25) and endothelium (58). Oxidized lipids and lipoproteins have been shown to accumulate in

33

atherosclerotic lesions and contribute to the pathogenesis of atherosclerosis (18, 170, 278) while oxidized low density lipoproteins (LDL) activate Nrf2. These data implicate Nrf2 as a sensor of the redox state of oxidized lipoproteins (7, 172, 181). The activation of Nrf2 by oxidized lipids has been hypothesized to occur through nitric oxide production (270), leaving room to speculate as to the role of Nrf2 in the pathogenesis of atherosclerosis. Nrf2-mediated protection in the vasculature may be due to the unique ability of Nrf2 to act as a redox sensor in the vasculature. Nrf2 activation in the vasculature has been reported in response reactive oxygen species such as oxidized lipoproteins, H_2O_2 and NO, but a correlation of Nrf2-mediated protection in the vasculature has not been made.

NRF2 IN THE RETINA The tubtub strain of mice are used as a model of adult onset obesity and is characterized by late-onset weight gain accompanied by progressive retinal and cochlear degeneration and tubtub mice (226, 227). Treatment of these mice with sulforaphane, a Nrf2 activator, increases antioxidant enzyme transcription through Nrf2, delaying the characteristic phenotype of photoreceptor degeneration (150). The role of Nrf2 in other aspects of the tubtub mouse phenotype has not been evaluated. However, Nrf2 may prove to play a role as oxidative stress has been shown to exacerbate many of the complications of obesity (13, 34-36, 77, 161, 240).

NRF2 IN THE KIDNEY In the kidney, ischemia-reperfusion often results in renal failure (263). Through microarray analysis after ischemia-reperfusion of the kidney, ARE-driven genes including glutathione S-transferases (GSTM5, GSTA2 and GSTP1),

and NAD(P)H quinone oxidoreductase (NQO1) were shown to be elevated. Nrf2 was also shown to be upregulated and, upon closer analysis, reoxygenation-specific nuclear accumulation was observed. These results suggest that Nrf2 might be involved in ischemic preconditioning through the activation of ARE-driven genes (171). Nrf2 has also been shown to be protective in other conditions of renal stress. α-lipoic acid, a known Nrf2 activator, has been implicated in protection against hypertension and nephrotoxicity after treatment with cyclosporine, a drug used after organ transplants (194). These reports suggest Nrf2 is involved in renal protection against ischemia-reperfusion and hypertension-induced nephrotoxicity through the activation of ARE-driven genes.

NRF2 IN THE LIVER Primary hepatocytes and the HepG2 cell line are considered good models of intact liver (32, 148) and with these useful tools, Nrf2 activation has been implicated as a protective mechanism against many diseases of the liver. Treatment with antioxidants such as BHA and tBHQ, or oxidants like H_2O_2, results in increased phase II enzyme expression in both primary hepatocytes and the HepG2 cell line (5, 141). Using the HepG2 hepatic cell model, Nrf2 was shown to mediate protection against oxidative stress from arachidonic acid-induced toxicity (92). It has been also been suggested that Nrf2 protects hepatocytes from the deleterious effects of alcohol. Activation of cytochrome P450 2E1 (CYP2E1) and the ethanol-derived oxidative stress therein, is a well characterized harmful byproduct of alcohol metabolism (185). CYP2E1 activation was shown to be reduced by Nrf2 in human hepatocytes (91, 299). These data cast Nrf2 as a possible protective agent against cirrhosis of the liver. In addition to protection

against alcohol, treatment with sulforaphane, a Nrf2 activator, results in increased clearance of arsenic in mouse hepatocytes (267). In support of Nrf2 aiding in the clearance of toxic chemicals, the hepatocyte-specific deletion of Keap1 results in increased resistance in acute drug toxicity and increased expression of phase II enzymes (228). In summary, activation of Nrf2 by oxidants or antioxidants protects the hepatocyte from oxidative stress that could occur by poisoning, drug overdose or alcoholism. These data suggest that Nrf2 aids in the clearance of harmful chemicals by the liver and might have far-reaching implications for Nrf2 in the treatment of toxicity of the liver.

NRF2 IN THE BRAIN Research on the Nrf2/ARE pathway in the brain has been extensive and, for the most part, pioneered by Jeffery Johnson's group at the University of Wisconsin (167, 168, 173, 175, 208, 264). The ARE has been shown to be activated by tBHQ and phorbol -12-myristate-13-acetate in neurobastoma cells (167, 175, 208). Pretreatment of tBHQ protects these cells from H_2O_2 induced apoptosis (175). Nrf2 has also been shown to protect primary neurons against mitochondrial complex inhibitors (168, 264) and human neural stem cells against H_2O_2-mediated cell death (173). Nrf2 activation by oxidants and antioxidants protects neuronal cell lines and primary cultures from oxidative stress.

A role in astrocyte mediated protection of neurons has been extended to Nrf2. Nrf2 has been shown to protect astrocytes from H_2O_2 (164) and, through the Nrf2/ARE pathway, astrocytes have been shown to protect neurons from H_2O_2 and nonexcitotoxic glutamate toxicity (152). Glia overexpressing Nrf2 have also been shown to protect neurons against glutamate toxicity associated with glutathione depletion (265). These

36

reports suggest that Nrf2 is associated with the well-characterized protection of neurons by their neighbors (reviewed in (9, 15, 80, 144)).

Nrf2 activation has also been reported to protect the brain against severe stresses including cerebral ischemia (266, 311) and oligemia (191). Nrf2 may even have a role in protecting against Parkinson's disease (PD). Nrf2 knockout mice had increased susceptibility to 1-methyl-4-phenyl-1,2,3,6-tetrahydropyridine (MPTP; a model of PD) toxicity as compared to wild-type (27). In addition, pretreatment of human neuroblastoma SH-SY5Y cells with apomorphine resulted in increased cell survival against 6-hydroxydopamine (6-OHDA) toxicity through the activation of Nrf2 and transcription of ARE-driven genes (101). Nrf2-mediated transcription of ARE-driven genes appear to protect against treatment with MPTP and 6-OHDA, mimicking many pathologies of Parkinson's disease.

Nrf2 protects various constituents of the brain, including neurons, astrocytes and glia against various oxidative stressors. Nrf2 also protects the brain against cerebral ischemia, oligemia and may play a role in neuroprotection in Parkinson's disease.

NRF2 IN CANCER   The pathogenesis of cancer is often caused by exposure to chemical insults. In response to these insults, the cellular defenses of antioxidant and detoxifying enzymes are coordinately activated by Nrf2 and aid in the clearance of these harmful substances. The use of the Nrf2 knockout mouse has been very useful in the study of the Nrf2/ARE system in cancer. Using the Nrf2 knockout mouse, chemotherapeutic agents have been shown to have decreased efficacy associated with decreased inducibility of antioxidant enzymes (116, 158, 250). Oltipraz, a

chemotherapeutic agent and Nrf2 activator, protects wild-type mice from the carcinogen benzo[a]pyrene, although increased tumor formation was observed in Nrf2 knockout mice (249, 250). Further, N-nitrosobutylamine caused increased lesion formation in the urinary tract and bladder of Nrf2 knockout mice compared to wild-type and treatment of wild type mice with oltipraz decreased lesion formation by 60-80% (114). Additionally, exposure to the well known carcinogens polycyclic aromatic hydrocarbons (PAH), derived from diesel exhaust, results in increased antioxidant enzyme levels in wild-type mice (179). The Nrf2 knockout mice, however, are more susceptible to DNA adduct formation in the lungs and increased inflammatory response in bronchial cells after treatment with PAHs (8). The selected studies outlined show a role for Nrf2 in cancer prevention through the increased expression of ARE enzymes. The role of the Nrf2/ARE pathway in cancer has been reviewed further (309).

NRF2 IN THE HEART While the role of Nrf2 in a cardiac setting has only recently been investigated, the protective nature of phase II antioxidants and detoxifying enzymes is well established (83, 108, 260, 303). Antioxidant enzymes protect against oxidative stress in many disease states, including myocardial infarction (105), hyperglycemia, (81) hypertension (54) and ischemia-reperfusion in both normal (261) and diabetic states (188). Furthermore, Nrf2 activators α-lipoic acid (30), resveratrol (29) and 1,2-dithiole-3-thione (D3T) (28) activate transcription of antioxidant enzymes and protect the cardiac cell from oxidative stress. Although the protective effects of Nrf2 inducers and the antioxidant enzymes controlled therein have been shown to protect against various

cardiac diseases, a direct link between Nrf2 and the cardiac cell was not made until 2005 (313).

In 2005, Zhu *et al* (313) reported that Nrf2 protects Nrf2 knockout primary cardiac fibroblasts against reactive oxygen and reactive nitrogen species. The Nrf2 activator D3T was unable to protect Nrf2 knockout cardiac fibroblasts from oxidative and nitrosative stress as compared to wild-type. Additionally, the Nrf2 knockout mice had decreased activity and protein levels of superoxide dismutase (SOD), catalase, glutathione reductase (GR), glutathione peroxidase (GPx), glutathione transferase (GST) and NADPH:quinone oxidoreductase 1 (NQO1). In support of Nrf2-mediated protection in the cardiac fibroblast, xanthane oxidase and the NO-generating drug 3-morpholinosydnonimine-N-ethylcarbamide (SIN-1) caused increased cell death in Nrf2 knockout cardiac fibroblasts. It was concluded that Nrf2 is involved in inducible and basal induction of antioxidant genes and Nrf2 is protective against reactive oxygen and nitrogen species (313).

In 2007, Purdom-Dickinson *et al.* isolated cardiac myocytes and fibroblasts and using microarray analysis, produced an extensive list of enzymes with altered expression after treatment with H_2O_2. The list included antioxidant enzymes, metabolic enzymes, cytokines, endocrine factors, cell cycle regulatory proteins, cytoskeletal proteins, contractile proteins, and channel proteins (for a complete list see appendix B). They reported that, in cardiac myocytes, the ARE is activated in a dose- and time-dependent manner in response to H_2O_2 using an ARE-luciferase reporter construct. Cardiac myocytes exhibited ARE binding and increased cell survival in response to doxycycline when preconditioned with H_2O_2. The investigators next examined if the preconditioning

39

effect seen by H_2O_2 pretreatment was Nrf2 dependent. They determined that transient transfection of cardiomyocytes with Nrf2 was unable to protect against treatment with doxycycline. From this observation it was suggested that up-regulation of Nrf2 alone is not protective. The authors concluded that activation of the Nrf2/ARE pathway is not responsible for the preconditioning effect seen by H_2O_2, and further hypothesized that the interaction of Nrf2 with other pathways was responsible for the observed preconditioning effect of H_2O_2 pretreatment.

The Nrf2 activators α-lipoic acid, resveratrol, and 1,2-dithiole-3-thione (D3T) are reported to protect the cardiac cell from oxidative stress. Cardiac fibroblasts and myocytes derived from the Nrf2 knockout mouse have decreased ARE-driven enzyme levels and increased susceptibility to oxidative stress, suggesting that Nrf2 protects the cardiac cell from oxidative stress. On the contrary, Nrf2 overexpression does not protect against doxycycline-induced cell death, like that of H_2O_2 pretreatment, suggesting that Nrf2 may not be involved in preconditioning the cardiac cell. It has been hypothesized that Nrf2 protects the cardiac cell through crosstalk with other protective pathways like NF-κB. It is unclear if the increased susceptibility to oxidative stress of Nrf2-deficient cardiac cells is due to direct actions of Nrf2 or a lack of crosstalk between Nrf2 and other pathways. The focus of the present study was therefore to determine if the transcription factor Nrf2 protects the cardiac-like H9c2 cell against oxidative stress.

In summary, Nrf2 activates phase II enzymes by recognition and direct binding to the ARE. Nrf2 activation can be attained through a direct reaction with an inducer or through a second messenger. MAPK, PI3K, and PKC have all been implicated in Nrf2 activation. Once activated, Nrf2 translocates into the nucleus where it binds to a co-

transcription factor, thought to be a small Maf protein, forming a heterodimer. The Nrf2:Maf heterodimer recognizes the ARE-initiating transcription of various antioxidants and detoxifying proteins. Nrf2 activation of ARE-driven genes is inducer-, gene- and tissue-specific and the differential regulation of ARE-driven transcription is thought to be mediated by both the sequence of the ARE and the Nrf2 co-transcription factor. Several negative regulators have been associated with the Nrf2/ARE system. Several proteins have been shown to form hetero- and homodimeric complexes occupying the ARE and preventing ARE-mediated transcription. The most important regulator of Nrf2, Keap1, binds directly to Nrf2, attaching it to the cytoskeleton and actively targeting it for proteosomal degradation (Figure 3). Nrf2 is ubiquitously expressed and reported to be protective in many tissues, earning it the title of the multi-organ protector. Protection by Nrf2 has been reported in tissues ranging from the skin and the lung, to the brain and the cardiovascular system. Taken together, the studies summarized here suggest that Nrf2 is protective in many disease states; overexpression and excessive Nrf2 activity can, however, be deleterious, thus ARE-driven transcription is heavily regulated.

MATERIALS

H9c2 Cell line: Rat cardiac-like H9c2 cells were obtained from the American Type Culture Collection (ATCC, Manassas, VA) and used as the cardiac model system.

Cell culture supplies: Dulbecco's Modified Eagle's Medium (DMEM), fetal bovine serum (FBS), penicillin/streptomycin/amphotericin B reagent, Hanks Balanced Salt Solution with and without calcium and magnesium (HBSS), trypsin, and phosphate buffered saline (PBS) were purchased from Invitrogen Co. (Calsbad, CA). Culture dishes including T-75, T-25, 10 cm, 6 cm, 12 well, 6 well, 96 well, as well as cryotubes were purchased from B.D. Falcon Co. (Franklin Lakes, NJ). Conical Tubes (15 and 50ml) were purchased from Corning, Inc. (Corning, NY).

Nucleic acid and siRNA supplies: TRIzol, blue juice gel loading buffer, siRNAs for Nrf2, Keap1 and their corresponding nonsense control siRNA, lipofectamine and OptiMEM media were purchased from Invitrogen. RNeasy mini kit was purchased from Qiagen, Inc. (Valencia, CA). Taq polymerase and its corresponding 10X buffer were obtained from Eppendorf, Inc. (Westbury, NY). The IQ supermix for real time PCR, iScript first strand synthesis kit, and the 96-well optical plates and sealing tape were purchased from Bio-Rad Laboratories (Hercules, CA). Agarose, NorthernMax denaturing gel buffer, MOPS gel running buffer, formaldehyde sample loading dye, RNase and DNase-free water and DEPC-water were purchased from Ambion, Inc.

(Austin, TX). The all-purpose molecular weight ladder was purchased from Bionexus Inc. (Oakland, CA). Tris-Acetate-EDTA (TAE) buffer, Tris-EDTA (TE) buffer, chloroform were purchased from Fisher Scientific (Pittsburg, PA). Thin-walled PCR tubes, 1.5 ml, and 2 ml tubes were purchased from LabScientific (Livingston, NJ).

Western Blotting Supplies: DC protein assay kit, Laemmli buffer, Tris-glycine-SDS buffer, β-mercaptoethanol, pre-stained SDS-PAGE broad range molecular weight marker and 12% SDS-PAGE ready-gels came from Bio-Rad laboratories (Hercules, CA). ECL plus western blotting detection kit and nitrocellulose membranes were purchased from Amersham Biosciences (Buckinghamshire, England). Methanol was purchased from Fisher Scientific. Nonfat dry milk came from Nestle (Glendale, Ca). Rabbit anti-goat Nuclear factor E2 like 2 (Nrf2) primary antibody, rabbit IgG anti-heme oxygenase 1 (HO1) primary antibody and goat anti-rabbit HRP-conjugated secondary antibody were purchased from Stressgen (Victoria, Canada). Keap1 primary antibody, goat IgG anti–NADPH:quinone oxidoreductase 1 (NQO1) primary antibody and rabbit anti-goat HRP-conjugated secondary antibody were obtained from Santa Cruz Biotechnology (Santa Cruz, CA).

CyQUANT Cell Proliferation Kit and the Image-iT live green ROS detection kit were purchased from Molecular Probes/Invitrogen.

All other chemicals not mentioned were purchased from Sigma-Aldrich-Fluka (St. Louis, MO).

METHODS

1 – Effect of tBHQ on HO1 and NQO1 gene expression of in the H9c2 cell line.

1.1 – Cell Culture:

All cell culture techniques were performed under a sterile level 2 biosafety cabinet. The H9c2 cells were thawed rapidly in a 37°C water bath until 1/8th of the total volume remained frozen. Cells were then triturated gently into a 5 ml pipette containing low glucose (5.5 mM) DMEM supplemented with 10% fetal bovine serum, 100 mg/ml streptomycin, 100 U/ml penicillin F and 0.25 mg/ml amphotericin B (DMEM growth media). This cell mixture was then transferred to a 15 ml conical tube, brought up to a total volume of 10 ml in DMEM growth medium, and centrifuged for 5 minutes at 500 x g at room temperature. The supernatant was aspirated and the cell pellet was resuspended in DMEM growth medium. Cells were plated into a T75 flask and grown at 37°C in a cell culture incubator under 95% air and 5% CO_2. Medium was changed after 24 hours.

After cell culture was established, medium was changed every three days and cells were passaged once per week at 90% confluence. For passage, cells were washed once with Hank's balanced salt solution (HBSS) without calcium and magnesium and trypsinized (0.05% trypsin w/v) for 5 minutes at 37°C. Cells were then gently rocked to remove any incompletely dislodged cells and 8 ml of DMEM growth medium was

added to the cells. Cells were then transferred to a 15 ml conical tube and centrifuged at 500 x g for 5 minutes at room temperature. Supernatant was removed and cells were resuspended in 10 ml of media and counted by trypan blue exclusion using a hemocytometer. Cells were plated at a density of 2.5 x 10^5 cells/ 75 cm^2.

The H9c2 cell line was derived from the left ventricles of neonatal rat hearts and can differentiate into either cardiac or skeletal muscle, depending on culture conditions (142, 205, 233). To ensure that our cells displayed the cardiac-like phenotype, mononucleation was verified by both 4',6-diamidino-2-phenylindole (DAPI) staining and hematoxylin-and-eosin (H&E) staining techniques.
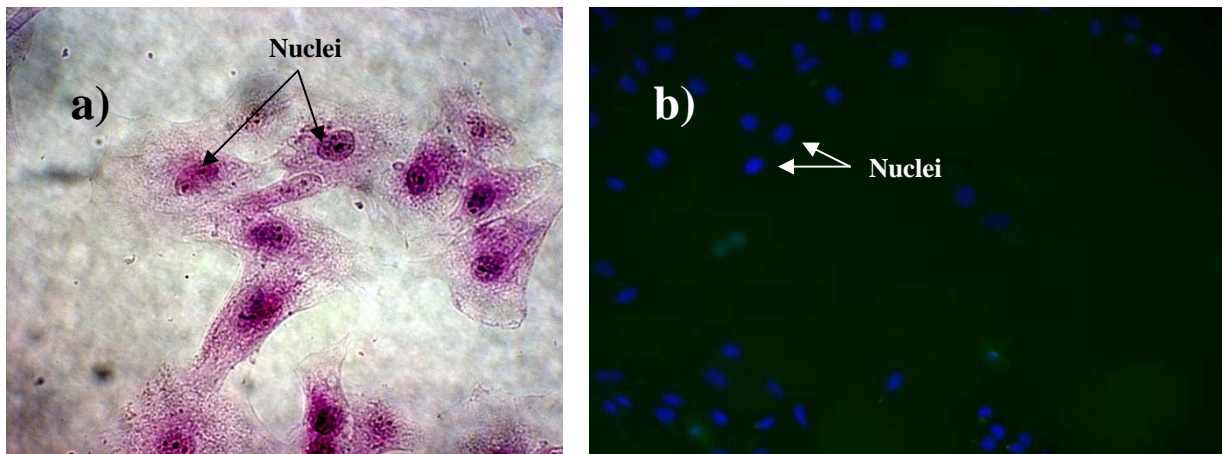
Figure 4: H9c2 mono-nucleation verified by a) hematoxylin-and-eosin (H & E) stain (40x magnification) and b) 4',6-diamidino-2-phenylindole (DAPI) staining (20X magnification).

1.2 – ARE-driven gene expression. To determine the expression of Antioxidant Response Element (ARE) containing genes, tert-butyl hydroquinone was used to drive ARE gene expression. As discussed in the literature review, tBHQ is a phenolic antioxidant and well known activator of Nrf2 (activators summarized in table 1, page 9

and appendix A, page108 (223)). The optimum concentration of tBHQ was determined

to be 10 μM, with the greatest increase of HO1 and NQO1 gene expression at the lowest

concentration of tBHQ. H9c2 cells were plated at a density of 5.0 x 10^5 cells per 10 cm

dish and grown to 80% confluence. Cells were treated with tBHQ (10 μM) or its vehicle

(1:20,000 dilution of DMSO) for 0, 4, 8, 12, 24, 36, 48 and 72 hours at 37°C in the cell

culture incubator. At each time point, the medium was aspirated and 1 ml of TRIzol was

added to each plate. Plates were mixed on a Belly Dancer (Stovall, Greensboro, NC) for

5 minutes, scraped into pre-labeled 1.5 ml tubes and stored at -80°C until use (see next

section for details). This experiment was repeated in three independent experiments.

1.3 – RNA isolation from H9c2 cells:

     1.3.1 Phase Separation: The tBHQ or vehicle treated H9c2 cell samples in TRIzol

were removed from the -80°C freezer and allowed to equilibrate to room temperature.

Once equilibrated, 200 μl of chloroform were added to each sample and samples were

shaken vigorously for 15 seconds. The samples were allowed to sit at room temperature

for three minutes, and centrifuged at 14,000 x g for 15 minutes at 4°C. Following

centrifugation, the samples were separated into 3 distinct layers. The lower fraction is the

organic phase and is red in color, the middle fraction, or interphase, is a white fluffy layer

containing DNA, and the top clear aqueous phase contains the RNA. The top phase was

carefully collected from the side, so as not to disturb the other phases. The extracted

aqueous phase should be clear with no white fraction. The aqueous phase was transferred

to a new, clean, pre-labeled 1.5 ml tube.

1.3.2 – Isolation of Total RNA Using the RNeasy Mini Kit: The aqueous phase obtained from the phase separation was combined with 350 μl of 70% EtOH (v/v), vortexed, transferred into a spin column and placed into a 2 ml collection tube. Samples were centrifuged at 10,000 x g for 30 seconds at room temperature and flow through was discarded. Samples were washed with 700 μl of RW1 buffer, centrifuged at 10,000 x g for 30 seconds and the flow through was discarded. To prevent contamination, the spin column was transferred to a new clean 2 ml collection tube, washed twice with 500 μl of RPE buffer and centrifuged at 10,000 x g for 30 seconds at room temperature. The collection tube was discarded and replaced with a new pre-labeled 1.5 ml tube. RNA was eluted by pipetting 50 μl of RNase- and DNase- free water directly onto the membrane of the silica gel column and incubating at room temperature for 5 minutes. The tube was centrifuged at 10,000 x g for 2 minutes and RNA in the flow through was either stored at -80°C or directly used in the next step.

1.3.3 – RNA Purity and Concentration Analysis: Sample RNA was analyzed spectrophotometrically for concentration and purity. The optical density of RNA samples was determined by UV spectroscopy using a SmartSpec plus spectrophotometer (Bio-Rad). Sample RNA was diluted 1:100 in TE buffer (10 mM Tris-HCl, pH 7.5, 1 mM EDTA), transferred into a clean cuvette and analyzed spectrophotometrically using TE buffer as a blank. An absorbance at 260 nm of 1 is equivalent to 40 μg/ml total RNA. Sample RNA concentrations ranged from 0.1 to 1.0 μg/μl. Purity was also assessed by the ratio of absorbances from 260 nm and 280 nm ($A_{260/280}$). If the $A_{260/280}$ ratio was not greater than or equal to 1.7, the RNA purity was in question and samples were subjected to denaturing agarose gel electrophoresis to assess RNA integrity further.

1.3.4 – RNA Integrity Assessment: The purity and integrity of sample RNA was determined using denaturing-formaldehyde agarose gel electrophoresis (Mattheus *et al.* 2003). Total RNA (1 µg) was diluted in three volumes of formaldehyde sample loading dye (1X denaturing gel running buffer, 50% glycerol, 1mM EDTA, pH 8.0, 0.25% bromophenol blue, 0.25% xylene cyanol) and heated to 65°C for 15 minutes.   Samples were then removed, condensed on ice, centrifuged at 1000 x g for 5 seconds and loaded on to the denaturing-formaldehyde agarose gel. A 1.2% (w/v) agarose gel was prepared in NorthernMax denaturing gel buffer per manufacturers instructions (1x MOPS, 50% formamide 6% formaldehyde; 1X MOPS buffer in DEPC water; 50% formamide, 6% formaldehyde). The gel was electrophoresed at 100 V for 30 minutes, removed from the chamber and stained for 15 minutes in 0.5 µg/ml of ethidium bromide in diethyl pyrocarbonate water (DEPC 0.1% w/v). The gel was destained in DEPC water for 1 hour, visualized via UV illumination, and an image was obtained using a FluorS multimager (Bio-Rad). The integrity of each RNA sample was determined by visual analysis of the 28S and 18S ribosomal RNA bands. Only samples where the 28S band were twice as dense as the 18S band (Figure 5) were used for further analysis.
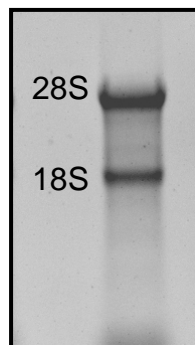

Figure 5: RNA Integrity Gel. The quality of isolated RNA was assessed following formaldehyde-denaturing agarose gel electrophoresis. This image depicts a representative gel for control RNA sample isolated from H9c2 cells. Both ribosomal RNA 28s and 18s bands are clearly visible, with the 28S band twice as dense as the 18S band.

1.4 – Analysis of Gene Expression:

1.4.1 – First Strand cDNA Synthesis: Total RNA was reverse transcribed to make cDNA using reverse transcriptase (RT). The cDNA was generated using the iScript first strand synthesis kit (4 μl of 5X RT buffer, 1 μl RT enzyme brought up to a total of 20 μl with water) and 1 μg of total RNA in a pre-labeled thin-walled PCR tube. The reaction was carried out on a Perkin Elmer model 2400 thermocycler under the following conditions: 25°C for 5 minutes followed by 42°C for 30 minutes then 85°C for 5 minutes with a final hold at 4°C.

1.4.2 – Real-Time PCR Primer Design: Primer design is crucial in reproducible and reliable gene expression analysis. Oligonucleotide primers were designed using vector NTI software (Invitrogen). General guidelines for primer design include a length of 18-24 base pairs, a GC content of 50-60%, a melting temperature (T_m) between 50 and 65°C, no secondary structure, no repeats of G's or C's longer than 3 base pairs, no G's or C's at ends of primers, no 3' complementarity (also known as primer dimerization; set at $\Delta G \geq -4$), a predicted amplicon size of 75-150 base pairs, and no secondary structure at binding sites. All criteria except the secondary structure can be programmed into the primer design tab of Vector NTI. Secondary structure of the gene and the amplicon were assessed using the mfold server provided by Dr. Michael Zuker (http://bioinfo.math.rpi.edu/~mfold/dna/form1.cgi). An 800 base pairs sequence of the gene to be amplified was analyzed for secondary structure under the following conditions: folding temperature 60°C, the ionic conditions of sodium (50 mM) and magnesium (3 mM). The derived secondary structure of the DNA was then used for

further primer design (Figure 6). Primers were designed in regions of no secondary structure. If an area of 150 base pairs without secondary structure was not found, the folding temperature was increased, keeping in mind that this then changed the temperature at which the primers were designed.
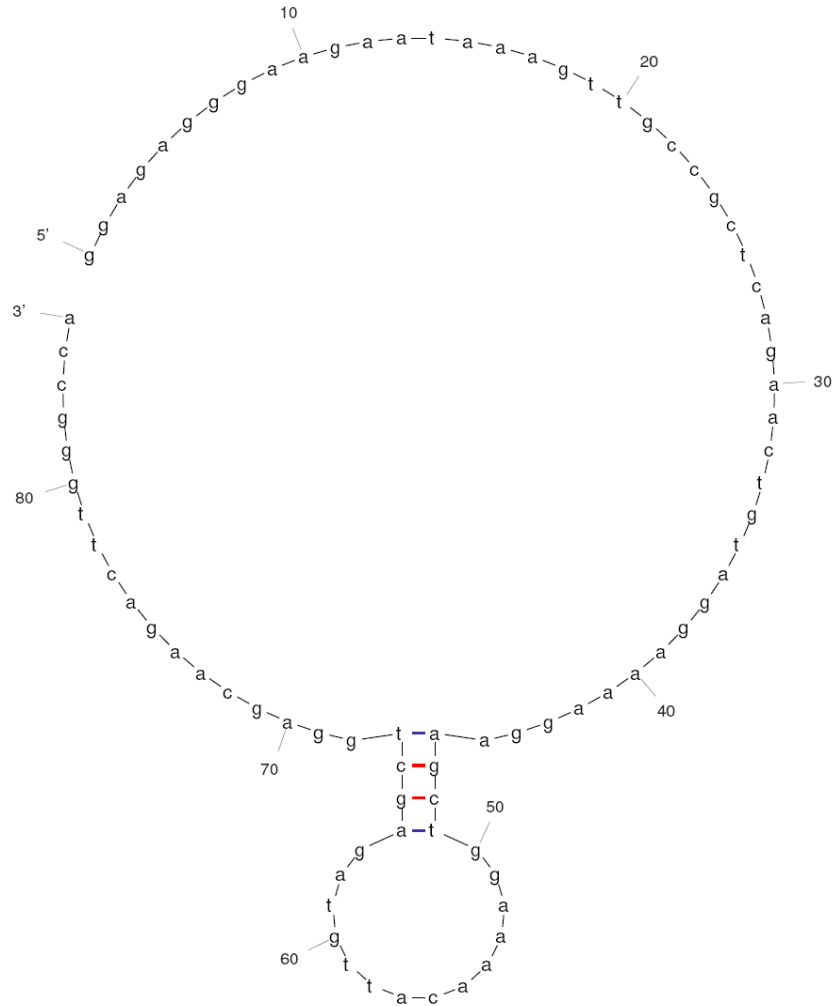
Figure 6: Mfold output. The secondary structure of the genes quantified by real-time PCR was assessed by the mfold server offered by Dr. M Zuker at Rensselaer Polytechnic Institute. This figure depicts the Nrf2 (Accession # NM_031789) amplicon folded at 55°C with 5 mM Na^+ and 3 mM Mg^{2+}.

The designed primer sequences were BLAST searched for gene specificity. BLAST is a search of all genes stored in the NCBI GenBank database and is available online at www.ncbi.nih.gov/Genbank. If a match occurred for a gene other than the gene in which the primers were designed with an expectation number below 0.01, the primers

51

were discarded and new primers designed. The expectation number is the number of times this match would be expected to occur by chance in a search of the entire database. Two primer sets for each gene were designed and synthesized by Sigma-Genosys (St. Louis, MO).

Gene-specific primers designed for real-time PCR were: NAD(P)H quinone oxidoreductase 1 (NQO1), heme oxygenase-1 (HO1), NF-E2 related factor 2 (Nrf2), kelch-like associated protein 1 (Keap1) and the two housekeeping genes glyceraldehyde 3-phosphate dehydrogenase (GAPDH), and acidic ribosomal phosphoprotein Po (Arbp) (Table 2).

Table 2. Gene Specific Primers for Real-Time PCR

NQO1 (rat)	sense 5'-CCTTGTATTGGTTTGGGGTG
Accession # NM_017000	antisense 5'-GCATACGTGTAGGCGAATCCTGCT
HO1 (rat)	sense 5'-CAGGTGTCCAGGGAAGGCTTTAAGC
Accession # NM_012580	antisense 5'-TTTCGCTCTATCTCCTCTTCCAGGG
Nrf2 (rat)	sense 5'-GGAGAGGGAAGAATAAAGTTGCCGC
Accession # NM_031789	antisense 5'-TGGCCCAAGTCTTGCTCCAGCTCT
Nrf2 (human)	sense 5'-ATTGCCTGTAAGTCCTGGTCA
Accession # NM_006164	antisense 5'-ACTGCTCTTTGGACATCATTTCG
Keap1 (rat)	sense 5'-GCTCAACCGCTTGCTGTATGC
Accession # NM_057152	antisense 5'-TCATCCGCCACTCATTCCTCTC
GAPDH (rat)	sense 5'-ATGATTCTACCCACGGCAAG
Accession # M17701	antisense 5'-CTGGAAGATGGTGATGGGTT
Arbp (rat)	sense 5'-AAGCGCGTCCTGGCATTGTCT
Accession # NM_007475	antisense 5'-CCGCAGGGGGCAGCAGTGGT
OAS2 (mouse)	sense 5'-TCAGAAGAGAAGCCAACGTGA,
Accession # NM_145227	antisense 5'-CGGAGACAGCGAGGGAAAT

1.4.3 – Primer Specificity and Efficiency Verification: Before primers were used for real time PCR, each set was tested for specificity and efficiency. To make certain each primer pair had only one amplicon, a standard PCR reaction (2 μl cDNA, 5 μl reaction buffer, 1 μl dNTPs (0.2 M), 1 μl Taq (1.25 U) polymerase, 41 μl ddH$_2$O) at the designated annealing temperature was performed (1 cycle 5 minutes @ 95°C; 40 cycles

15 seconds @ 95°C, then 30 seconds @ 60°C, then 15 seconds @ 72°C; and a final hold at 4°C) using control cDNA generated from the H9c2 cells. The PCR product was run on a 1.2% agarose gel, and the number and size of the band(s) were determined. Only primers with one amplicon of the correct size were used.
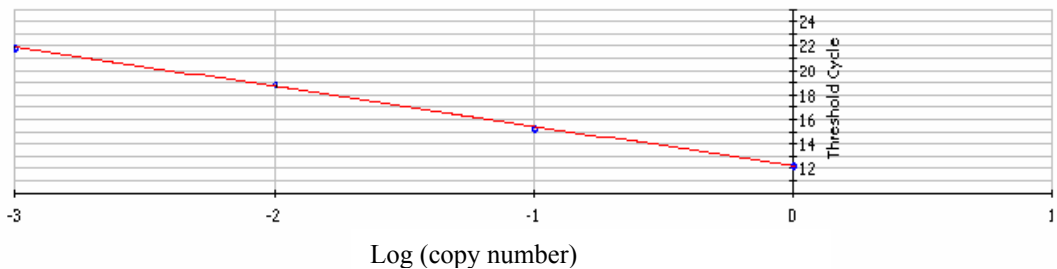
Primer PCR efficiency was determined by real-time PCR using a myIQ iCycler real-time PCR detection system (Bio-Rad). A standard curve was generated using 10-fold dilutions of control cDNA and the newly designed primers (Figure 7). The reaction condition mixture consisted of 1.25 U platinum Taq polymerase, 20 mM Tris, pH 8.4, 3 mM $MgCl_2$, 0.2 M each of the dNTPs, 50 mM KCl, 1:75,000 dilution of the DNA intercalating dye SYBR green (Platinum SYBR Green Supermix, Invitrogen), and the conditions were as follows: an initial denaturation at 94°C for 2 min, followed by 35 cycles of 94°C for 15 seconds, 60°C for 30 seconds and 68°C for 1 minute followed by a melt curve of 80 cycles starting at 55°C, increasing 0.5°C each cycle. The cycle threshold (Ct) was plotted against the cDNA dilution and the slope of the line was derived using the formula $E= (10^{-1/slope})-1$. E represents the efficiency of the reaction. Only primers with efficiencies of 80-120% were used for experimentation. In addition, the dilution series provided information regarding the correlation coefficient and only coefficients above 0.995 were used in these experiments.
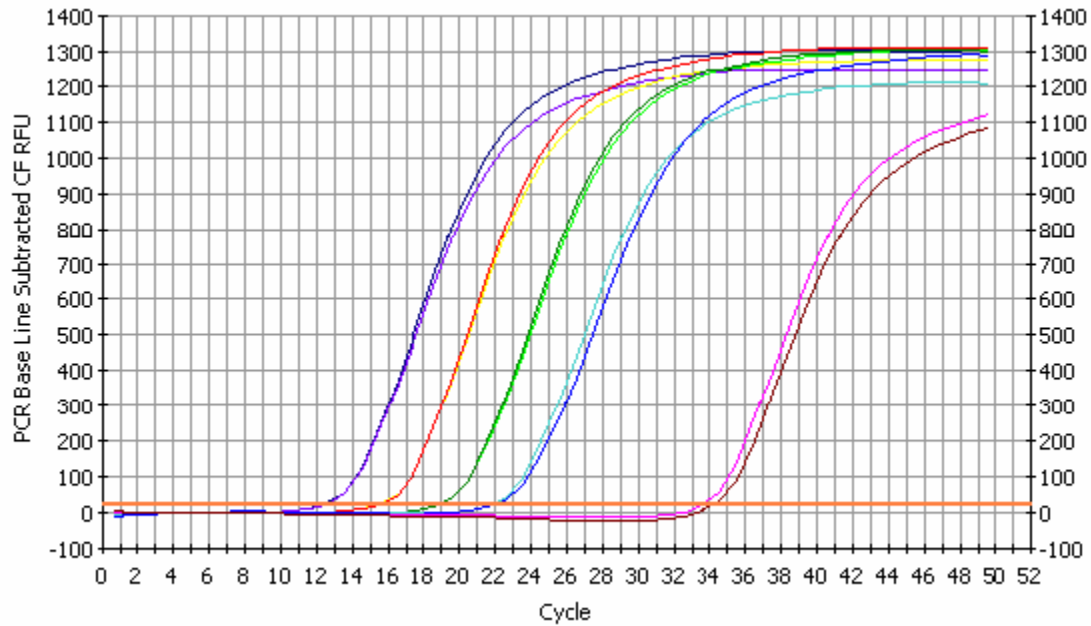
Correlation Coefficient = 0.999   Y=-3.227+12.223
PCR Efficiency = 104.1

□ Unknowns
▫ Standards

Figure 7: Real Time PCR standard curve for rat Nrf2 PCR efficiency.   The primer efficiency was determined by a standard curve of serial dilutions of cDNA.   The top graph is a representative real-time PCR quantification graph.   The horizontal orange line is the cycle threshold (Ct), at which point the copies of the gene reach a threshold of fluorescence.   Each curve represents a reaction with a certain dilution of cDNA in duplicate.   The curves with the lowest Ct, represent the highest concentration of cDNA.   The last 2 curves represent the blank (cDNA free) samples.   The lower graph is a standard curve with cDNA concentration on the X axis and Ct on the Y axis.   The PCR efficiency is 104.1% with a correlation coefficient of 0.999.

The data was further analyzed for efficient primer binding and for complete reaction elongation (Figure 8). To ensure efficiency of the primers, each curve should start above the previous curve and should increase exponentially at the start and plateau at the end. If these criteria were not met, the primers were discarded.
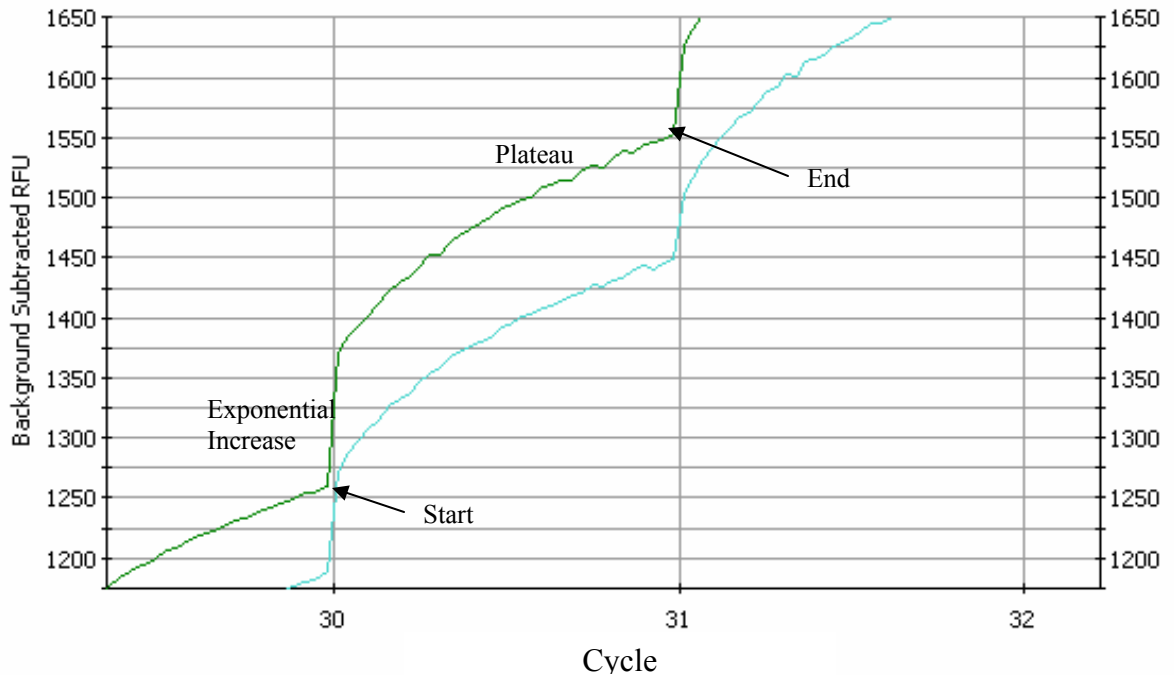
Figure 8: Primer binding and reaction elongation analysis. This graph represents a single cycle reaction of primer binding, elongation and primer unbinding of the gene heme oxygenase 1. Each trace represents a duplicate of a real-time PCR sample. Starting at cycle 30, an exponential increase in fluorescence is observed. This represents the primer binding to the template and the amplification of the target gene. The plateau phase represents the slowing and then end of the reaction when the next cycle begins with the 95°C segment.

To ensure that no 3' complementarity was present (primer dimerization), a melt curve was also performed (Figure 9). Each primer pair should have only one peak, indicative of one PCR product, and no secondary peak formation at 68-72°C (primer dimerization). If these criteria were not met, the primers were discarded.
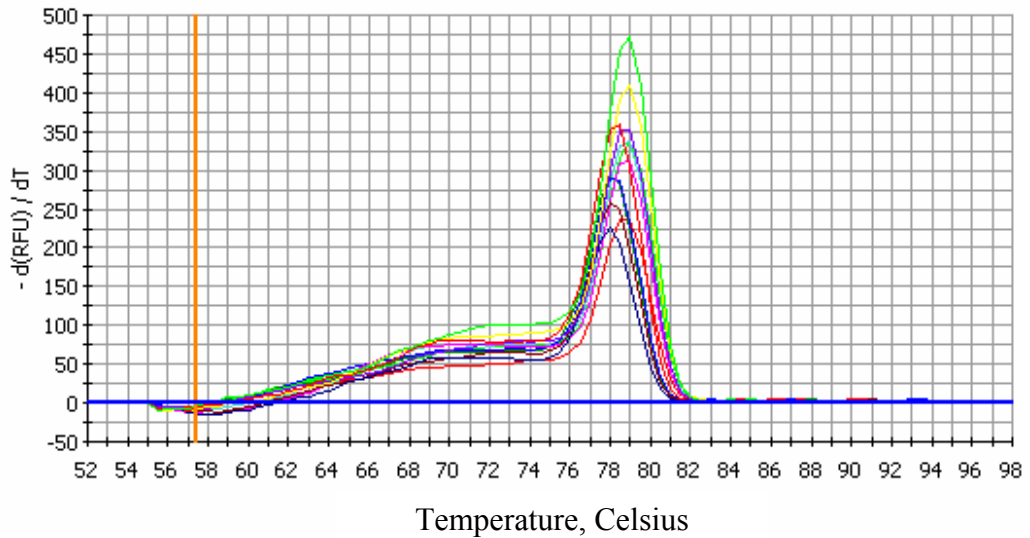
Figure 9: Melt Curve analysis for primer dimerization. A melt curve of a representative Nrf2 amplification reaction. The single peak represents one amplicon with a distinct melting temperature T_m. The DNA synthesis is detected through dsDNA intercalation of the dye SYBR green. Little binding was present at 68-72°C, showing no primer dimerization.

1.4.4 – Primer Annealing Temperature: The last of the optimization experiments was an analysis of the annealing temperature. This consisted of running identical reactions using control cDNA at different temperatures and the temperature gradient function on the MyIQ real time unit. This tests annealing temperatures across a 20°C range, 10 degrees above and 10 below the designed annealing temperatures. As a rule of thumb, the temperature with the lowest Ct was chosen as the ideal temperature for the reaction to proceed.

1.4.5 – Real-Time PCR: Once primer and RNA quality was assessed, real-time PCR analysis of the ARE-containing genes was performed. H9c2 cells were treated with tBHQ and RNA isolated at time points of 0, 4, 8, 12, 24, 36, 48 and 72 hours. Expression of heme oxygenase 1 (HO1) and NADPH:quinone oxidoreductase 1 (NQO1) as well as the two housekeeping genes, glyceraldehyde 3-phosphate dehydrogenase

56

(GAPDH) and acidic ribosomal phosphoprotein Po (Arbp) were measured in duplicate on the myIQ iCycler real-time PCR detection system. No change was detected in housekeeping gene expression. The reaction mixture (conditions described in section 1.3.3) was as follows; 13 μl SYBR green supermix, 10 μl nuclease-free H_2O, 1 μl of 5 μM primer mix (both sense and antisense suspended in 1X TE buffer) and 1 μl experimental cDNA. The thermocycler program was as follows: an initial denaturation at 94°C for 2 minutes, followed by 35 cycles of 94°C for 15 seconds, 60°C for 30 seconds and 68°C for 1 minute. Each experiment was performed three to five times in duplicate and a cDNA-free sample (blank) was run with each primer to ensure contamination was not present.

1.4.6 – Real-Time PCR Analysis: Changes in gene expression of the ARE-containing genes HO1 and NQO1 were calculated relative to the gene expression at time zero. Matched-time vehicle-treated controls were checked prior to these experiments to verify no change in expression levels over time. The modified ΔΔCt method as described by Vandesompele *et. al* (292) was programmed into a Microsoft Excel macro (Bio-Rad) and used for analyses of gene expression. This method was modified from the ΔΔCt method described in Livak and Schmittgen in 2001 (190) and uses complex algorithms that allow for use of multiple housekeeping genes.

2 – Effects of tBHQ on protein expression of HO1 and NQO1 in the H9c2 cell line.

2.1 – Cell Culture:

H9c2 cells were plated in 10 cm dishes and grown to 80% confluence as described in section 1.1. Cells were treated with 10 μM tBHQ or its vehicle for 12 and 24 hours. Experiments were repeated four times in duplicate

2.2 – Preparation of Whole Cell Lysates:

At each time point the medium was aspirated, dishes were placed on ice and 1 ml of ice-cold HBSS was added to each plate. Cells were scraped into pre-chilled 1.5 ml centrifuge tubes, centrifuged at 500 x g for 5 minutes at 4°C, the supernatant was aspirated, and cell pellets were resuspended in 100 μl radioimmunoprecipitation (RIPA) lysis buffer (KH_2PO_4 10.6 mmoles/L, NaCl 1.5 moles/L, $Na_2HPO_4.7H_2O$ 29.7 mmoles/L, 1% Igepal, 0.5% sodium deoxycholate, 0.1% SDS, supplemented with 100 μg/ml PMSF, 50 KIU/ml apoprotin and 100 μl/ml of sodium orthovanadate), triturated through 100 μl pipette tip and centrifuged at 10,000 x g at 4°C for 15 minutes. The pellet was discarded and the supernatant was stored at -20°C until further analysis.

2.3 – Determination of Protein Concentration:

Protein concentration was determined using the DC protein assay (Bio-Rad), a colorimetric assay modified from *Bradford, 1976* (23). A standard curve was generated using BSA at concentrations ranging from 0.1 to 1.5 μg/μl. The absorbance was measured at 750 nm on a SpectraMax Plus microplate reader (Molecular Devices Corp.,

Palo Alto, CA). Sample protein concentrations were determined based on the generated

standard curve.

2.4 – Western Blot:

Cell lysate samples were standardized to 20 μg protein and boiled in equal

volumes of Laemmli buffer (BioRad) containing 5% β-mercaptoethanol for 5 minutes.

Samples were separated in a 12% total monomer polyacrylamide gel in the presence of

sodium dodecyle sulfate (SDS) polyacrylamide gel electrophoresis (SDS-PAGE).

Following procedures for SDS-PAGE, the gel was then transferred electrophoretically to

a nitrocellulose membrane. Membranes were blocked at room temperature in 5% non-fat

dry milk in 1X TBS-T (20 mM Tris, 137 mM NaCl, pH 7.6; and 0.1% Tween 20) for 1

hour. Membranes were incubated with rabbit IgG anti-heme oxygenase 1 (HO1) primary

antibody or goat IgG anti–NADPH:quinone oxidoreductase 1 (NQO1) primary antibody

(1:3000 dilution) in 5% milk overnight at 4°C. Membranes were then washed three times

for five minutes each with 1X TBS-T, and incubated in 5% milk containing either goat

anti-rabbit IgG: horseradish peroxidase (HRP) conjugated secondary antibody or rabbit

anti-goat conjugated IgG:HRP conjugated secondary antibody (1:5,000 dilution) at room

temperature for 1 hour. Membranes were washed five times for five minutes each with

1X TBS-T, and immunoreactive bands were detected by chemiluminescence using the

ECL Plus Western Blotting Detection System on a FluorS Multi Imaging System (Bio-

Rad). Densities of the resulting bands were quantified using Quantity One software (Bio-

Rad). Each western blot was performed twice to account for inter-assay variation.

3 –The effect of tBHQ on nuclear translocation of the transcription factor Nrf2.

3.1 – Cell culture:

H9c2 cells were plated in 10 cm dishes and grown to 80% confluence as described in section 1.1, and treated with t-BHQ (10 μM) or vehicle for 15 minutes.

3.2 – Cytoplasmic and nuclear extractions:

Cytoplasmic and nuclear extracts were isolated using the NE-PER Nuclear Extraction Kit (PIERCE Biotechnology, Rockford, IL). Cells were scraped into 1 ml of HBSS and centrifuged for 5 minutes at 1000 x g at room temperature. The cell pellet was then resuspended in 100 μl of cytoplasmic extraction reagent (CER) I (proprietary recipe supplemented with 100 μg/ml Phenylmethanesulfonyl fluoride (PMSF), 50 KIU/ml apoprotin and 100 μl/ml of sodium orthovanadate), vortexed vigorously for 15 seconds and incubated on ice for 10 minutes. CERII buffer (5.5 μl) was added, the sample was vortexed and the cytoplasmic fraction separated from the nuclear fraction by centrifugation at 15,000 x g for 5 minutes at 4°C. The supernatant (cytoplasm) was separated from the pellet (nucleus) and transferred to a pre-chilled tube. Nuclei were then lysed with the addition of 50 μl of the Nuclear Extraction Reagent (NER; supplemented with 100 μg/ml PMSF, 50 KIU/ml apoprotin and 100 μl/ml of sodium orthovanadate), followed by four repeats of vortexing and incubation on ice for 10 minutes. Samples were centrifuged at 16,000 x g at 4°C for 10 min and the supernatant was stored at -80°C until use.

3.3 – Western Blot for Nrf2:

Protein concentrations were determined as described in section 2.3. Western blot protocol was as described in section 2.4. Rabbit anti-goat Nuclear factor E2 like 2 (Nrf2) primary antibody was used at a 1:1000 dilution, and goat anti-rabbit IgG:HRP conjugated secondary antibody was used at 1:5000 dilution. Each sample was also probed with antibodies for β-tubulin to assess contamination from the cytoplasmic fraction into the nuclear fraction.

4 –Reactive oxygen species generation produced by the oxidant tert-butyl hydroperoxide.

4.1 – Measurement of Intracellular ROS generation using microscopy:

Intracellular reactive oxygen species (ROS) levels were determined using the Image-it Live Green ROS detection kit (Molecular Probes) (200). This protocol uses the fluorescent probe, 5-(and 6)-carboxy-2',7'-dichlorodihydrofluorescein diacetate (carboxy-H_2DCFDA), a cell permeant dye that enters the cell and is cleaved by cellular esterases to the non-cell permeant non-fluorescent H_2DCF. H_2DCF is oxidized by ROS to the green fluorescent compound carboxy-DCF that can be detected by fluorescent microscopy.

H9c2 cells were plated on electrically charged cover slips (Fisher Scientific, Pittsburg, PA), and grown to 80% confluence. Cells were then treated in duplicate with tBHQ (10 μM) or its vehicle for 24 hrs. After 24 hours, tert butyl hydroperoxide (tBHP, 100 μM), an organic peroxide, or its vehicle was added for 2 hours. The cells were washed with 1 ml HBSS with calcium and magnesium and labeled with 25 μM carboxy-

H$_2$DCFDA in HBSS with calcium and magnesium for 30 min at 37°C in the dark. During the last five minutes, the nuclei were stained with the blue-fluorescent cell permeant nucleic acid stain Hoechst 33342 (1 μM). Cells were then washed five times with 1 ml HBSS with calcium and magnesium and coverslips mounted upside down on glass slides for ROS to be visualized in a double blind fashion using 40X magnification at Ex/Em 495/529 nm (green) and 350/461 (blue) on a Nikon 2000E fluorescence microscope. Images were merged and saved as JPEG files. Each experiments was repeated four times in duplicate.

4.2 – Measurement of Intracellular ROS generation using a microplate reader:

H9c2 cells were plated in 10 cm dishes and grown to 80% confluence as described in section 1.1. Cells were then treated in duplicate with tBHQ (10 μM) or its vehicle for 24 hrs. After 24 hours, tBHP (100 μM) or its vehicle was added for 2 hours. The cells were washed with 5 ml HBSS with calcium and magnesium, trypsinized and centrifuged at 500 x g for 5 minutes at room temperature. The supernatant was removed and cells were resuspended in 250 μl of carboxy-H$_2$DCFDA (25 μM) in HBSS with calcium and magnesium for 30 minutes at 37°C in the dark. Each sample was washed once with 200 μl HBSS with calcium and magnesium, centrifuged at 500 x g for 5 minutes at room temperature, resuspended in 1 ml phenol red-free phosphate buffered saline (PBS) and counted (as described in section 1.1). Cells were added to black 96 well plates at a density of 50,000 cells per well in a volume of 200 μl. Plates were then read on a Fusion Universal microplate analyzer (Packard Instruments, Meriden, CT) at

excitation and emission wavelengths of 480 nm and 530 nm, respectively. Each experiments was repeated four times in duplicate.

5 – Effects of Nrf2 siRNA treatment on the protective effects of tBHQ.

5.1 – RNA interference:

RNA interference (RNAi) is a pathway in cellular defense against viral infection and transposons as well as functions as a method for post-transcriptional modification (100, 204, 262, 290, 307). It has recently been utilized as a unique form of post-translational gene silencing post-transcriptionally. The mechanism of RNAi starts with dsRNA that is recognized by the protein Dicer, which cleaves dsRNA into smaller (73, 169, 215) dsRNA fragments (19, 73, 74, 98). These fragments are then unwound and separated by the multi-protein RNA-Induced Silencing Complex (RISC) resulting in a single strand RNA-RISC complex (33, 99, 118, 225). The RNA-RISC complex binds to the target mRNA using the RNA as a probe and the RNA-RISC complex cleaves the mRNA in a site-specific manner. The cleaved products are then released and degraded, leaving the RNA-RISC complex to seek out more copies of the target mRNA and deplete the remaining pool of target mRNAs, resulting in gene knockdown (Figure 10) (73).
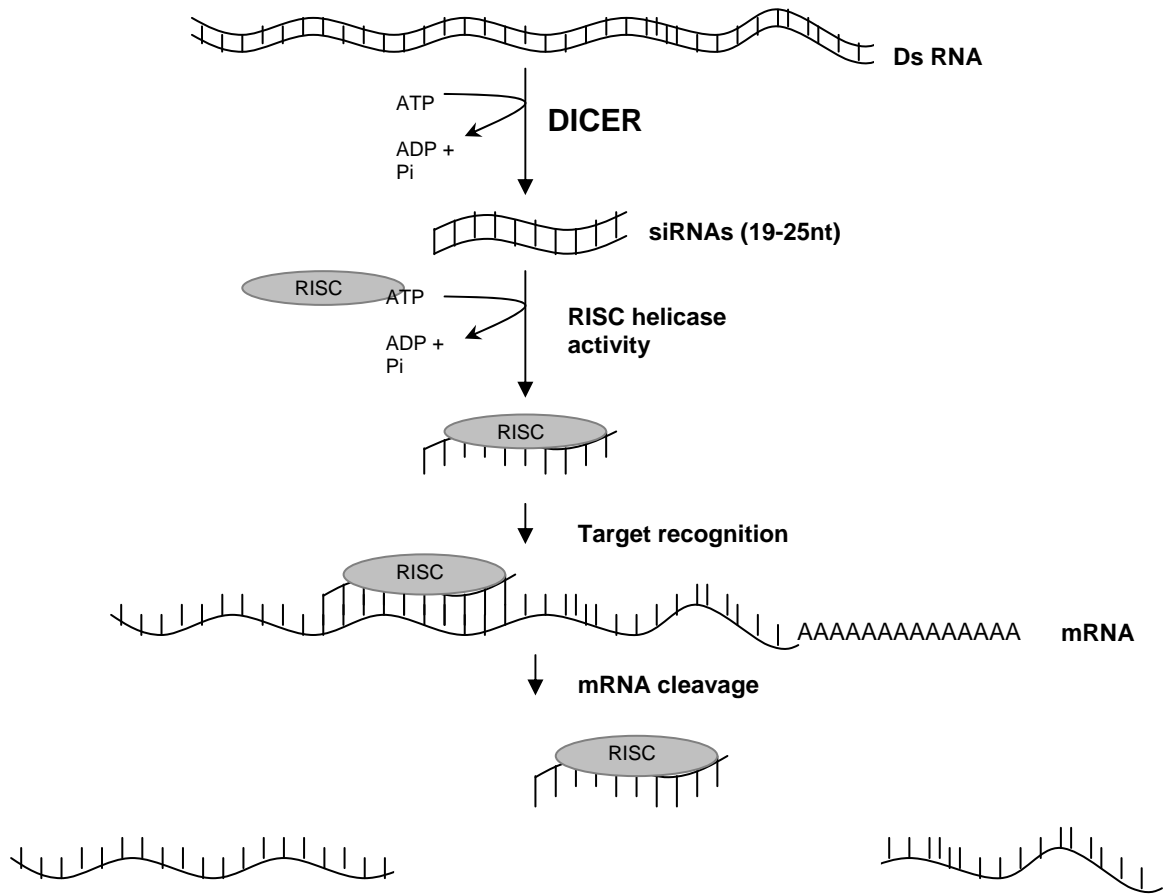
Figure 10: RNA interference. RNAi starts in the presence of dsRNA. dsRNA is recognized by the protein Dicer and cleaved into smaller (19-25nt) dsRNA fragments. These fragments are then unwound and separated by the multi-protein RNA-Induced Silencing Complex (RISC) resulting in a single strand RNA-RISC complex. This complex is then guided by the single strand of RNA to the target mRNA where it binds via complementarity and the mRNA undergoes site-specific cleavage.

A successful transfection of siRNAs is vital to investigating a biological role associated with gene silencing. For this reason, RNAi technology was validated using siTOX transfection control (Invitrogen). SiTOX is a cytotoxic, RNA-based reagent that is used to optimize transfection efficiencies. In addition, a positive control siRNA directed against the housekeeping gene glyceraldehyde 3-phosphate dehydrogenase

64

(GAPDH) was used determine knockdown efficiency. To ensure that the siRNAs did not stimulate the antiviral interferon response, we measured the gene expression of a member of the antiviral response, 2'-5'-oligoadelylate synthetase (OAS2) (55), using real-time PCR in nonsense and siRNA transfected H9c2 cells.

5.2 – siRNA transfection efficiency:

As mentioned on the previous page, transfection efficiency of the siRNAs was assessed by the siTOX transfection control (Dharmacon). Cells were grown to 25% confluence and treated with the proprietary siTOX RNA based cytotoxic agent. This agent results in cell death within 48 hours and correlates with transfection efficiency. H9c2 cells were plated at 50% confluence and treated with siTOX siRNA transfection control or nonsense siRNA. Cell survival after siTOX treatment was determined using the cell proliferation assay in duplicate (section 5.6.1) and transfection efficiency was found to be 42%. This experiment was repeated 3 times.

5.3 – Nrf2 siRNA treatment:

H9c2 Cells were plated in antibiotic-free low glucose (5.5 mM) DMEM supplemented with 10% fetal bovine serum at a density of 3×10^5 cells per 24 well plate. The cells were incubated overnight in normal growth conditions. The next day, cells were treated with 40 pmoles of all three non-overlapping Stealth™ (Invitrogen) siRNAs directed against rat Nrf2 (Accession number NM_031789) or nonsense GC matched siRNAs (proprietary sequence) and delivered by Lipofectamine 2000 (Invitrogen) in OptiMEM medium (Invitrogen). Lipofectamine transfection reagent utilizes cationic

lipid-mediated transfection where siRNAs interact with the cell membrane in the form of a lipid:siRNA complex. This detergent-like structure is partially hydrophobic and hydrophilic, and enters the cell through endocytosis (11). The siRNAs (Table 3) were prepared in a 1:50 dilution of 20 μM in OptiMEM (6 well plate: 10 μl each siRNA into 500 μl OptiMEM per well), and lipofectamine was prepared in a 1:100 dilution in OptiMEM medium (5 μl lipofectamine per 500 μl of OptiMEM per well) and incubated at room temperature for 5 minutes. Equal volumes of lipofectamine and siRNA mixtures (500 μl of RNA mixture + 500 μl of lipofectamine mixture per well of six well plate) were then combined and incubated for another 20 minutes at room temperature. The RNA/lipofectamine mixture was then added to the cells in addition to 1 ml of full growth medium (1 ml per well of six well plate) and incubated over night. Medium was changed 12 hours later to normal full growth medium containing antibiotic.

Table 3: siRNA sequences.

Nrf2 siRNAs	UUUAAGUGGCCCAAGUCUUGCUCCA
	UGGAGCAAGACUUGGGCCACUUAAA
	UACUCACUGGGAGAGUAAGGUUUCC
	GGAAACCUUACUCUCCCAGUGAGUA
	UGAAGGUUCGGUUACCAUCCUGCGA
Keap1 siRNAs	UGAAGGUUCGGUUACCAUCCUGCGA
	UCGCAGCAUGGUAACCGAAACUUCA
	CUGUCAAUCUGGUACAUGACUGCCC
	GGGCAGUCAUGUACCAGAUUGACAG
	AUUUGACCCAGUGGAUGCACGCAUG
	CAUGAGUGCAUCGACUGGGUCAAAU

5.4 – siRNA knockdown verification:

 After treatment with siRNAs, cells were incubated for a total of 64 hours and subsequently treated with tBHQ (10 µM) or its vehicle for 8 hours. To verify gene knockdown, mRNA and protein levels for Nrf2 and Keap1 were measured and repeated in three independent experiments. Immunoblots for Nrf2 protein expression were preformed as described in section 3.3 and repeated in three independent experiments. Nrf2 gene expression was determined using conventional (section 1.3.3) and real-time PCR (section 1.3.5) and repeated in three independent experiments. As mentioned previously, siRNAs mediated activation of the interferon (antiviral response) response was not detected using real-time PCR of 2'–5'-oligoadenylate synthetase (OAS2) (table 2) (55).

5.5 –ROS generation in Nrf2 siRNA treated H9c2 cells in response to tBHP:

 To determine the effect of Nrf2 on ROS production in the H9c2 cell line, cells were treated as described above with Nrf2 siRNAs, incubated for 48 hours and subsequently treated with tBHQ (10 µM) or its vehicle for 24 hours. Cells were then challenged with either 100 µM tBHP or 200 µM H_2O_2 for 2 hours. Cells were trypsinised for 5 minutes, pelleted by centrifugation at 500 x g for 5 minutes at room temperature, and resuspended in HBSS containing carboxy-H_2DCFDA (25 µM) without Ca^{++} and Mg^{++}. Cells were incubated in the dark for 30 minutes at 37°C. Cells were then pelleted, washed in HBSS, counted using a hemocytometer (as described in section 1.1), and 50,000 cells were resuspended in 200 µl of PBS without phenol red, plated per well of a black 96 well plate and read on a Fusion universal microplate analyzer at excitation

and emission wavelengths of 480 nm and 530 nm, respectively. Experiments were repeated three times and performed in duplicate.

5.6 – Effect of oxidative stress on H9c2 cell survival following Nrf2 knockdown:

To determine the effect of Nrf2 on cell survival in response to H_2O_2 and tBHP, cells were treated as described above with Nrf2 siRNAs, incubated for a total of 48 hours and subsequently treated with tBHQ (10 μM) or its vehicle for 24 hours. Cells were challenged with either tBHP (100 μM) or H_2O_2 (200 μM) or their vehicle and incubated for 48 hours. Medium was aspirated and cells were immediately frozen and stored at -80°C. Control cells were counted, pelleted by centrifugation and stored at -80°C for the standard curve.

5.6.1 – Cell Proliferation Assay: The CyQUANT Cell Proliferation Assay Kit was used to estimate cell number. The kit utilizes CyQUANT GR, a green fluorescent dye, which fluoresces when bound to nucleic acids. Fluorescence from the DNA-bound dye is directly proportional to cell number and a standard curve was generated using control cells relating fluorescence to cell number. The standard curve is linear from 50 to 50,000 cells. A representative standard curve can be found in appendix D. Cell lysates from experimental samples and control cells for the standard curve were thawed to room temperature and resuspended in 500 μl lysis buffer containing the fluorescent dye CyQUANT GR (working lysis buffer). Control cells were also thawed and resuspended in the working lysis buffer. Samples were transferred in duplicate to a black 96-well plate (200 μl/well) and read on a Fusion Universal Microplate Analyzer at excitation and emission wavelengths of 480 nm and 530 nm.

68

6 – Effects of Keap1 siRNA treatment on the protective effects of tBHQ.

6.1 – Keap1 siRNA treatment:

H9c2 cells were plated in antibiotic-free low glucose (5.5 mM) DMEM supplemented with 10% fetal bovine serum at a density of 3 x 10^5 cells per plate. The cells were incubated overnight in normal growth conditions. The next day, H9c2 cells were treated with 40 pmoles of three non-overlapping Stealth^{TM} (Invitrogen) siRNAs directed against rat Keap1 (Accession number NM_057152) or nonsense GC matched siRNAs and delivered by Lipofectamine 2000 (Invitrogen) in OptiMEM medium (Invitrogen) (Table 3). SiRNAs were prepared in a 1:50 dilution in OptiMEM (6 well plate: 10 μl each siRNA into 500 μl OptiMEM per well), and lipofectamine was prepared in a 1:100 dilution in OptiMEM medium (5 μl lipofectamine per 500 μl of OptiMEM per well) and incubated at room temperature for 5 minutes. Equal volumes of lipofectamine and siRNA mixtures (500 μl of RNA mixture + 500 μl of lipofectamine mixture per well of six well plate) were then combined and incubated for another 20 minutes at room temperature. The RNA/lipofectamine mixture was then added to the cells in addition to 1ml of full growth medium (1 ml per well of six well plate) and incubated over night. Medium was changed 12 hours later to normal full growth medium-containing antibiotic.

6.2– siRNA knockdown verification:

After treatment with siRNAs, cells were incubated for 64 hours and subsequently treated with tBHQ (10 μM) or its vehicle for 8 hours. In the absence of Keap1, tBHQ treatment should have little effect on ARE gene transcription, as Nrf2 would already be activated. To verify gene knockdown of Keap1, mRNA and protein levels were

69

measured. Immunoblots for Keap1 protein expression were preformed as described in section 3.3 using primary Keap1 IgG (1:250 dilution) and secondary antibody rabbit anti-goat IgG:HRP (1:5000 dilution). Keap1 gene expression was determined using conventional (section 1.3.3) and real-time PCR (section 1.3.5). To ensure the siRNAs did not activate the interferon (antiviral) response, real-time PCR of 2'–5'-oligoadenylate synthetase (OAS2) was performed. Experiments were repeated three times and performed in duplicate.

6.3 – Effect of Oxidative Stress on cell survival following Keap1 Knockdown.

After treatment with siRNAs for Keap1, H9c2 cells were then incubated for a total of 48 hours and subsequently treated with tBHQ (10 μM) or its vehicle for 24 hours. Cells were then challenged with either tBHP (100 μM) or H_2O_2 (200 μM) and incubated for an additional 48 hours. Medium was aspirated and cells were immediately frozen and stored at -80°C. Control cells were counted pelleted by centrifugation and stored at -80°C for the standard curve. Cell proliferation was assessed using the CyQUANT Cell Proliferation Assay Kit to quantify cell survival as described in section 5.5.1.

7 – The effect of Nrf2 overexpression in the H9c2 cell line.

7.1 – Transfection of the H9c2 cells with Nrf2.

The vector encoding Nrf2 tagged with green fluorescent protein (Nrf2-GFP) was a generous gift from Manabu Furukawa at the University of Nebraska, and was used in studies published by Furukawa *et al.* in 2005 (89). H9c2 cells were grown to 80% confluence and transfected with 0.5 μg DNA containing Nrf2-GFP or empty vector

pcDNA 3.1 (p3.1), the same vector containing the Nrf2 construct.   DNA was diluted in 500 μM OptiMEM and lipofectamine was prepared in a 1:100 dilution in OptiMEM medium 5 μl lipofectamine per 500 μl of OptiMEM) and incubated at room temperature for 5 minutes. Equal volumes of lipofectamine and DNA mixtures were then combined and incubated for another 20 minutes at room temperature.   The DNA/lipofectamine mixture was then added to the cells in addition to 1ml of full growth medium and incubated over night. Medium was changed 12 hours later to normal full growth medium containing antibiotic.

7.2 – Nrf2 overexpression verification.

H9c2 cells were transfected with both Nrf2-GFP and p3.1 as described in section 7.1 and RNA was isolated 48 hours later as described in section 1.3.   cDNA was generated and real-time PCR was performed using primers for HO1, NQO1 and Nrf2 as described in sections 1.4.   Protein levels of Nrf2 were verified by western blot as described in section 3.3.

7.3 – Subcellular localization of Nrf2-GFP.

Cells were plated and transfected as described in the previous section. Cells were then passaged and grown to 80% confluence on electrically charged cover slips (Fisher Scientific, Pittsburg, PA). Cells were treated with tBHQ (10 μM) or vehicle for 1 hour and then coverslips were placed upside down onto glass slides.   Cells were then visualized using a 40X magnification at Ex/Em 495/529 nm (green) and 350/461 nm (blue) on a Nikon 2000E fluorescence microscope.   Images were saved as JPEG files.

7.4 – The effect of Nrf2 overexpression on cell survival in response to H₂O₂ and tBHP.

H9c2 cells were transfected with both Nrf2-GFP and p3.1 as described in section 7.1 and passaged into 6 identical wells of a 24 well plate. The next day cells were treated with tBHQ (10 μM) for 24 hours. Cells were then challenged with H_2O_2 (200 μM) and tBHP (100 μM) and grown for 48 hours. The cell medium was then removed and the cell culture plate was frozen at -80°C. Cell survival was assessed by the cell proliferation assay as described in section 5.6.1.

8 – Experimental Design

8.1 – Gene Expression. H9c2 cells treated with tBHQ (10 μM) or vehicle and at each time point RNA was isolated. Sample quality was verified, quantified and reverse transcribed. Real-time PCR was performed on each sample in duplicate. Each experiment was repeated three times.

8.2 – Protein Expression. H9c2 cells were treated with vehicle and tBHQ (10 μM) for 12 and 24 hours. Sample protein content normalized and western Blot analysis was performed in duplicate. Each experiment was repeated four times.

8.3 - Nuclear Translocation. H9c2 cells were treated for 15 minutes with tBHQ (10 μM) and nuclear and cytoplasmic compartments separated by differential centrifugation.

Sample protein content was normalized and western Blot analysis was performed in duplicate. Each experiment was repeated three times.

8.4 - ROS generation. H9c2 cells were treated with vehicle, tBHP (100 µM), tBHQ (10 µM), tBHQ (10 µM) + tBHP (10 µM) in duplicate. ROS generation was measured using the green fluorescent dye carboxy-H2DCFDA and cell nuclei were marked by DAPI staining. Each experiment was repeated 4 times.

8.5 – ROS generation of Nrf2 transfected cells. H9c2 cells transfected with siRNAs directed against Nrf2 or GC matched siRNAs. Both sets of siRNA transfected cells were treated with vehicle, tBHP (100 µM), tBHQ (10 µM), tBHP (100 µM) and ROS generation measured using the dye carboxy-H2DCFDA on the fluorescence plate reader. Each experiment was repeated three times.

8.6 – Cell survival of Nrf2 transfected cells. H9c2 cells transfected with nonsense or Nrf2 siRNAs. Both sets of siRNA transfected cells were treated with vehicle, H_2O_2 (200 µM), tBHP (100 µM), tBHQ (10 µM), tBHQ (10 µM) + tBHP (100 µM) and tBHQ (100 µM) + H_2O_2 (200 µM) and cell survival was measured using cell proliferation assay. Each experiment was repeated six times.

8.7 – Cell survival of Keap1 siRNA transfected cells. H9c2 cells transfected with nonsense and Keap1 siRNAs. Following transfection cells were treated with vehicle, H_2O_2 (200 µM), tBHP (100 µM), tBHQ (10 µM), tBHQ (10 µM) + tBHP (100 µM) and

tBHQ (100 μM) + H_2O_2 (200 μM) and cell survival was measured using cell proliferation assay. Each experiment was repeated three times.

8.8 – Nuclear localization of Nrf2-GFP. H9c2 cells were transfected with p3.1 or Nrf2-GFP. Following transfection cells were treated with tBHQ or vehicle for 12 hour. Cells were then visualized by fluorescence microscopy.

8.9 – Cell survival of Nrf2 transfected cells. H9c2 cells were transfected with p3.1 or Nrf2-GFP. Following transfection, cells were treated in duplicate with vehicle, H_2O_2 (200 μM), tBHP (100 μM), tBHQ (10 μM), tBHQ (10 μM) + tBHP (100 μM) and tBHQ (100 μM) + H_2O_2 (200 μM). Cell survival was measured using cell proliferation assay and this experiment was repeated three times.

9 – Statistical Analysis

All statistical procedures were conducted using Minitab (State College, PA). A paired t-test was used when samples were paired with a control. For example, the western blots for both HO1 and NQO1 were compared to time-specific vehicle-treated control. Differences between groups were assessed using a one-way ANOVA for multiple comparisons. Where differences were observed, a Tukey-Kramer *post-hoc* test was used. Statistical significance was set at $p < 0.05$. In real-time PCR experiments, significance cannot be assessed due to the constraints of the gene expression MACRO. Using this MACRO the expression of the control samples is automatically set to 1, preventing statistical analysis. However, the MACRO does assign a standard deviation to

the control samples and through comparisons of standard deviations one can assess significance.

RESULTS

tBHQ- induced increase in HO1 and NQO1 gene expression:

It has been reported that heme oxygenase 1 (HO1) and NADPH oxidoreductase 1 (NQO1) gene expression are regulated by the transcription factor Nrf2 after oxidative stress (3, 64, 124). Therefore we examined whether the expression of the antioxidant enzymes HO1 and NQO1 increased after treatment with the Nrf2 activator tBHQ (149, 165). H9c2 cells were treated with tert-butyl hydroquinone (tBHQ) (10 μM) for 0, 4, 8, 12, 24 and 48 hours and RNA was isolated. Basal gene expression of HO1 and NQO1 did not change in vehicle-treated cells over a 48 hour period (data not shown). tBHQ (10 μM) caused a significant ($p > 0.05$) increase in both HO1 and NQO1 gene expression by 4 hours and each peaked at 8 hours (Figure 11). tBHQ caused a 7.6 +/- 0.5 fold and a 4.4 +/- 0.5 fold increase in expression at 8 hours compared to vehicle treated cells for HO1 and NQO1, respectively. By 48 hours, HO1 and NQO1 expression was not significantly different from the control. These data suggest that Nrf2 activation by tBHQ treatment resulted in increased transcription of the ARE-containing genes HO1 and NQO1.

76
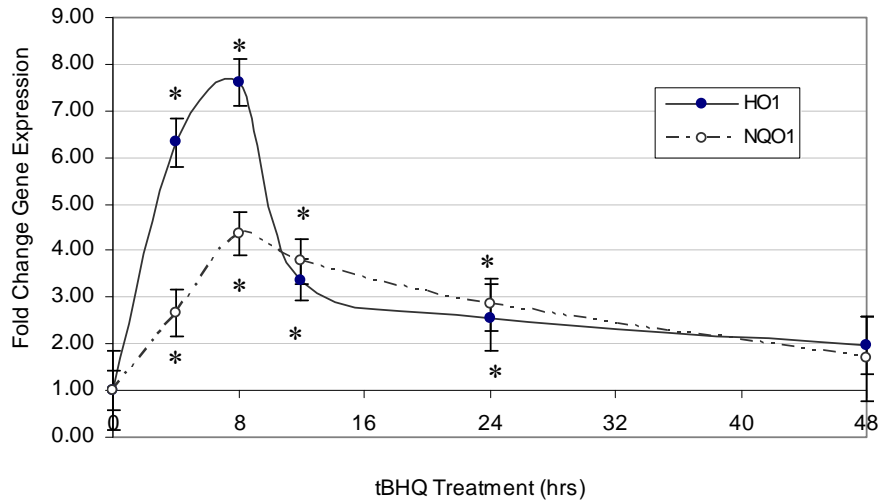
Figure 11. Effect of tBHQ ($10\mu M$) on the expression of HO1 and NQO1. Cells were treated with tBHQ for up to 48 hrs and HO1 and NQO1 gene expression was measured by real time RT-PCR (n=3 independent experiments). Solid circle and line indicates HO1 gene expression. Open circle dotted line indicates NQO1 gene expression. Each time point is normalized to 2 housekeeping genes, glyceraldehyde 3-phosphate dehydrogenase (GAPDH) and acidic ribophosphoprotein (Abrp). Error bars represent standard error. * Indicates significantly different from vehicle treatment at indicated time-point ($p<0.05$).

tBHQ-induced increase in HO1 and NQO1 protein expression:

To verify that HO1 and NQO1 protein levels increased after tBHQ treatment, HO1 and NQO1 immunoreactivity after tBHQ treatment was measured. Cells were treated with tBHQ (10 µM) or vehicle for 12 and 24 hours, lysed and normalized for total protein. Basal levels of HO1 and NQO1 were detected in the lysate of vehicle treated cells. tBHQ significantly ($p > 0.05$) increased the expression of HO1 1.3 ± 0.1 fold after 12 hours and 1.9 ± 0.1 fold after 24 hours relative to vehicle-treated cells (Figure 12.B), whereas the increase in NQO1 expression was only significant at 24 hrs. tBHQ increased NQO1 expression 1.4 ± 0.1 fold after 12 hours and 1.8 ± 0.2 fold after 24 hours relative to vehicle-treated cells (Figure 12.A). These data suggest that tBHQ increases HO1 and NQO1 translation.
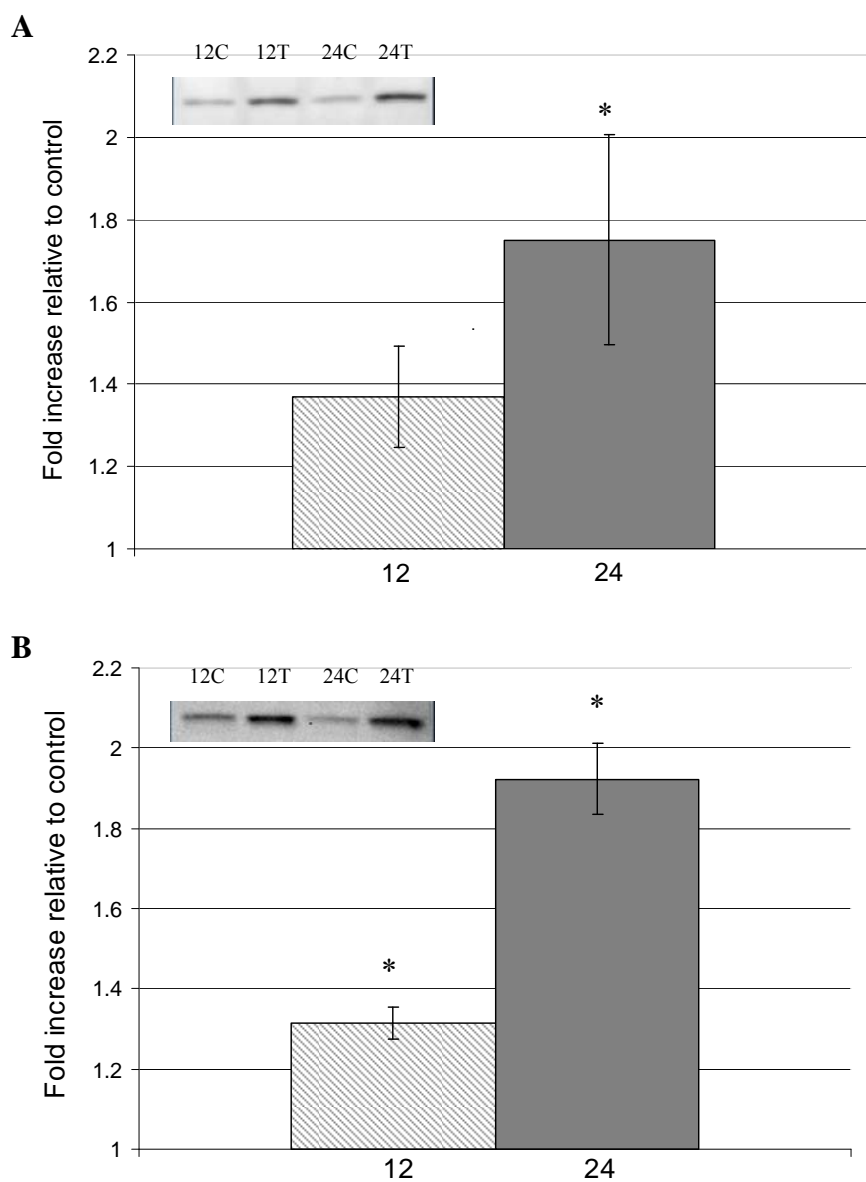
Figure 12. Effect of tBHQ on protein levels of **A)** heme oxygenase-1 (HO1) and **B)** NAD(P)H:quinone oxidoreductase 1 (NQO1) immunoreactivity after 12 and 24 hour treatment (n=4 independent experiments). Protein levels were measured with specific antibodies for HO1 and NQO1 and data are expressed as fold increase compared to vehicle treatment for the same time point. Inlays are a representative western blot. Error bars represent standard error. * Indicates significantly different from vehicle treatment at indicated time-point (p<0.05).

Nrf2 translocation into the nucleus after treatment with tBHQ:

The transcription factor Nrf2 is sequestered and subsequently degraded in the cytoplasm in non-stressed cells (89). Upon activation, Nrf2 is released from Keap1 and translocates into the nucleus, increasing expression of ARE-driven genes. To determine whether treatment with tBHQ activates Nrf2 and causes its translocation from the cytoplasm to the nucleus, cells were treated with tBHQ and cytoplasmic and nuclear fractions were analyzed for Nrf2 immunoreactivity. Nrf2 immunoreactivity was detected in the cytoplasm at time zero of treatment and did not change after 15 minutes treatment with tBHQ. Nrf2 immunoreactivity was also detected at time zero in the nuclear fraction and its content increased significantly after treatment with tBHQ for 15 minutes. β-tubulin was used as a cytosolic marker and was detected in the cytosolic fraction but not the nuclear fraction. We also measured cytoplasmic and nuclear after tBHQ treatment for up to 8 hours. Nrf2 levels increased in both cytoplasmic and nuclear compartments in response to tBHQ treatment compared to time zero with, cytoplasmic Nrf2 levels remaining elevated 8 hours after tBHQ treatment. In the nuclear extract Nrf2 levels returned to basal levels by four hours of tBHQ treatment (Figure 13.C). These data suggest that tBHQ treatment activates Nrf2 and causes its translocation from the cytoplasm to the nucleus.
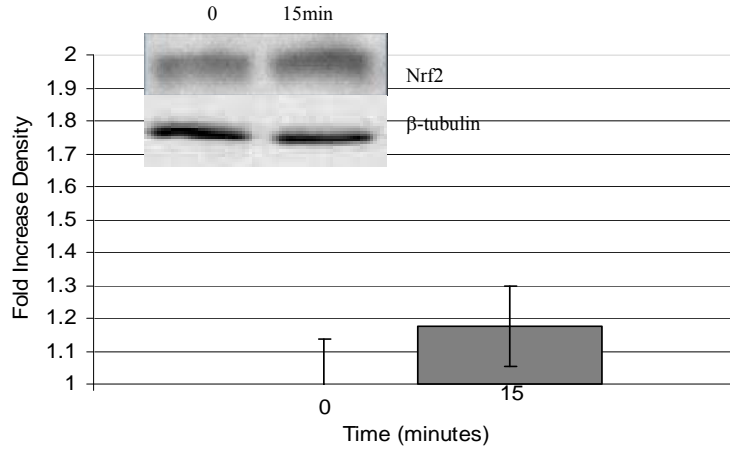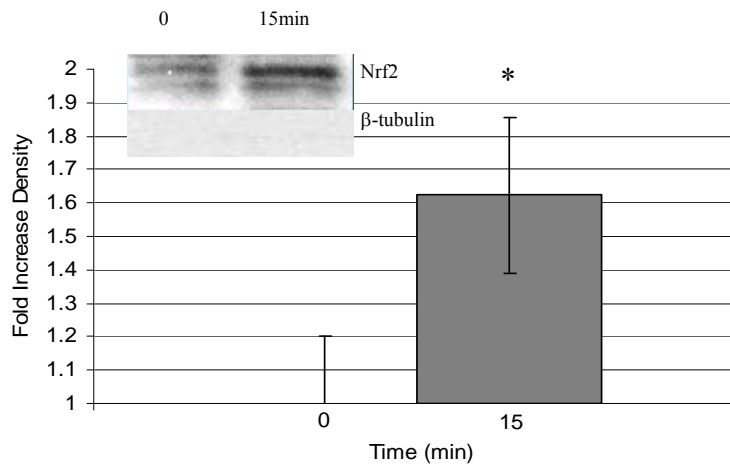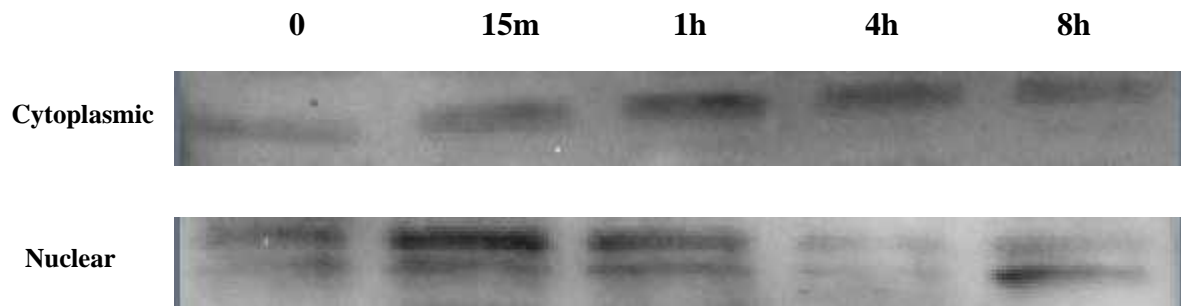
Figure 13. Effect of tBHQ on Nrf2 protein expression in **A)** cytoplasmic and **B)** nuclear compartments (n=4 independent experiments). Cells were treated for 15 minutes with tBHQ (10 μM) and Nrf2 immunoreactivity was measured in the cytoplasmic and nuclear fractions. Protein levels were normalized and data are expressed as fold increase compared to vehicle treatment for the same time point. Inlays are a representative western blot. Error bars represent standard error. β-tubulin was used as a cytosolic marker. * Indicates significantly different from 0 time point ($p < 0.05$) **C)** Nrf2 levels after treatment with tBHQ (10 μM) in the cytoplasmic and nuclear extracts (Representative figure of three independent experiments).

81

Nrf2 siRNA treatment attenuates HO1 and NQO1 expression:

To determine the role of Nrf2 in mediating the expression of ARE-driven genes in response to tBHQ, a set of three Stealth[TM] RNAi directed against rat Nrf2 to knockdown Nrf2 were used. Treatment of H9c2 cells with the Nrf2 siRNAs for 12 hours decreased Nrf2 mRNA expression by 80% as compared to cells treated with nonsense (NS) siRNAs. In Nrf2 knockdown cells treated with tBHQ (10 μM) for 12 hours there was also an 80% suppression of Nrf2 mRNA expression (Figure 14.A & B). Similarly, Nrf2 protein levels were also reduced following Nrf2 siRNA treatment for 12 hours (Figure 14.C).

Next whether Nrf2 siRNA treatment altered expression of the ARE-containing genes HO1 and NQO1 was examined. Basal gene expression of HO1 and NQO1 was decreased by 65% and 80%, respectively, in H9c2 cells treated with the Nrf2 siRNA compared to cells treated with nonsense siRNAs. In addition, tBHQ-induced induction of HO1 and NQO1 gene expression was reduced in Nrf2 siRNA treated cells. The increase in HO1 and NQO1 expression in response to tBHQ was reduced by 55% and 65% respectively, in Nrf2 knockdown cells as compared to nonsense siRNA treated cells (Figure 14.D) The increase in HO1 and NQO1 expression in response to tBHQ in nonsense siRNA treated cells was not different from that seen in control cells. These data suggest that Nrf2 knockdown attenuates the ARE-driven gene expression of HO1 and NQO1 in response to tBHQ treatment.
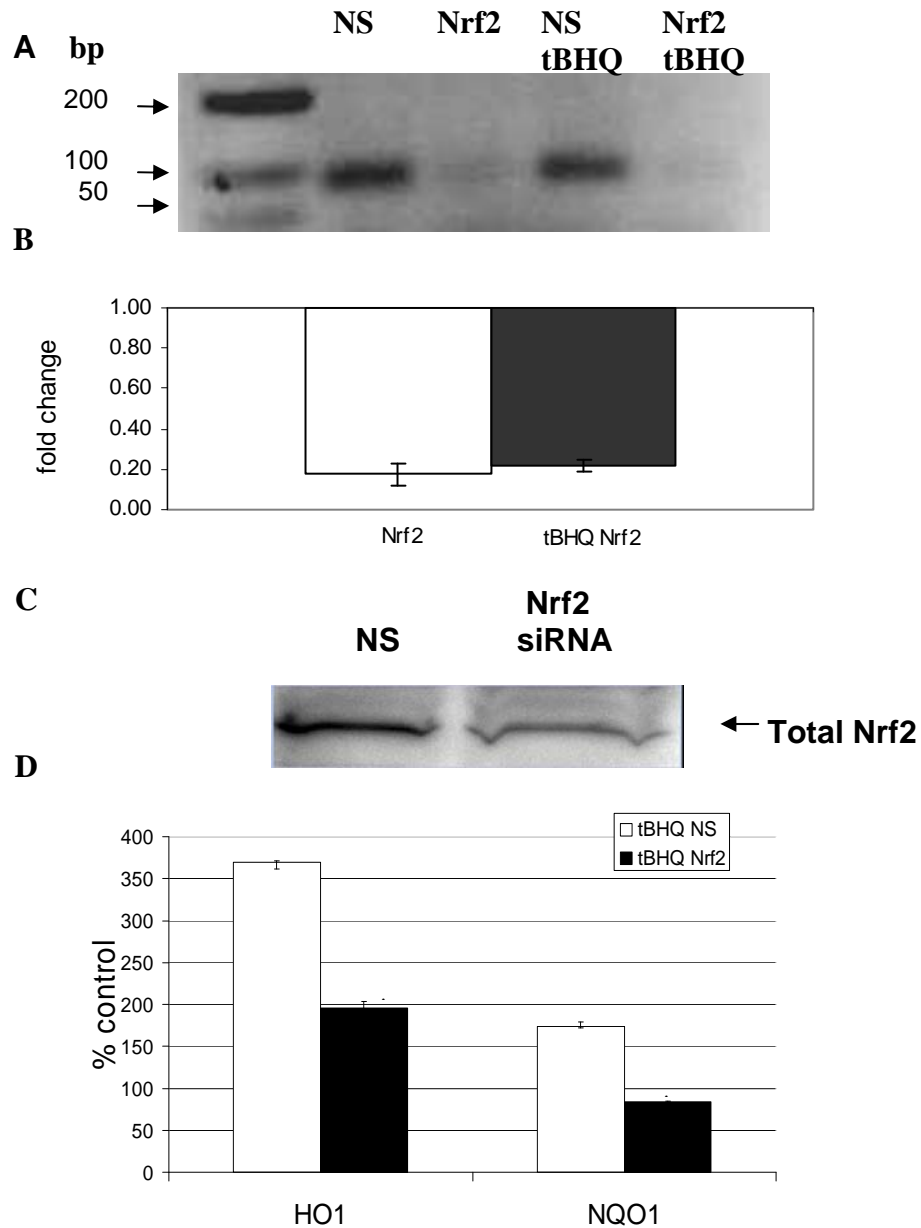
Figure 14. Effect of Nrf2 siRNA on Nrf2 gene and protein expression (n=3 independent experiments for each figure). **A)** Representative graph of RT-PCR of Nrf2 gene expression. **B)** Graphical representation of real-time RT-PCR of Nrf2 expression. The white bar represents a decrease in Nrf2 mRNA levels compared to nonsense siRNA treated basal conditions; whereas the black bar represents the decrease in Nrf2 levels as compared to nonsense (NS) siRNA treated with tBHQ. **C)** Representative western blot depicting protein expression of Nrf2 in whole cell lysates of nonsense (NS) siRNA and Nrf2 siRNA transfected cells. **D)** Effect of tBHQ (10 μM) on HO1 and NQO1 gene expression in cells transfected with nonsense (NS) siRNA and Nrf2 siRNA after tBHQ treatment. Error bars represent standard error.

Activation of Nrf2 protects H9c2 cells against oxidative stress:

To assess whether Nrf2 activation protects cells against subsequent oxidative stress, H9c2 cells were pretreated with tBHQ (10 μM), challenged 24 hours later with tBHP (100μM) or its vehicle for two hours, and reactive oxygen species (ROS) generation was measured. ROS were measured using the Image-it Live Green ROS detection kit (Molecular Probes). This protocol was used for both the qualitative assessment of ROS generation using fluorescent microscopy and the quantitative measurement of fluorescent intensity. Cells were treated with vehicle, tBHQ, tBHP and a combination of pretreatment with tBHQ (10 μM) then treatment with tBHP (100 μM). In vehicle-treated cells, only blue nuclei were detected upon inspection with fluorescent microscopy. The nuclei appeared rounded with little to no visible green fluorescence (Figure 15.A.i). Treatment of cells for two hours with tBHP (100 μM) caused the generation of green fluorescence throughout the cells indicative of ROS generation (Figure 15.A.ii). Pretreatment of H9c2 cells with tBHQ (10 μM) had no effect on ROS generation, irrespective of whether it was measured at two hours (data not shown) or 24 hours after treatment (Figure 15.A.iii). However, the increase in ROS generation in response to tBHP was completely abrogated in H9c2 cells pretreated with tBHQ (10 μM) for 24 hours (Figure 15.A.iv). Quantitative analysis of ROS generation measured by fluorescence intensity in suspended cells revealed similar results (Figure 15.B). tBHP (100 μM for 2 hours) increased the fluorescent intensity significantly ($p > 0.05$) compared to vehicle treated cells. Pretreatment with tBHQ (10 μM) for 24 hours blocked this increase in ROS generation in response to tBHP (100 μM). These data can be interpreted

to suggest that tBHQ, at a concentration demonstrated to activate Nrf2, is sufficient to decrease the cellular oxidative state even in the presence of the oxidant tBHP.

A

B
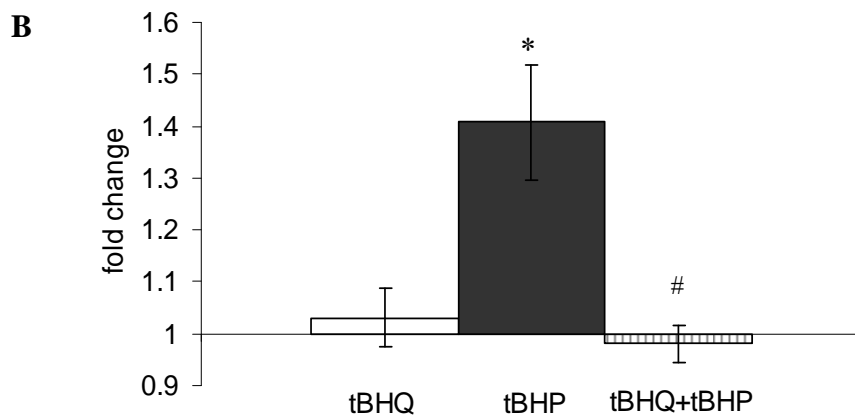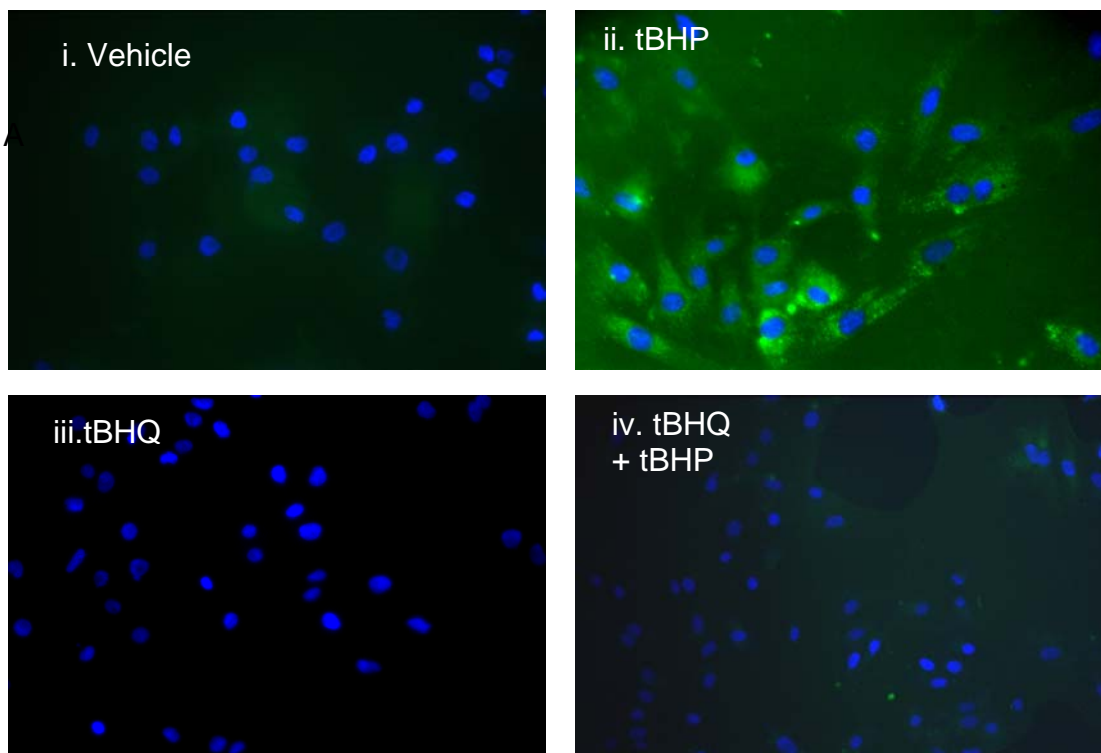
Figure 15. Reactive oxygen species generation. (n=4 independent experiments). A) ROS generation was visualized (40x magnification) using carboxy-H_2DCFDA and the nuclei with the blue-fluorescent cell permeant nucleic acid stain Hoechst 33342. ROS generation is seen as green fluorescence and the nuclei are seen as blue. i-iv are representative fluorescence micrographs of four independent experiments. i) Vehicle treated. ii) 100 μM tBHP for 2 hours iii) 10 μM tBHQ for 24 hours iv) tBHQ (10 μM) pretreatment for 24 hours, followed by 100 μM tBHP for 2 hours. B) Quantitative measurement of ROS generation using fluorescence intensity in suspended cells. For the same conditions described above, bars and lines represent the mean and SE of for independent experiments performed in duplicate. * Indicates significant difference from tBHQ (p<0.05). # Indicates significant difference from tBHP (p<0.05).

Nrf2 knockdown increases tBHP-induced ROS generation:

To further investigate the role of Nrf2 in protecting H9c2 cells against oxidative stress, cells were treated with Nrf2 siRNAs and ROS generation was measured in response to tBHP. tBHP (100 μM for 2 hours) increased ROS generation in nonsense siRNA treated cells from 1480 $\pm$ 35 in control to 2109 $\pm$ 37 fluorescent units (FU). The tBHP-induced increase in ROS were enhanced in cells pretreated with Nrf2 siRNAs. In Nrf2 knockdown cells, tBHP approximately doubled the increase in fluorescence compared to nonsense siRNA treated cells. As described earlier in control cells (figure 15) tBHQ pretreatment also decreased tBHP-induced ROS generation in nonsense siRNA treated cells. However, this protective effect of tBHQ was lost in Nrf2 knockdown cells. ROS accumulation increased from control at 1197 $\pm$ 2 FU to 4268 $\pm$ 438 FU in Nrf2 knockdown cells pretreated with tBHQ (10 μM) and then challenged with tBHP (100μM). Therefore, the inhibitory effect of tBHQ on tBHP-induced ROS accumulation was decreased in cells when Nrf2 was knocked-down by treatment with Nrf2 siRNAs (Figure 16).

NS siRNA	+	-	+	-	+	-	+	-
Nrf2 siRNA	-	+	-	+	-	+	-	+
tBHQ	-	-	+	+	-	-	+	+
tBHP	-	-	-	-	+	+	+	+
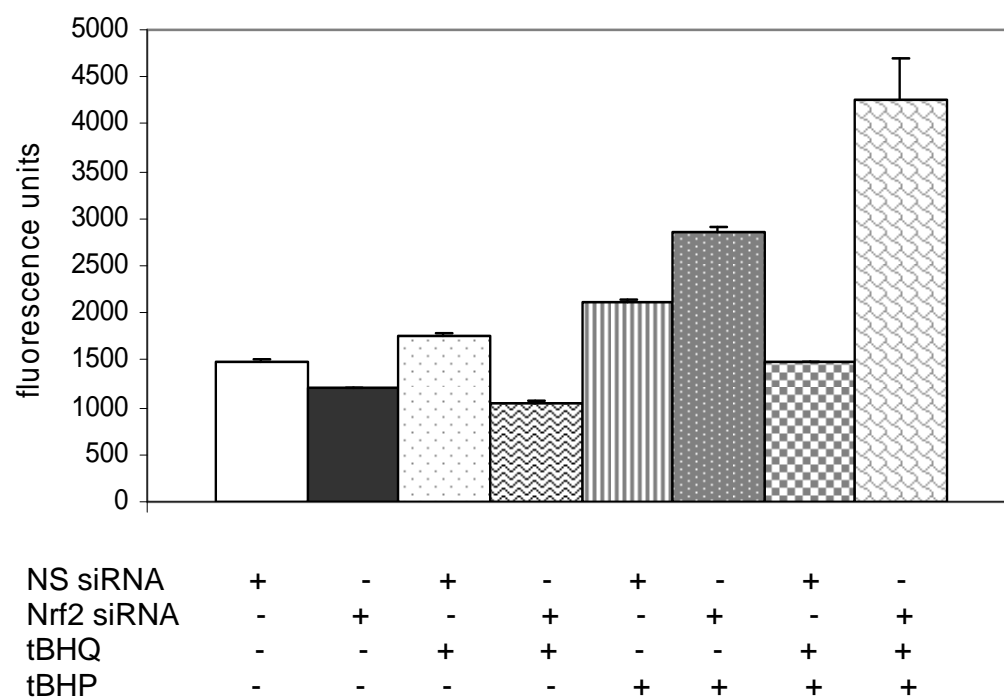
Figure 16. Effect of Nrf2 siRNA treatment and tBHQ on intracellular ROS generation (representative graph of three independent experiments). Cells were treated with either the nonsense (NS) siRNA or the Nrf2 siRNA followed by pretreatment with tBHQ (10 μM) or its vehicle for 24 hours. Cells were then exposed to 100 μM tBHP for 2 hours, suspended, counted and ROS measured using carboxy-H_2DCFDA. Error bars represent standard deviation within one experiment.

Nrf2 knockdown decreased cell survival after oxidative stress:

Data from Figure 16 suggests that Nrf2 activation protects H9c2 cells against ROS accumulation in response to the prooxidant tBHP. To determine whether activation of Nrf2 can protect H9c2 cells from oxidant-induced cell death, cells were treated with Nrf2 or NS siRNAs and the effects of tBHP and H_2O_2 on cell survival measured. In NS siRNA transfected cells, H_2O_2 caused a 72.8 ± 4.1 % decrease in cell number and tBHP caused a 62.7 ± 12.6 % decrease in cell number. Pretreatment of NS siRNA transfected cells with tBHQ for 24 hours reduced the effect of tBHP to remote cell death. In Nrf2 siRNA transfected cells H_2O_2 and tBHP caused a 66.8 ± 11.7 % and 72.8 ± 9.7 % decrease in cell number, respectively. tBHQ pretreatment had no effect on basal cell number but did not protect the cells from death in response to tBHP or H_2O_2 as was seen in NS siRNA transfected cells. Therefore the ability of tBHQ to protect H9c2 cells from death in response to tBHP or H_2O_2 was lost in Nrf2 knockdown cells.

NS siRNA	+	+	+	+	+	+	-	-	-	-	-	-
Nrf2 siRNA	-	-	-	-	-	-	+	+	+	+	+	+
tBHQ	-	-	-	+	+	+	-	-	-	+	+	+
H$_2$O$_2$	-	+	-	-	+	-	-	+	-	-	+	-
tBHP	-	-	+	-	-	+	-	-	+	-	-	+
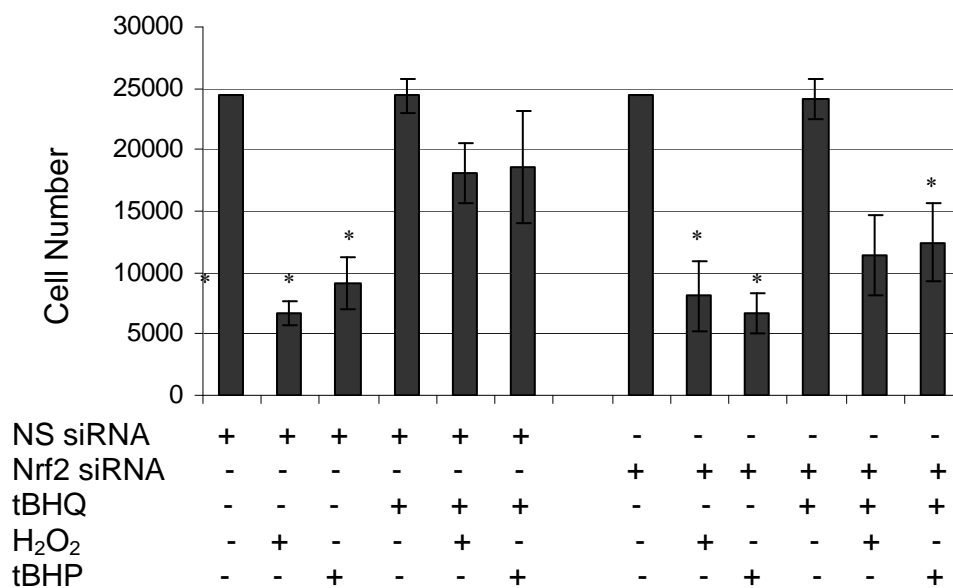
Figure 17. Effects of Nrf2 knockdown on cell survival. H9c2 cells were transfected with either nonsense (NS siRNA) or Nrf2 siRNAs (n=6 independent experiments). Cell survival was measured by cell proliferation assay after the following treatments: vehicle (C), 200 μM H$_2$O$_2$ (2h), 100 μM tBHP (2h), 10 μM tBHQ (2h), 10 μM tBHQ followed by 200 μM H$_2$O$_2$ (24h followed by 2 h respectively), and 10 μM tBHQ followed by 100 μM tBHP (24h followed by 2 h respectively). For the same conditions described above, bars and lines represent the mean and SE of for independent experiments performed in duplicate. *Indicates significant difference from vehicle treated control (p<0.05).

Keap1 knockdown increases HO1 and NQO1 expression:

Keap1 is an inhibitory protein that sequesters and marks Nrf2 for proteosomal degradation. To determine if the protective effect of Nrf2 was enhanced by decreasing expression of Keap1 using siRNAs, H9c2 cells were treated with either nonsense (NS) or Keap1 siRNAs. H9c2 cells treated with Keap1 siRNAs had a tendency to be reduced as measured by real-time PCR and western blot (Figure 18.A&B). In Keap1 knocked down cells, basal HO1 and NQO1 gene expression increased 2.6 ± 0.5 fold and 4.6 ± 0.6 (SE) fold, respectively, as compared to NS siRNA transfected cells with fold change of 1. In addition, Nrf2 basal expression levels increased 2.2 ± 0.3 fold. Pretreatment with tBHQ for 8 hours increased HO1 and NQO1 gene expression by 9.3 ± 0.5 and 8.32 ± 3.8 fold, respectively, in cells with Keap1 knockdown (Figure 18.C).

A

B

C
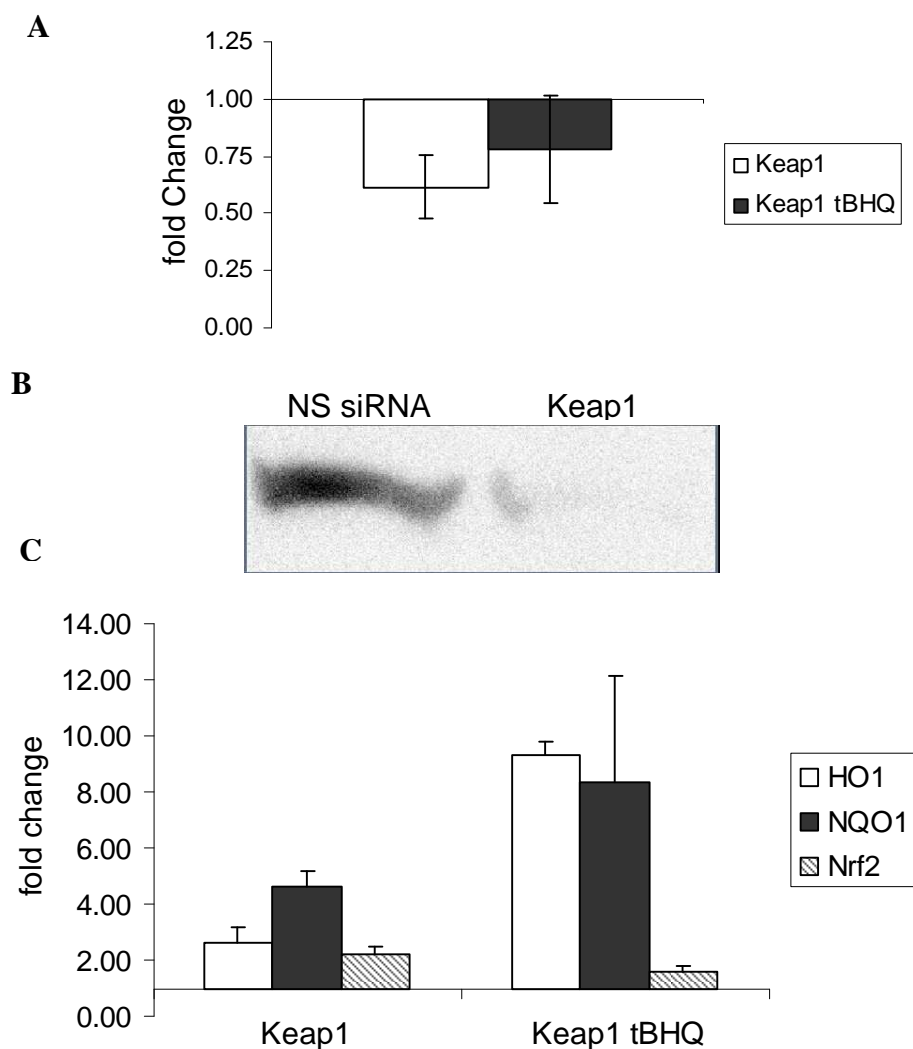
Figure 18. The effect of Keap1 siRNA on gene and protein expression. **A)** Real-time PCR of Keap1 mRNA levels after treatment with Keap1 siRNAs followed by treatment with 10 μM tBHQ or vehicle for 8 hours as compared to nonsense (NS) siRNA treated control. **B)** Western blot of Keap1 protein levels after treatment with Keap1 siRNAs as normalized to nonsense (NS) siRNA treated control. **C)** Real-time PCR of HO1, NQO1 and Nrf2 mRNA levels after treatment with Keap1 siRNAs and after exposure to 10 μM tBHQ or vehicle as compared to nonsense (NS) siRNA treated control. Error bars represent standard error.

Keap1 knockdown increases cell survival after oxidative stress:

Under basal conditions, Keap1 knockdown increases HO1 and NQO1 gene expression (Figure 18). To determine whether Keap1 knockdown enhanced cell survival during oxidative stress, H9c2 cells were transfected with NS and Keap1 siRNAs, challenged with tBHP or H_2O_2, and cell survival was measured. In NS transfected cells, H_2O_2 (200 μM) decreased cell number by 73.8 ± 3.0 %. Pretreatment with tBHQ 24 hours prior to exposure to H_2O_2 inhibited the cell death by 27.3 ± 6.8 % in NS transfected cells. In contrast, cells transfected with Keap1 siRNAs H_2O_2 did not cause a significant decrease in cell number both in the absence or present of tBHQ.

A similar trend was observed with tBHP (100 μM) treatment. In NS treated cells, tBHP reduced cell number to 49.14 ± 16.7 % as compared to control; whereas tBHQ treatment protected H9c2 cells from tBHP-mediated cell death (24.1 ± 15.0 %). In Keap1 knockdown cells, tBHP did not significantly decrease cell number (25.2 ± 12.2) and tBHQ pretreatment did not further increase cell survival (20.5 ± 13.3 %). These data suggest that Keap1 knockdown is sufficient to protect the H9c2 cells against oxidative stress caused by H_2O_2 and tBHP. The protective effect of Keap1 is similar to that of NS siRNA treated control cells pretreated with tBHQ (Figure 19).

NS siRNA	+	+	+	+	+	+	-	-	-	-	-	-
Nrf2 siRNA	-	-	-	-	-	-	+	+	+	+	+	+
tBHQ	-	-	-	+	+	+	-	-	-	+	+	+
H_2O_2	-	+	-	-	+	-	-	+	-	-	+	-
tBHP	-	-	+	-	-	+	-	-	+	-	-	+
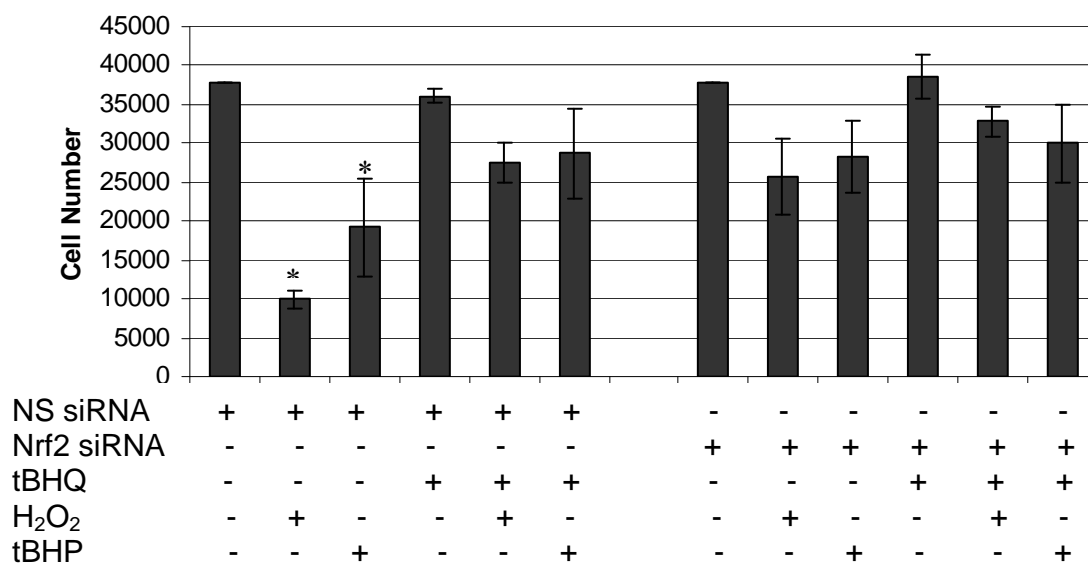
Figure 19. Effects of Keap1 knockdown on cell survival. H9c2 cells were transfected with either nonsense (NS siRNA) or Keap1 siRNAs (n=3 independent experiments). Cell survival was measured after the following treatments: vehicle (C), 200 μM H_2O_2 (2h), 100 μM tBHP (2h), 10 μM tBHQ (2h), 10 μM tBHQ followed by 200 μM H_2O_2 (24h followed by 2 h respectively), and 10 μM tBHQ followed by 100 μM tBHP (24h followed by 2 h respectively). For the same conditions described above, bars and lines represent the mean and SE of for independent experiments performed in duplicate. *Indicates significant difference from vehicle treated control (p<0.05).

Nrf2 - GFP overexpression does not increase HO1 and NQO1 expression:

Nrf2 has been shown to protect against oxidative stress, however Nrf2 overexpression has been reported to be unable to protect cardiac myocytes against doxorubicin toxicity (248). Therefore, it was next determined whether Nrf2 overexpression could activate ARE driven transcription and protect the H9c2 cells from oxidative stress. H9c2 cells were transiently transfected with human Nrf2 tagged with green fluorescent protein (Nrf2-GFP) or with empty pcDNA 3.1 vector. Nrf2-GFP was a generous gift from Dr. Furukawa at the University of Nebraska (89). Nrf2-GFP transfection increased basal human Nrf2 mRNA levels as compared to empty vector transfected control (Figure 20.A). H9c2 cells transfected with Nrf2-GFP had and increase in Nrf2 immunoreactivity, however there was no difference in HO1 and NQO1 mRNA expression as compared to empty vector transfected cells (Figure 20.C). tBHQ (10 μM 24 hours) increased Ho1 and NQO1 gene expression similarly in both empty vector and Nrf2-GFP transfected cells (Figure 20).
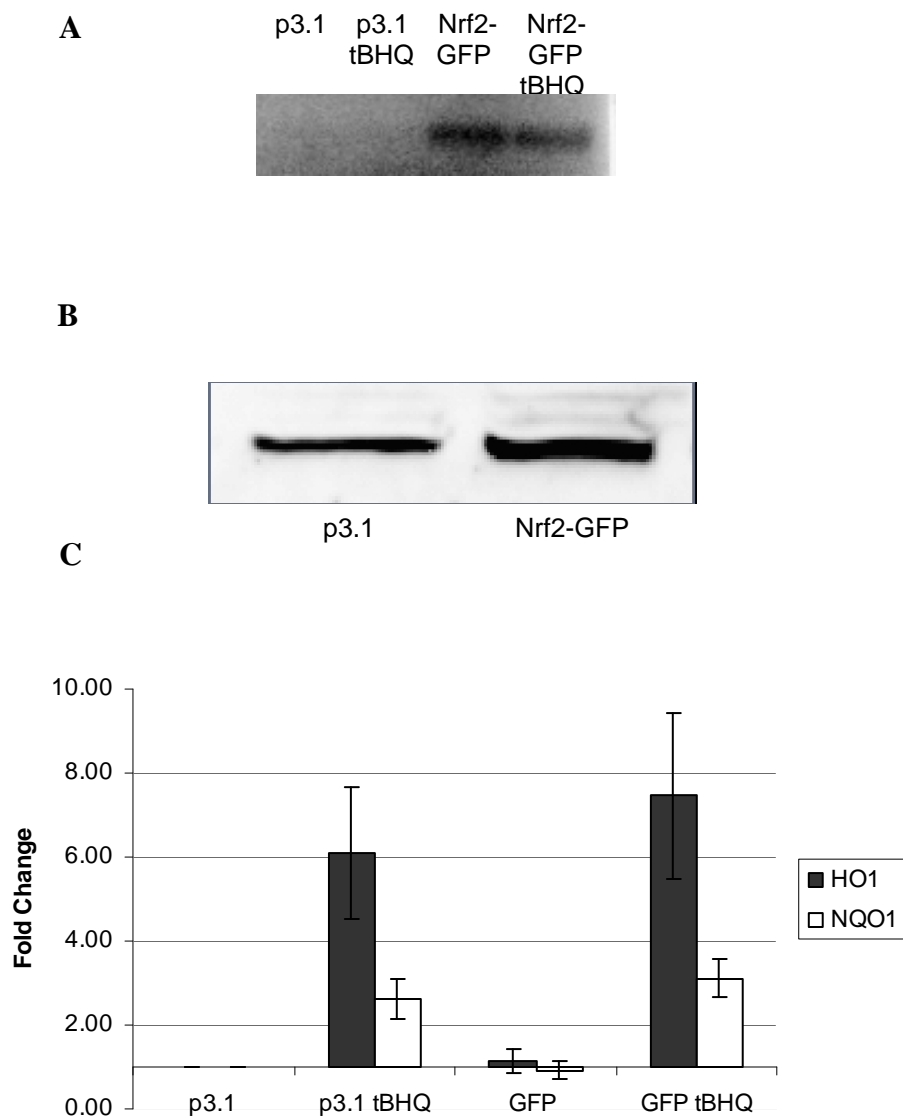
Figure 20. Effect of Nrf2 overexpression on gene and protein expression. H9c2 cells were transfected with either Nrf2 tagged with green fluorescent protein (Nrf2-GFP) or empty pcDNA 3.1 vector (p3.1). **A)** RT-PCR of gene expression in empty vector and Nrf2-GFP transfected cells after treatment with tBHQ (10 μM) or it vehicle for 24 hours.(n=2 independent experiments). **B)** Protein expression of Nrf2 in empty vector (p3.1) and Nrf2-GFP transfected cells (n=3 independent experiments). **C)** Real-time PCR on the effect of tBHQ (10 μM for 8hrs) on HO1 and NQO1 gene expression in cells transfected with Nrf2-GFP or empty vector (p3.1) (n=3 independent experiments). Error bars represent standard error.

H9c2 cells overexpressing Nrf2 - GFP require tBHQ for nuclear translocation:

In an effort to investigate why Nrf2 overexpression did not increase transcription of ARE-driven genes, H9c2 cells were transfected with human Nrf2 tagged with green fluorescent protein (Nrf2-GFP) or empty pcDNA 3.1 vector and plated on charged coverslips. Cells were treated with tBHQ (10 μM) or its vehicle for 1 hour and visualized via fluorescent microscopy. Background fluorescence was detected in the H9c2 cells transfected with empty vector and treated with vehicle (Figure 21.i). In H9c2 cells transfected with Nrf2-GFP, fluorescence was detected and appeared to be localized throughout the cytoplasm (Figure 21.ii). H9c2 cells transfected with empty vector and treated with tBHQ showed no significant fluorescence (Figure 21.iii), whereas H9c2 cells transfected with Nrf2-GFP and treated with tBHQ displayed localization of fluorescence in the nucleus (Figure 21.iv). These data suggest that overexpressed Nrf2-GFP remains predominantly in the cytoplasm until activated by tBHQ, at which point it translocates into the nucleus.
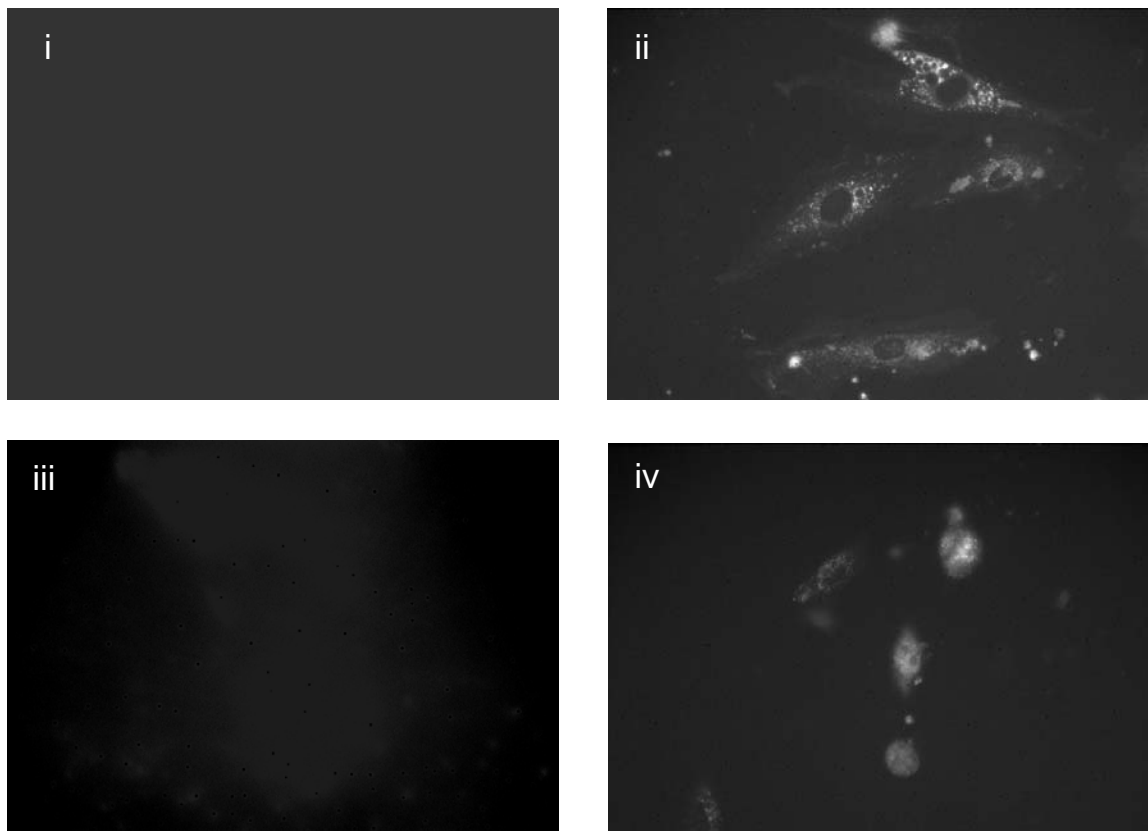
Figure 21. Cellular localization of Nrf2 tagged with green fluorescent protein (Nrf2-GFP) (40x magnification). H9c2 cells were transfected with either Nrf2-GFP or empty pcDNA 3.1 vector. **i.** Fluorescence of H9c2 cells transfected with pcDNA 3.1 empty vector and treated with vehicle for 1 hour. **ii.** Fluorescence of H9c2 cells transfected with Nrf2-GFP and treated with vehicle for 1 hour. **iii.** Fluorescence of H9c2 cells transfected with pcDNA 3.1 empty vector and treated with 10 μM tBHQ for 1 hour. **iv.** Fluorescence of H9c2 cells transfected with Nrf2-GFP and treated with 10 μM tBHQ for 1 hour. Representative figure of four independent experiments.

Nrf2 overexpression is not protective:

To address whether Nrf2 overexpression protects H9c2 cells against lethal levels of oxidative stress, cells were transfected with Nrf2-GFP or pcDNA 3.1, challenged with H_2O_2 or tBHP and cell survival was measured (Figure 22). In empty vector transfected cells, H_2O_2 treatment increased cell death 59.0 ± 6.6 % and tBHP treatment increased cell death to 77.4 ± 6.4 % as compared to control. A similar trend was observed in cells overexpressing Nrf2. H_2O_2 treatment increased cell death 56.7 ± 7.11 % and tBHP treatment increased cell death 67.4 ± 10.7 %. tBHQ treatment protected both Nrf2 overexpressing and empty vector control. In empty vector transfected cells, tBHQ treatment decreased cell death 16.3 ± 16.4 % in H_2O_2 treated and 31.4 ± 5.7 % in tBHP treated cells. In Nrf2 overexpressing cells, tBHQ treatment decreased cell death 10.7 ± 7.0 % after H_2O_2 treatment and 13.3 ± 8.1 % after tBHP treatment. While Nrf2 activation protected against oxidative stress and cell death, Nrf2 overexpression alone did not.
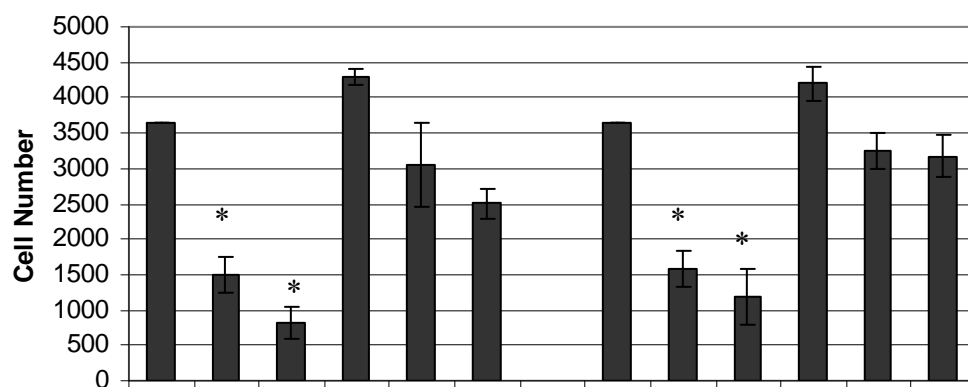
pcDNA 3.1	+	+	+	+	+	+	-	-	-	-	-	-
Nrf2-GFP	-	-	-	-	-	-	+	+	+	+	+	+
tBHQ	-	-	-	+	+	+	-	-	-	+	+	+
H_2O_2	-	+	-	-	+	-	-	+	-	-	+	-
tBHP	-	-	+	-	-	+	-	-	+	-	-	+

Figure 22. Effect of Nrf2 overexpression on cell survival (n=3 independent experiments). H9c2 cells were transfected with Nrf2-GFP or empty vector (pcDNA 3.1) and cell survival was measured after the following treatments: vehicle (C), 200 μM H_2O_2 (2h), 100 μM tBHP (2h), 10 μM tBHQ (2h), 10 μM tBHQ followed by 200 μM H_2O_2 (24h followed by 2 h, respectively), and 10 μM tBHQ followed by 100 μM tBHP (24h followed by 2 h, respectively). For the same conditions described above, bars and lines represent the mean and SE of for independent experiments performed in duplicate. *Indicates significant difference from vehicle treated control (p<0.05).

100

DISCUSSION

These studies evaluated the protective nature of Nrf2 against oxidative stress in the H9c2 cardiac-like cell line. We used the antioxidant *tert*-butyl hydroquinone (tBHQ) to activate Nrf2. tBHQ treatment resulted in nuclear accumulation of Nrf2 and increased transcription of the ARE-driven genes, HO1 and NQO1. tBHQ treatment also protected H9c2 cells from reactive oxygen species (ROS) generation and prooxidant-induced cell death. The protective effects of tBHQ were mediated through Nrf2, as Nrf2 knockdown prevented transcription of HO1 and NQO1. Nrf2 knockdown increased ROS generation in response to the prooxidant tert-butyl hydroperoxide (tBHP) and increased cell death in response to H_2O_2 and tBHP. In cells with reduced Nrf2 levels, tBHQ did not protect against ROS or cell death.

Knockdown of the inhibitory protein Keap1 increased expression of HO1, NQO1, and Nrf2. Keap1 knockdown was protective against prooxidant mediated cell death which was not further augmented by tBHQ treatment. Overexpression of Nrf2 did not cause increased transcription of HO1 and NQO1. This is likely due to nuclear exclusion of Nrf2. Only after tBHQ treatment did cells overexpressing Nrf2 exhibit increased enzyme transcription and nuclear localization. Thus Nrf2 appears to protect the cardiac-like H9c2 cells from oxidative stress when activated by Nrf2 or by the removal of Keap1. Nuclear exclusion of Nrf2 prevents increased gene transcription by Nrf2 overexpression unless Nrf2 is activated by tBHQ.

The rat cardiac-like H9c2 cells were used as the model cell system for this study. The H9c2 cells were developed in 1976 from the lower half of the embryonic rat heart consisting of mostly ventricular tissue (142). The H9c2 cell is a mononucleated spindle shaped large myoblast. At low densities, H9c2 cells retain their cardiac like phenotype which includes mononucleation, the ability to generate an overshooting action potential when stimulated, and a pattern of creatine phosphokinase CPK isoenzyme expression consistent with cardiac tissues. H9c2 cells also contain sarcomeres in the same pattern, diameter and structure of cardiac tissue. The H9c2 cell line can be used to represent both cardiac-like and skeletal muscle-like cells depending on growth conditions. To promote a cardiac-like phenotype, H9c2 cells were grown in the presence of 10% FBS and cultures were passaged every three days. These cells must reach confluence and grow for a period of three weeks before attaining the skeletal muscle phenotype (142). The mononucleated cardiac phenotype of H9c2 cells was verified periodically by both DAPI staining and hematoxylin-and-eosin (H&E) staining (Figure 4). To ensure that the H9c2 cells did not differentiate during the course of experimentation, only cells within the first 10 passages were used and gene expression analysis of HO1, NQO1, GAPDH and ABRP were measured to verify that the gene expression profile of H9c2 cell cultures remained consistent.

In the present study, we used the well known Nrf2 activator tBHQ to activate Nrf2. tBHQ caused an increase in mRNA expression of the genes HO1 and NQO1. tBHQ has been shown to activate Nrf2-mediated transcription using ARE-luciferase reporter constructs (149) and in ARE-hPAP reporter transgenic mice (125). In these studies, tBHQ activated Nrf2 resulting in ARE binding and transcription of ARE

responsive genes. In addition, a host of genes has been reported to be transcribed by Nrf2 after treatment with tBHQ including γ-glutamyl transpeptidase, γ glautamylcysteine synthase (187) HO1 (141), NQO1 (149) and many more, as determined by microarray analysis (173, 176).

The expression of protective enzymes has been shown to be controlled by Nrf2 in many tissues and cell lines, thereby supporting the hypothesis that Nrf2 is a multi-organ protector (166). In this study we found increased expression of the classical ARE-driven genes HO1 and NQO1 in cardiac H9c2 cells, consistent with the idea that the observed protective effect is a result of the activation of Nrf2.

Heme oxygenase-1 (HO1), the inducible form of the HO proteins, is activated in response to a host of oxidant and antioxidant stimuli (51). By degrading the reactive free heme into the antioxidants bilirubin and the anti-inflammatory agent CO, HO1 has been reported to protect cells against oxidative stress (52, 301, 302). HO1 has been shown to protect the heart in a variety of situations including after transplantation and against atherosclerotic lesion formation, while the lack of HO1 has been reported to exacerbate cardiac lesion formation after ischemia-reperfusion in normal and diabetic rats (188, 273, 300-302). Furthermore, HO1 transcription has been shown to be activated by the antioxidant response element (2). These studies, taken together, emphasize the importance of ARE-mediated HO1 expression in a cardiac system and make it an ideal reporter gene to analyze ARE activation.

NAD(P)H:quinone oxidoreductase 1 (NQO1) is an enzyme that catalyzes a two electron reduction of both exogenous and endogenous quinones, and quinone containing compounds including the tumor drug mitomyocin C, vitamins K and E, and benzene

quinones (218, 223, 244). A lack of NQO1 or reduction of its activity has been linked to a number of cancers including leukemia and myelogenous hyperplasia as well as being associated with increased benzene hematoxicity and a decreased response to chemotherapy. Thus, NQO1 has the beneficial effect of chemoprotection (16, 82, 162, 192, 212, 271, 272). NQO1 is constitutively expressed in most mammalian tissues and its induction requires the Nrf2-ARE pathway, making it a very useful reporter gene for studying the Nrf2-ARE system (196).

In the present study we did not investigate direct protective effects of HO1 or NQO1 induction. Instead, expression of HO1 and NQO1 was used as an index of ARE activation by Nrf2. HO1 and NQO1 are ideal reporter genes of ARE activation because they have sequence differences within the ARE and are differentially expressed in response to tBHQ treatment (Figure 13). Many other genes have been reported to contain AREs and to protect the cardiac cell after oxidative stress including glutathione reductase, glutathione peroxidase, glutathione S-transferase, superoxide dismustase, and catalase (28-30, 54, 83, 108, 199, 260, 302, 303).

RNA interference (RNAi) has recently been utilized as a unique form of post-transcriptional gene silencing. (100, 204, 262, 290, 307). siRNA technology works on the basis of creating RNA duplexes. The double-stranded RNA is recognized by the cells multi-protein RNA-Induced Silencing Complex (RISC) and degraded (for more information see section 5.1 of the methods section).

RNAi has several limitations. The cellular antiviral response is the most adverse side effect of siRNA technology. The antiviral response is characterized by the production of cytotoxic interferons and inflammatory cytokines. To overcome this

limitation we measured gene expression of a member of the interferon response cascade, 2'-5'-oligoadelylate synthetase (OAS2). We detected no change from control, suggesting that our siRNA transfection protocol does not activate the antiviral interferon response. In addition, lipid-mediated transfection is inherently toxic to the cell and can result in off-target or non-specific effects of the transfection. The nonsense siRNA control was used in parallel to the experimental siRNA in every experiment to ensure that observed effects were due to gene knockdown and not to nonspecific effects of the transfection.

Another limitation of RNAi is that gene expression is not completely eliminated and the effectiveness of different siRNAs varies. A positive control siRNA directed against the housekeeping gene glyceraldehyde 3-phosphate dehydrogenase (GAPDH) was used to determine knockdown efficiency. Using siRNAs generated against GAPDH, mRNA levels were reduced 90%, thus only 10% of the normal number of GAPDH transcripts were present. We observed variation in the transfection of different siRNAs with relative knockdown at 80% for Nrf2 and only 40% for Keap1. Although the level of knockdown of Keap1 was low, it translated to a measurable Keap1 protein reduction, increased HO1 and NQO1 transcription by free Nrf2, and increased cell survival when exposed to prooxidants. The insufficient knockdown of Keap1 may partially explain why tBHQ treatment was able to increase gene expression of ARE-driven genes in the presence of Keap1 siRNA (Figure 18.C). If Keap1 knockdown was complete, all Nrf2 would be free and tBHQ would not be likely to affect ARE-driven gene transcription. The knockdown of Keap1 was sufficient to protect cells against the effects of prooxidants, suggesting that the increase in expression of ARE-driven proteins was

enough to elicit a protective response. We concluded that although Keap1 knockdown was low, it was sufficient to analyze the effect of reduced Keap1 levels.

Another concern using siRNA technology is that of transfection efficiency. Transfection efficiency is expressed as the percentage of cells that take up the siRNA. Transfection efficiency was found to be 42%. While this transfection efficiency is low, gene knockdown specific effects could be detected. These data support the use of siRNA technology in the H9c2 cells and by addressing its inherent limitations (interferon response, transfection efficiency and housekeeping gene normalization) provide us with reasonable assurance that we are using a reliable model with observed due specifically to gene knockdown.

In this study increased gene expression and protein levels of HO1 and NQO1 were observed in response to tBHQ treatment. Activation of Nrf2 by tBHQ and the subsequent increase in expression of stress proteins have been described in numerous tissues (111, 125, 152, 264, 266) and other cell lines (64, 165, 183, 220, 223). Here it is shown that tBHQ activates antioxidant transcription through a Nrf2-dependent mechanism. After treatment with tBHQ a rapid translocation of Nrf2 from the cytoplasm to the nucleus was observed. This translocation occurred within 15 minutes of tBHQ treatment and Nrf2 levels remained elevated in the nucleus for up to 4 hours. This correlates with other studies showing elevated Nrf2 levels from 1-12 hours after activation (89, 173, 222, 310). Similar results were reported in human neuroblastoma cells where tBHQ treatment resulted in dramatic nuclear translocation of Nrf2(167).

Using HO1 and NQO1 mRNA levels as an index of Nrf2-mediated activation of the ARE, Nrf2 knockdown resulted in decreased basal and tBHQ-stimulated HO1 and

NQO1 gene expression. These data suggest that Nrf2 is involved in both basal and stimulated expression of ARE-induced genes. These observations agree with results of studies involving other tissues in which Nrf2 knockout decreased antioxidant-mediated induction of antioxidant genes. For example, in murine prenatal fibroblasts, tBHQ induced HO1 expression in wild-type but not Nrf2 knockout cells, suggesting that Nrf2 is necessary for tBHQ-induced HO1 induction (141). It has also been reported that, in the absence of Nrf2, there is a marked impairment in the expression of genes encoding a number of detoxifying enzymes, including GSH biosynthetic enzymes, in the liver and GI tract (42, 119, 201).

In addition to Nrf2 involvement in ARE-induced gene expression, Nrf2 is also necessary to facilitate the protective effects of tBHQ against cytotoxic effects of oxidative stress. H_2O_2 was chosen because it is a commonly produced ROS in ischemia-reperfusion injury and is more stable than its more reactive counterparts O_2^- and OH^- (289). tBHP was chosen because of similarities to the byproducts of lipid peroxidation (207). tBHP has been reported to induce apoptosis in rat hepatocytes (96), HepG2 cells (241) and N_2A and SH-SY5Y neuronal cells (312) through opening of the mitochondrial permeability transition pore (96, 241).

In the present study, tBHP increased generation of reactive oxygen species and decreased cell viability of H9c2 cells. The effect of tBHP on ROS generation was blocked by pretreatment with tBHQ at the concentration and time frame in which ARE-induced genes are expressed. Additionally, the protective effect of tBHQ on tBHP-induced ROS generation was lost following Nrf2 knockdown using Nrf2 siRNAs. This suggests that Nrf2 activation is necessary for tBHQ-mediated protection of cardiac H9c2

cells. These data agree with many studies demonstrating a relationship between Nrf2 activation and cytoprotection from oxidative stress. Dhakshinamoorthy and Porter (66) reported that siRNA-mediated knockdown of Nrf2 sensitized neuroblastoma cells to NO-induced apoptosis. Nrf2 knockout in primary astrocytes and neurons were more sensitive to oxidative damage and mitochondrial toxins than wild-type cells (164, 168) and overexpression of Nrf2 in astrocytes increased the survival of neurons under conditions associated with non-excitotoxic glutamate toxicity (152). Nrf2 has also been shown to protect the lung from butylated hydroxytoluene-induced acute respiratory distress syndrome (40), hyperoxic injury (47), and bleomycin-mediated pulmonary fibrosis (50) through increased detoxification and antioxidant potentials. Nrf2 knockout mice also show increased sensitivity to acetaminophen-induced hepatotoxicity as well as increased levels of lipid peroxidation and DNA damage (39, 75, 177). These data reinforce the pivotal role of the Nrf2-ARE pathway in protecting multiple tissues and cells from oxidative stress and suggest a universal role for Nrf2 in the protective pathway.

Nrf2 activation is responsible for protection against oxidative stress elicited by tBHQ. Normal cells are susceptible to reactive oxygen species generation caused by H_2O_2 and tBHP. Pretreatment with tBHQ for 24 hours protected H9c2 cells against H_2O_2- and tBHP-mediated reactive oxygen species generation. However, in Nrf2-deficient cells oxidative stress results in an increase in ROS even when pretreated with tBHQ. These data can be interpreted to suggest that the protective nature of tBHQ is due solely to its ability to activate Nrf2, not through the inherent antioxidative nature of tBHQ.

In normal H9c2 cells, Nrf2 activation by tBHQ protects cells against death caused by tBHP and H_2O_2. This protective effect is due to the activation of antioxidant enzymes prior to an oxidative event, leaving the cell in a state predisposed for oxidative stress. Upon knockdown of Nrf2, pretreatment with tBHQ did not protect against H_2O_2 or tBHP, further supporting the idea that Nrf2 is a major player in this protective mechanism. This suggests that Nrf2 is responsible for protection against oxidative stress mediated by both tBHP and H_2O_2.

These data are somewhat in contrast to those of Purdom-Dickenson *et al.* (248). They showed that pretreatment with H_2O_2 protected the cells from subsequent doxorubicin-induced apoptosis, whereas Nrf2 overexpression did not. In an effort to determine if the observed increased survival was mediated through the Nrf2 protein, these investigators overexpressed Nrf2 and treated cells with doxorubicin. Because overexpression of Nrf2 was not protective, the authors concluded that the cytoprotective effect of H_2O_2 pretreatment is not dependent on Nrf2 activation. They hypothesized that cross talk between Nrf2 and another protein, possibly nuclear factor κ β, was responsible for the observed cytoprotection.

In an attempt to clarify the role of Nrf2 in the protective response against oxidative stress we knocked down the inhibitory protein Keap1 using siRNAs. By removing Keap1 it was possible to evaluate the direct effects of Nrf2 in the absence of the activator tBHQ. Keap1 knockdown resulted in low constitutive levels of ARE-containing gene expression, presumably through the constitutive activation of the ARE. In Keap1 deficient cells, the oxidative stressors H_2O_2 and tBHP had no effect on cell death. These data also suggest that protective effects seen with tBHQ can be attributed

directly to Nrf2 activation. Treatment with Keap1 siRNA mimicked the protective response seen with tBHQ treatment. In the absence of Keap1, Nrf2 is free to activate the expression of antioxidant and detoxifying genes, thus leaving the cell in a protected state. These cells are resistant to the oxidative effects of H_2O_2 and tBHP at concentrations that are lethal to untreated cells.

To examine the effects of exogenous Nrf2 in protecting the cardiac cells against oxidative stress, H9c2 cells were transiently transfected with human Nrf2 tagged with green fluorescent protein (Nrf2-GFP). Under basal conditions, Nrf2-GFP was localized exclusively in the cytoplasm indicative of nuclear exclusion of Nrf2 and suggesting a negative regulator was preventing nuclear translocation. Furthermore, when Nrf2-GFP cells were treated with tBHQ, fluorescence was localized in the nucleus indicating nuclear translocation of Nrf2. To verify these results we measured transcription of ARE-containing genes. In Nrf2 overexpressing cells, HO1 and NQO1 mRNA remained at basal levels; whereas Nrf2 mRNA and protein levels were elevated. tBHQ treatment resulted in increased HO1 and NQO1 expression, suggesting that Nrf2 is excluded from the cardiac cell by Keap1 or another regulatory mechanism. The observation that Nrf2 translocation and gene transcription occurs only after tBHQ treatment suggests that Nrf2 must be activated in order to protect the cell.

A limitation to the above described experiment is that expression of exogenous human Nrf2 (hNrf2) in rat H9c2 cells may result in problems with nuclear import and ARE-driven gene transcription due to species differences. To evaluate this inherent problem, nuclear translocation of Nrf2 was measured in H9c2 cells. hNrf2 was able to enter the nucleus after tBHQ treatment. tBHQ caused translocation of hNrf2 at the same

110

concentration and in the same time frame as observed endogenous Nrf2 in H9c2 cells, suggesting that human Nrf2 is able to enter the nucleus of the rat H9c2 cells to initiate gene transcription.

These data can be interpreted to suggest that Nrf2 overexpression was not protective to cardiac cells as described in Purdom-Dickenson *et al.*, 2006 (248). In our experiments, cells overexpressing Nrf2 did not enter the nucleus unless activated by tBHQ. This could explain why Nrf2 overexpression alone was not sufficient to protect the cardiomyocyte against DOX treatment. The observed nuclear exclusion of Nrf2 could be through negative control by Keap1 and/or the nuclear export signal. As indicated in the literature review, the Nrf2 protein contains a redox-insensitive nuclear export signal (NES) (122, 182) and deletion of the NES results in increased localization of Nrf2 after treatment with tBHQ (122). While we did not investigate the contribution of the NES, it is a possible explanation for the observed nuclear exclusion of Nrf2.

Studies discussed in this dissertation are the first to look directly at the effects of Nrf2 in a cardiac model using siRNAs. The use of siRNAs overcomes limitations associated with gene (i.e. loss of function models) knockout mouse because it involved temporary gene knockdown. Knockout mice have many limitations caused by the absence of a gene from the genome at the start of development. Complications include death, chronic health problems, functional compensation by other closely related gene family members, and multiple copies of genes or pseudogenes in genome (239). By temporarily knocking down a gene, siRNA technology reduces the risk of death due to the removal of a protein, reduces the likelihood of functional compensation by other members a protein family and does not discriminate against mRNA created by different

copies of a gene. In fact, development of technology facilitating the use of siRNAs in the whole animal is in progress to bypass the limitations of the knockout mouse (243).

Studies reported here are the first to examine the effects of Keap1 knockdown in a cardiac cell model system. This is especially valuable considering that the Keap1 knockout mutation is lethal in the whole animal. The herein data suggest that reduction of Keap1 actively protects the cardiac cell against lethal levels of prooxidants to an extent similar to that observed for Nrf2 activation by tBHQ. These data suggest that removal of the inhibitory protein Keap1 results in free Nrf2 that translocates into the nucleus initiating gene transcription. This study is also the first to show that overexpressing Nrf2 does not result in nuclear translocation of Nrf2 or ARE-driven gene transcription unless activated by tBHQ. The regulatory mechanism causing nuclear exclusion of Nrf2 is involve both Keap1 and the nuclear export signal.

In summary, Nrf2 was shown to protect H9c2 cells against two forms of lethal oxidative stress associated to exposure to H_2O_2 and tBHP, through increased antioxidant enzyme levels when stimulated by tBHQ. Activation of Nrf2 is necessary for Nrf2-mediated protection against ROS generation and cell death. Keap1 knockdown protected cells in a similar fashion to that observed with tBHQ treatment, supporting the hypothesis that effects seen after treatment with tBHQ reflect activation of Nrf2 and that Nrf2 must be activated in order to protect cells from oxidative stress. Fluorescent microscopy and gene expression analyses showed that Nrf2 is not present in the nucleus in unstimulated cells overexpressing Nrf2. Thus, Nrf2 overexpression alone does not protect the cell due to retention of Nrf2 in the cytoplasm. From these data it is concluded that Nrf2 protects H9c2 cardiac-like cells from oxidative stress when activated, or in the absence of its

inhibitory protein Keap1. These studies point to Nrf2 as a protective protein that may have therapeutic implications in the fight against cardiovascular disease.

CONCLUSIONS

The Nrf2 protein coordinately activates antioxidant enzymes in many tissues. The role of Nrf2 as a multi-organ protector holds true in the H9c2 cardiac-like cell line. However, Nrf2 must be activated in order to exhibit its protective effects. Removal of Keap1 protects the cardiac like cell from oxidative stress by freeing Nrf2; however the cell exhibits mechanisms that regulate the transcription of ARE-driven genes, which in turn, prevents the overexpression of Nrf2 from being inherently protective. Nrf2 activation protects H9c2 cells against oxidative stress and as such, may be valuable in therapeutic strategies for the treatment of cardiovascular disease.

REFERENCES

1.   Effect of enalapril on survival in patients with reduced left ventricular ejection fractions and congestive heart failure. The SOLVD Investigators. *The New England journal of medicine* 325: 293-302, 1991.

2.   **Alam J, Stewart D, Touchard C, Boinapally S, Choi AM, and Cook JL.** Nrf2, a Cap'n'Collar transcription factor, regulates induction of the heme oxygenase-1 gene. *J Biol Chem* 274: 26071-26078, 1999.

3.   **Alam J, Wicks C, Stewart D, Gong P, Touchard C, Otterbein S, Choi AM, Burow ME, and Tou J.** Mechanism of heme oxygenase-1 gene activation by cadmium in MCF-7 mammary epithelial cells. Role of p38 kinase and Nrf2 transcription factor. *J Biol Chem* 275: 27694-27702, 2000.

4.   **Albagli O, Dhordain P, Deweindt C, Lecocq G, and Leprince D.** The BTB/POZ domain: a new protein-protein interaction motif common to DNA- and actin-binding proteins. *Cell Growth Differ* 6: 1193-1198, 1995.

5.   **Alia M, Ramos S, Mateos R, Bravo L, and Goya L.** Response of the antioxidant defense system to tert-butyl hydroperoxide and hydrogen peroxide in a human hepatoma cell line (HepG2). *Journal of biochemical and molecular toxicology* 19: 119-128, 2005.

6.   **Andrews NC, Erdjument-Bromage H, Davidson MB, Tempst P, and Orkin SH.** Erythroid transcription factor NF-E2 is a haematopoietic-specific basic-leucine zipper protein. *Nature* 362: 722-728, 1993.

7.   **Anwar AA, Li FY, Leake DS, Ishii T, Mann GE, and Siow RC.** Induction of heme oxygenase 1 by moderately oxidized low-density lipoproteins in human vascular smooth muscle cells: role of mitogen-activated protein kinases and Nrf2. *Free Radic Biol Med* 39: 227-236, 2005.

8.   **Aoki Y, Sato H, Nishimura N, Takahashi S, Itoh K, and Yamamoto M.** Accelerated DNA adduct formation in the lung of the Nrf2 knockout mouse exposed to diesel exhaust. *Toxicology and applied pharmacology* 173: 154-160, 2001.

9.   **Araque A.** Astrocyte-neuron signaling in the brain--implications for disease. *Curr Opin Investig Drugs* 7: 619-624, 2006.

10.   **auf dem Keller U, Huber M, Beyer TA, Kumin A, Siemes C, Braun S, Bugnon P, Mitropoulos V, Johnson DA, Johnson JA, Hohl D, and Werner S.** Nrf transcription factors in keratinocytes are essential for skin tumor prevention but not for wound healing. *Mol Cell Biol* 26: 3773-3784, 2006.

11.   **Ausubel FM.** New York: John Wiley & Sons, Inc, 2001.

12.   **Azen SP, Qian D, Mack WJ, Sevanian A, Selzer RH, Liu CR, Liu CH, and Hodis HN.** Effect of supplementary antioxidant vitamin intake on carotid arterial wall intima-media thickness in a controlled clinical trial of cholesterol lowering. *Circulation* 94: 2369-2372, 1996.

13.   **Balkau B, Bertrais S, Ducimetiere P, and Eschwege E.** Is there a glycemic threshold for mortality risk? *Diabetes Care* 22: 696-699, 1999.

14.   **Bardwell VJ and Treisman R.** The POZ domain: a conserved protein-protein interaction motif. *Genes Dev* 8: 1664-1677, 1994.

15.   **Benarroch EE.** Neuron-astrocyte interactions: partnership for normal function and disease in the central nervous system. *Mayo Clinic proceedings* 80: 1326-1338, 2005.

16.   **Benson AM, Hunkeler MJ, and Talalay P.** Increase of NAD(P)H:quinone reductase by dietary antioxidants: possible role in protection against carcinogenesis and toxicity. *Proc Natl Acad Sci U S A* 77: 5216-5220, 1980.

17.   **Berger SP, Hunger M, Yard BA, Schnuelle P, and Van Der Woude FJ.** Dopamine induces the expression of heme oxygenase-1 by human endothelial cells in vitro. *Kidney international* 58: 2314-2319, 2000.

18.   **Berliner JA and Watson AD.** A role for oxidized phospholipids in atherosclerosis. *The New England journal of medicine* 353: 9-11, 2005.

19.   **Bernstein E, Caudy AA, Hammond SM, and Hannon GJ.** Role for a bidentate ribonuclease in the initiation step of RNA interference. *Nature* 409: 363-366, 2001.

20.   **Beyer TA, Auf dem Keller U, Braun S, Schafer M, and Werner S.** Roles and mechanisms of action of the Nrf2 transcription factor in skin morphogenesis, wound repair and skin cancer. *Cell Death Differ*, 2007.

21.   **Blank V, Kim MJ, and Andrews NC.** Human MafG is a functional partner for p45 NF-E2 in activating globin gene expression. *Blood* 89: 3925-3935, 1997.

22.   **Bonnesen C, Eggleston IM, and Hayes JD.** Dietary indoles and isothiocyanates that are generated from cruciferous vegetables can both stimulate apoptosis and confer protection against DNA damage in human colon cell lines. *Cancer Res* 61: 6120-6130, 2001.

23.   **Bradford MM.** A rapid and sensitive method for the quantitation of microgram quantities of protein utilizing the principle of protein-dye binding. *Analytical biochemistry* 72: 248-254, 1976.

24.   **Braun S, Hanselmann C, Gassmann MG, auf dem Keller U, Born-Berclaz C, Chan K, Kan YW, and Werner S.** Nrf2 transcription factor, a novel target of keratinocyte growth factor action which regulates gene expression and inflammation in the healing skin wound. *Mol Cell Biol* 22: 5492-5505, 2002.

25.   **Brunt KR, Fenrich KK, Kiani G, Tse MY, Pang SC, Ward CA, and Melo LG.** Protection of human vascular smooth muscle cells from H2O2-induced apoptosis through functional codependence between HO-1 and AKT. *Arteriosclerosis, thrombosis, and vascular biology* 26: 2027-2034, 2006.

26.   **Buckley BJ, Marshall ZM, and Whorton AR.** Nitric oxide stimulates Nrf2 nuclear translocation in vascular endothelium. *Biochem Biophys Res Commun* 307: 973-979, 2003.

27.   **Burton NC, Kensler TW, and Guilarte TR.** In vivo modulation of the Parkinsonian phenotype by Nrf2. *Neurotoxicology* 27: 1094-1100, 2006.

116

28.   **Cao Z and Li Y.** The chemical inducibility of mouse cardiac antioxidants and phase 2 enzymes in vivo. *Biochem Biophys Res Commun* 317: 1080-1088, 2004.

29.   **Cao Z and Li Y.** Potent induction of cellular antioxidants and phase 2 enzymes by resveratrol in cardiomyocytes: protection against oxidative and electrophilic injury. *Eur J Pharmacol* 489: 39-48, 2004.

30.   **Cao Z, Tsang M, Zhao H, and Li Y.** Induction of endogenous antioxidants and phase 2 enzymes by alpha-lipoic acid in rat cardiac H9C2 cells: protection against oxidative injury. *Biochem Biophys Res Commun* 310: 979-985, 2003.

31.   **Cao Z, Zhu H, Zhang L, Zhao X, Zweier JL, and Li Y.** Antioxidants and phase 2 enzymes in cardiomyocytes: Chemical inducibility and chemoprotection against oxidant and simulated ischemia-reperfusion injury. *Experimental biology and medicine (Maywood, NJ* 231: 1353-1364, 2006.

32.   **Casey CA, Nanji A, Cederbaum AI, Adachi M, and Takahashi T.** Alcoholic liver disease and apoptosis. *Alcoholism, clinical and experimental research* 25: 49S-53S, 2001.

33.   **Caudy AA, Myers M, Hannon GJ, and Hammond SM.** Fragile X-related protein and VIG associate with the RNA interference machinery. *Genes Dev* 16: 2491-2496, 2002.

34.   **Ceriello A.** New insights on oxidative stress and diabetic complications may lead to a "causal" antioxidant therapy. *Diabetes Care* 26: 1589-1596, 2003.

35.   **Ceriello A and Motz E.** Is oxidative stress the pathogenic mechanism underlying insulin resistance, diabetes, and cardiovascular disease? The common soil hypothesis revisited. *Arteriosclerosis, thrombosis, and vascular biology* 24: 816-823, 2004.

36.   **Ceriello A, Taboga C, Tonutti L, Quagliaro L, Piconi L, Bais B, Da Ros R, and Motz E.** Evidence for an independent and cumulative effect of postprandial hypertriglyceridemia and hyperglycemia on endothelial dysfunction and oxidative stress generation: effects of short- and long-term simvastatin treatment. *Circulation* 106: 1211-1218, 2002.

37.   **Chan JY, Han XL, and Kan YW.** Cloning of Nrf1, an NF-E2-related transcription factor, by genetic selection in yeast. *Proc Natl Acad Sci U S A* 90: 11371-11375, 1993.

38.   **Chan JY, Kwong M, Lu R, Chang J, Wang B, Yen TS, and Kan YW.** Targeted disruption of the ubiquitous CNC-bZIP transcription factor, Nrf-1, results in anemia and embryonic lethality in mice. *The EMBO journal* 17: 1779-1787, 1998.

39.   **Chan K, Han XD, and Kan YW.** An important function of Nrf2 in combating oxidative stress: detoxification of acetaminophen. *Proc Natl Acad Sci U S A* 98: 4611-4616, 2001.

40.   **Chan K and Kan YW.** Nrf2 is essential for protection against acute pulmonary injury in mice. *Proc Natl Acad Sci U S A* 96: 12731-12736, 1999.

41.   **Chan K, Lu R, Chang JC, and Kan YW.** NRF2, a member of the NFE2 family of transcription factors, is not essential for murine erythropoiesis, growth, and development. *Proc Natl Acad Sci U S A* 93: 13943-13948, 1996.

42.   **Chanas SA, Jiang Q, McMahon M, McWalter GK, McLellan LI, Elcombe CR, Henderson CJ, Wolf CR, Moffat GJ, Itoh K, Yamamoto M, and Hayes JD.** Loss of the Nrf2 transcription factor causes a marked reduction in constitutive and inducible

117

expression of the glutathione S-transferase Gsta1, Gsta2, Gstm1, Gstm2, Gstm3 and Gstm4 genes in the livers of male and female mice. *Biochem J* 365: 405-416, 2002.

43.   **Chen L, Kwong M, Lu R, Ginzinger D, Lee C, Leung L, and Chan JY.** Nrf1 is critical for redox balance and survival of liver cells during development. *Mol Cell Biol* 23: 4673-4686, 2003.

44.   **Chen XL, Dodd G, Thomas S, Zhang X, Wasserman MA, Rovin BH, and Kunsch C.** Activation of Nrf2/ARE pathway protects endothelial cells from oxidant injury and inhibits inflammatory gene expression. *Am J Physiol Heart Circ Physiol* 290: H1862-1870, 2006.

45.   **Chen XL, Varner SE, Rao AS, Grey JY, Thomas S, Cook CK, Wasserman MA, Medford RM, Jaiswal AK, and Kunsch C.** Laminar flow induction of antioxidant response element-mediated genes in endothelial cells. A novel anti-inflammatory mechanism. *J Biol Chem* 278: 703-711, 2003.

46.   **Chenais B, Derjuga A, Massrieh W, Red-Horse K, Bellingard V, Fisher SJ, and Blank V.** Functional and placental expression analysis of the human NRF3 transcription factor. *Molecular endocrinology (Baltimore, Md* 19: 125-137, 2005.

47.   **Cho HY, Jedlicka AE, Reddy SP, Kensler TW, Yamamoto M, Zhang LY, and Kleeberger SR.** Role of NRF2 in protection against hyperoxic lung injury in mice. *Am J Respir Cell Mol Biol* 26: 175-182, 2002.

48.   **Cho HY and Kleeberger SR.** Genetic mechanisms of susceptibility to oxidative lung injury in mice. *Free Radic Biol Med* 42: 433-445, 2007.

49.   **Cho HY, Reddy SP, and Kleeberger SR.** Nrf2 defends the lung from oxidative stress. *Antioxidants & redox signaling* 8: 76-87, 2006.

50.   **Cho HY, Reddy SP, Yamamoto M, and Kleeberger SR.** The transcription factor NRF2 protects against pulmonary fibrosis. *Faseb J* 18: 1258-1260, 2004.

51.   **Choi AM and Alam J.** Heme oxygenase-1: function, regulation, and implication of a novel stress-inducible protein in oxidant-induced lung injury. *Am J Respir Cell Mol Biol* 15: 9-19, 1996.

52.   **Clark JE, Foresti R, Green CJ, and Motterlini R.** Dynamics of haem oxygenase-1 expression and bilirubin production in cellular protection against oxidative stress. *Biochem J* 348 Pt 3: 615-619, 2000.

53.   **Clerk A and Sugden PH.** Untangling the Web: specific signaling from PKC isoforms to MAPK cascades. *Circ Res* 89: 847-849, 2001.

54.   **Csonka C, Pataki T, Kovacs P, Muller SL, Schroeter ML, Tosaki A, and Blasig IE.** Effects of oxidative stress on the expression of antioxidative defense enzymes in spontaneously hypertensive rat hearts. *Free Radic Biol Med* 29: 612-619, 2000.

55.   **Dahlgren C, Wahlestedt C, and Thonberg H.** No induction of anti-viral responses in human cell lines HeLa and MCF-7 when transfecting with siRNA or siLNA. *Biochem Biophys Res Commun* 341: 1211-1217, 2006.

56.   **Davies SP, Reddy H, Caivano M, and Cohen P.** Specificity and mechanism of action of some commonly used protein kinase inhibitors. *Biochem J* 351: 95-105, 2000.

57.   **Davis RC, Hobbs FD, and Lip GY.** ABC of heart failure. History and epidemiology. *BMJ (Clinical research ed* 320: 39-42, 2000.

58.	**Day RM, Suzuki YJ, and Fanburg BL.** Regulation of glutathione by oxidative stress in bovine pulmonary artery endothelial cells. *Antioxidants & redox signaling* 5: 699-704, 2003.
59.	**DeLong MJ, Prochaska, H.J., Talalay, P.** *Protective Agents In Cancer*. London: Academic London, 1986.
60.	**Denison MS, Fisher JM, and Whitlock JP, Jr.** Protein-DNA interactions at recognition sites for the dioxin-Ah receptor complex. *J Biol Chem* 264: 16478-16482, 1989.
61.	**Derjuga A, Gourley TS, Holm TM, Heng HH, Shivdasani RA, Ahmed R, Andrews NC, and Blank V.** Complexity of CNC transcription factors as revealed by gene targeting of the Nrf3 locus. *Mol Cell Biol* 24: 3286-3294, 2004.
62.	**Devling TW, Lindsay CD, McLellan LI, McMahon M, and Hayes JD.** Utility of siRNA against Keap1 as a strategy to stimulate a cancer chemopreventive phenotype. *Proc Natl Acad Sci U S A* 102: 7280-7285A, 2005.
63.	**Dhakshinamoorthy S, Jain AK, Bloom DA, and Jaiswal AK.** Bach1 competes with Nrf2 leading to negative regulation of the antioxidant response element (ARE)-mediated NAD(P)H:quinone oxidoreductase 1 gene expression and induction in response to antioxidants. *J Biol Chem* 280: 16891-16900, 2005.
64.	**Dhakshinamoorthy S and Jaiswal AK.** Functional characterization and role of INrf2 in antioxidant response element-mediated expression and antioxidant induction of NAD(P)H:quinone oxidoreductase1 gene. *Oncogene* 20: 3906-3917, 2001.
65.	**Dhakshinamoorthy S and Jaiswal AK.** Small maf (MafG and MafK) proteins negatively regulate antioxidant response element-mediated expression and antioxidant induction of the NAD(P)H:Quinone oxidoreductase1 gene. *J Biol Chem* 275: 40134-40141, 2000.
66.	**Dhakshinamoorthy S and Porter AG.** Nitric oxide-induced transcriptional up-regulation of protective genes by Nrf2 via the antioxidant response element counteracts apoptosis of neuroblastoma cells. *J Biol Chem* 279: 20096-20107, 2004.
67.	**Ding Y, Schwartz D, Posner P, and Zhong J.** Hypotonic swelling stimulates L-type Ca2+ channel activity in vascular smooth muscle cells through PKC. *Am J Physiol Cell Physiol* 287: C413-421, 2004.
68.	**Dinkova-Kostova AT, Holtzclaw WD, Cole RN, Itoh K, Wakabayashi N, Katoh Y, Yamamoto M, and Talalay P.** Direct evidence that sulfhydryl groups of Keap1 are the sensors regulating induction of phase 2 enzymes that protect against carcinogens and oxidants. *Proc Natl Acad Sci U S A* 99: 11908-11913, 2002.
69.	**Dinkova-Kostova AT, Massiah MA, Bozak RE, Hicks RJ, and Talalay P.** Potency of Michael reaction acceptors as inducers of enzymes that protect against carcinogenesis depends on their reactivity with sulfhydryl groups. *Proc Natl Acad Sci U S A* 98: 3404-3409, 2001.
70.	**Durchdewald M, Beyer TA, Johnson DA, Johnson JA, Werner S, and auf dem Keller U.** Electrophilic chemicals but not UV irradiation or reactive oxygen species activate Nrf2 in keratinocytes in vitro and in vivo. *The Journal of investigative dermatology* 127: 646-653, 2007.
71.	**Eckel RH, York DA, Rossner S, Hubbard V, Caterson I, St Jeor ST, Hayman LL, Mullis RM, and Blair SN.** Prevention Conference VII: Obesity, a worldwide

epidemic related to heart disease and stroke: executive summary. *Circulation* 110: 2968-2975, 2004.

72.   **Eggler AL, Liu G, Pezzuto JM, van Breemen RB, and Mesecar AD.** Modifying specific cysteines of the electrophile-sensing human Keap1 protein is insufficient to disrupt binding to the Nrf2 domain Neh2. *Proc Natl Acad Sci U S A* 102: 10070-10075, 2005.

73.   **Elbashir SM, Lendeckel W, and Tuschl T.** RNA interference is mediated by 21- and 22-nucleotide RNAs. *Genes Dev* 15: 188-200, 2001.

74.   **Elbashir SM, Martinez J, Patkaniowska A, Lendeckel W, and Tuschl T.** Functional anatomy of siRNAs for mediating efficient RNAi in Drosophila melanogaster embryo lysate. *The EMBO journal* 20: 6877-6888, 2001.

75.   **Enomoto A, Itoh K, Nagayoshi E, Haruta J, Kimura T, O'Connor T, Harada T, and Yamamoto M.** High sensitivity of Nrf2 knockout mice to acetaminophen hepatotoxicity associated with decreased expression of ARE-regulated drug metabolizing enzymes and antioxidant genes. *Toxicol Sci* 59: 169-177, 2001.

76.   **Esper RJ, Nordaby RA, Vilarino JO, Paragano A, Cacharron JL, and Machado RA.** Endothelial dysfunction: a comprehensive appraisal. *Cardiovascular diabetology* 5: 4, 2006.

77.   **Evans JL, Goldfine ID, Maddux BA, and Grodsky GM.** Are oxidative stress-activated signaling pathways mediators of insulin resistance and beta-cell dysfunction? *Diabetes* 52: 1-8, 2003.

78.   **Favreau LV and Pickett CB.** The rat quinone reductase antioxidant response element. Identification of the nucleotide sequence required for basal and inducible activity and detection of antioxidant response element-binding proteins in hepatoma and non-hepatoma cell lines. *J Biol Chem* 270: 24468-24474, 1995.

79.   **Favreau LV and Pickett CB.** Transcriptional regulation of the rat NAD(P)H:quinone reductase gene. Identification of regulatory elements controlling basal level expression and inducible expression by planar aromatic compounds and phenolic antioxidants. *J Biol Chem* 266: 4556-4561, 1991.

80.   **Fellin T, Sul JY, D'Ascenzo M, Takano H, Pascual O, and Haydon PG.** Bidirectional astrocyte-neuron communication: the many roles of glutamate and ATP. *Novartis Foundation symposium* 276: 208-217; discussion 217-221, 233-207, 275-281, 2006.

81.   **Fiordaliso F, Bianchi R, Staszewsky L, Cuccovillo I, Doni M, Laragione T, Salio M, Savino C, Melucci S, Santangelo F, Scanziani E, Masson S, Ghezzi P, and Latini R.** Antioxidant treatment attenuates hyperglycemia-induced cardiomyocyte death in rats. *J Mol Cell Cardiol* 37: 959-968, 2004.

82.   **Fleming RA, Drees J, Loggie BW, Russell GB, Geisinger KR, Morris RT, Sachs D, and McQuellon RP.** Clinical significance of a NAD(P)H: quinone oxidoreductase 1 polymorphism in patients with disseminated peritoneal cancer receiving intraperitoneal hyperthermic chemotherapy with mitomycin C. *Pharmacogenetics* 12: 31-37, 2002.

83.   **Foresti R, Goatly H, Green CJ, and Motterlini R.** Role of heme oxygenase-1 in hypoxia-reoxygenation: requirement of substrate heme to promote cardioprotection. *Am J Physiol Heart Circ Physiol* 281: H1976-1984, 2001.

84.   **Fornerod M, Ohno M, Yoshida M, and Mattaj IW.** CRM1 is an export receptor for leucine-rich nuclear export signals. *Cell* 90: 1051-1060, 1997.

85.   **Forstermann U and Munzel T.** Endothelial nitric oxide synthase in vascular disease: from marvel to menace. *Circulation* 113: 1708-1714, 2006.

86.   **Friling RS, Bensimon A, Tichauer Y, and Daniel V.** Xenobiotic-inducible expression of murine glutathione S-transferase Ya subunit gene is controlled by an electrophile-responsive element. *Proc Natl Acad Sci U S A* 87: 6258-6262, 1990.

87.   **Fujita S, Peisach J, Ohkawa H, Yoshida Y, Adachi S, Uesugi T, Suzuki M, and Suzuki T.** The effect of Sudan III on drug metabolizing enzymes. *Chemico-biological interactions* 48: 129-143, 1984.

88.   **Fujita S, Suzuki M, and Suzuki T.** Structure-activity relationships in the induction of hepatic drug metabolism by azo compounds. *Xenobiotica; the fate of foreign compounds in biological systems* 14: 565-568, 1984.

89.   **Furukawa M and Xiong Y.** BTB protein Keap1 targets antioxidant transcription factor Nrf2 for ubiquitination by the Cullin 3-Roc1 ligase. *Mol Cell Biol* 25: 162-171, 2005.

90.   **Genc S, Egrilmez MY, and Genc K.** Endothelial nitric oxide-mediated Nrf2 activation as a novel mechanism for vascular and neuroprotection by erythropoietin in experimental subarachnoid hemorrhage. *Medical hypotheses* 67: 424, 2006.

91.   **Gong P and Cederbaum AI.** Nrf2 is increased by CYP2E1 in rodent liver and HepG2 cells and protects against oxidative stress caused by CYP2E1. *Hepatology (Baltimore, Md* 43: 144-153, 2006.

92.   **Gong P and Cederbaum AI.** Transcription factor Nrf2 protects HepG2 cells against CYP2E1 plus arachidonic acid-dependent toxicity. *J Biol Chem* 281: 14573-14579, 2006.

93.   **Gong P, Hu B, Stewart D, Ellerbe M, Figueroa YG, Blank V, Beckman BS, and Alam J.** Cobalt induces heme oxygenase-1 expression by a hypoxia-inducible factor-independent mechanism in Chinese hamster ovary cells: regulation by Nrf2 and MafG transcription factors. *J Biol Chem* 276: 27018-27025, 2001.

94.   **Griendling KK and FitzGerald GA.** Oxidative stress and cardiovascular injury: Part I: basic mechanisms and in vivo monitoring of ROS. *Circulation* 108: 1912-1916, 2003.

95.   **Griendling KK and FitzGerald GA.** Oxidative stress and cardiovascular injury: Part II: animal and human studies. *Circulation* 108: 2034-2040, 2003.

96.   **Haidara K, Morel I, Abalea V, Gascon Barre M, and Denizeau F.** Mechanism of tert-butylhydroperoxide induced apoptosis in rat hepatocytes: involvement of mitochondria and endoplasmic reticulum. *Biochimica et biophysica acta* 1542: 173-185, 2002.

97.   **Hamby RI, Zoneraich S, and Sherman L.** Diabetic cardiomyopathy. *Jama* 229: 1749-1754, 1974.

98.   **Hammond SM, Bernstein E, Beach D, and Hannon GJ.** An RNA-directed nuclease mediates post-transcriptional gene silencing in Drosophila cells. *Nature* 404: 293-296, 2000.

121

99.   **Hammond SM, Boettcher S, Caudy AA, Kobayashi R, and Hannon GJ.** Argonaute2, a link between genetic and biochemical analyses of RNAi. *Science (New York, NY* 293: 1146-1150, 2001.

100.   **Hannon GJ.** RNA interference. *Nature* 418: 244-251, 2002.

101.   **Hara H, Ohta M, and Adachi T.** Apomorphine protects against 6-hydroxydopamine-induced neuronal cell death through activation of the Nrf2-ARE pathway. *Journal of neuroscience research* 84: 860-866, 2006.

102.   **He CH, Gong P, Hu B, Stewart D, Choi ME, Choi AM, and Alam J.** Identification of activating transcription factor 4 (ATF4) as an Nrf2-interacting protein. Implication for heme oxygenase-1 gene regulation. *J Biol Chem* 276: 20858-20865, 2001.

103.   **Heidkamp MC, Bayer AL, Martin JL, and Samarel AM.** Differential activation of mitogen-activated protein kinase cascades and apoptosis by protein kinase C epsilon and delta in neonatal rat ventricular myocytes. *Circ Res* 89: 882-890, 2001.

104.   **Hertel M, Braun S, Durka S, Alzheimer C, and Werner S.** Upregulation and activation of the Nrf-1 transcription factor in the lesioned hippocampus. *The European journal of neuroscience* 15: 1707-1711, 2002.

105.   **Hill MF and Singal PK.** Antioxidant and oxidative stress changes during heart failure subsequent to myocardial infarction in rats. *The American journal of pathology* 148: 291-300, 1996.

106.   **Ho KK, Pinsky JL, Kannel WB, and Levy D.** The epidemiology of heart failure: the Framingham Study. *Journal of the American College of Cardiology* 22: 6A-13A, 1993.

107.   **Hommes FA, Everts RS, and Havinga H.** The development of DT-diaphorase in rat liver and its induction by benzo(a)pyrene. *Biology of the neonate* 34: 248-252, 1978.

108.   **Hoshida S, Nishida M, Yamashita N, Igarashi J, Aoki K, Hori M, Kuzuya T, and Tada M.** Heme oxygenase-1 expression and its relation to oxidative stress during primary culture of cardiomyocytes. *J Mol Cell Cardiol* 28: 1845-1855, 1996.

109.   **Hosoya T, Maruyama A, Kang MI, Kawatani Y, Shibata T, Uchida K, Warabi E, Noguchi N, Itoh K, and Yamamoto M.** Differential responses of the Nrf2-Keap1 system to laminar and oscillatory shear stresses in endothelial cells. *J Biol Chem* 280: 27244-27250, 2005.

110.   **Huang HC, Nguyen T, and Pickett CB.** Phosphorylation of Nrf2 at Ser-40 by protein kinase C regulates antioxidant response element-mediated transcription. *J Biol Chem* 277: 42769-42774, 2002.

111.   **Huang HC, Nguyen T, and Pickett CB.** Regulation of the antioxidant response element by protein kinase C-mediated phosphorylation of NF-E2-related factor 2. *Proc Natl Acad Sci U S A* 97: 12475-12480, 2000.

112.   **Ide T, Tsutsui H, Kinugawa S, Suematsu N, Hayashidani S, Ichikawa K, Utsumi H, Machida Y, Egashira K, and Takeshita A.** Direct evidence for increased hydroxyl radicals originating from superoxide in the failing myocardium. *Circ Res* 86: 152-157, 2000.

113.   **Igarashi K, Kataoka K, Itoh K, Hayashi N, Nishizawa M, and Yamamoto M.** Regulation of transcription by dimerization of erythroid factor NF-E2 p45 with small Maf proteins. *Nature* 367: 568-572, 1994.

114.   **Iida K, Itoh K, Kumagai Y, Oyasu R, Hattori K, Kawai K, Shimazui T, Akaza H, and Yamamoto M.** Nrf2 is essential for the chemopreventive efficacy of oltipraz against urinary bladder carcinogenesis. *Cancer Res* 64: 6424-6431, 2004.

115.   **Iizuka T, Ishii Y, Itoh K, Kiwamoto T, Kimura T, Matsuno Y, Morishima Y, Hegab AE, Homma S, Nomura A, Sakamoto T, Shimura M, Yoshida A, Yamamoto M, and Sekizawa K.** Nrf2-deficient mice are highly susceptible to cigarette smoke-induced emphysema. *Genes Cells* 10: 1113-1125, 2005.

116.   **Ishii T, Itoh K, Takahashi S, Sato H, Yanagawa T, Katoh Y, Bannai S, and Yamamoto M.** Transcription factor Nrf2 coordinately regulates a group of oxidative stress-inducible genes in macrophages. *J Biol Chem* 275: 16023-16029, 2000.

117.   **Ishii Y, Itoh K, Morishima Y, Kimura T, Kiwamoto T, Iizuka T, Hegab AE, Hosoya T, Nomura A, Sakamoto T, Yamamoto M, and Sekizawa K.** Transcription factor Nrf2 plays a pivotal role in protection against elastase-induced pulmonary inflammation and emphysema. *J Immunol* 175: 6968-6975, 2005.

118.   **Ishizuka A, Siomi MC, and Siomi H.** A Drosophila fragile X protein interacts with components of RNAi and ribosomal proteins. *Genes Dev* 16: 2497-2508, 2002.

119.   **Itoh K, Chiba T, Takahashi S, Ishii T, Igarashi K, Katoh Y, Oyake T, Hayashi N, Satoh K, Hatayama I, Yamamoto M, and Nabeshima Y.** An Nrf2/small Maf heterodimer mediates the induction of phase II detoxifying enzyme genes through antioxidant response elements. *Biochem Biophys Res Commun* 236: 313-322, 1997.

120.   **Itoh K, Wakabayashi N, Katoh Y, Ishii T, Igarashi K, Engel JD, and Yamamoto M.** Keap1 represses nuclear activation of antioxidant responsive elements by Nrf2 through binding to the amino-terminal Neh2 domain. *Genes Dev* 13: 76-86, 1999.

121.   **Itoh K, Wakabayashi N, Katoh Y, Ishii T, O'Connor T, and Yamamoto M.** Keap1 regulates both cytoplasmic-nuclear shuttling and degradation of Nrf2 in response to electrophiles. *Genes Cells* 8: 379-391, 2003.

122.   **Jain AK, Bloom DA, and Jaiswal AK.** Nuclear import and export signals in control of Nrf2. *J Biol Chem* 280: 29158-29168, 2005.

123.   **Jain AK and Jaiswal AK.** Phosphorylation of tyrosine 568 controls nuclear export of Nrf2. *J Biol Chem* 281: 12132-12142, 2006.

124.   **Jaiswal AK.** Nrf2 signaling in coordinated activation of antioxidant gene expression. *Free Radic Biol Med* 36: 1199-1207, 2004.

125.   **Johnson DA, Andrews GK, Xu W, and Johnson JA.** Activation of the antioxidant response element in primary cortical neuronal cultures derived from transgenic reporter mice. *J Neurochem* 81: 1233-1241, 2002.

126.   **Jones CI, 3rd, Zhu H, Martin SF, Han Z, Li Y, and Alevriadou BR.** Regulation of Antioxidants and Phase 2 Enzymes by Shear-Induced Reactive Oxygen Species in Endothelial Cells. *Ann Biomed Eng*, 2007.

127.   **Kahl R.** Synthetic antioxidants: biochemical actions and interference with radiation, toxic compounds, chemical mutagens and chemical carcinogens. *Toxicology* 33: 185-228, 1984.

128.   **Kang KW, Cho MK, Lee CH, and Kim SG.** Activation of phosphatidylinositol 3-kinase and Akt by tert-butylhydroquinone is responsible for antioxidant response element-mediated rGSTA2 induction in H4IIE cells. *Mol Pharmacol* 59: 1147-1156, 2001.

129.   **Kang KW, Choi SH, and Kim SG.** Peroxynitrite activates NF-E2-related factor 2/antioxidant response element through the pathway of phosphatidylinositol 3-kinase: the role of nitric oxide synthase in rat glutathione S-transferase A2 induction. *Nitric Oxide* 7: 244-253, 2002.

130.   **Kang KW, Ryu JH, and Kim SG.** The essential role of phosphatidylinositol 3-kinase and of p38 mitogen-activated protein kinase activation in the antioxidant response element-mediated rGSTA2 induction by decreased glutathione in H4IIE hepatoma cells. *Mol Pharmacol* 58: 1017-1025, 2000.

131.   **Kang MI, Kobayashi A, Wakabayashi N, Kim SG, and Yamamoto M.** Scaffolding of Keap1 to the actin cytoskeleton controls the function of Nrf2 as key regulator of cytoprotective phase 2 genes. *Proc Natl Acad Sci U S A* 101: 2046-2051, 2004.

132.   **Kannan S and Jaiswal AK.** Low and High Dose UVB Regulation of Transcription Factor NF-E2-Related Factor 2. *Cancer Res* 66: 8421-8429, 2006.

133.   **Kannel WB and McGee DL.** Diabetes and cardiovascular risk factors: the Framingham study. *Circulation* 59: 8-13, 1979.

134.   **Kataoka K, Igarashi K, Itoh K, Fujiwara KT, Noda M, Yamamoto M, and Nishizawa M.** Small Maf proteins heterodimerize with Fos and may act as competitive repressors of the NF-E2 transcription factor. *Mol Cell Biol* 15: 2180-2190, 1995.

135.   **Katoh Y, Itoh K, Yoshida E, Miyagishi M, Fukamizu A, and Yamamoto M.** Two domains of Nrf2 cooperatively bind CBP, a CREB binding protein, and synergistically activate transcription. *Genes Cells* 6: 857-868, 2001.

136.   **Katsuoka F, Motohashi H, Engel JD, and Yamamoto M.** Nrf2 transcriptionally activates the mafG gene through an antioxidant response element. *J Biol Chem* 280: 4483-4490, 2005.

137.   **Kawamoto Y, Nakamura Y, Naito Y, Torii Y, Kumagai T, Osawa T, Ohigashi H, Satoh K, Imagawa M, and Uchida K.** Cyclopentenone prostaglandins as potential inducers of phase II detoxification enzymes. 15-deoxy-delta(12,14)-prostaglandin j2-induced expression of glutathione S-transferases. *J Biol Chem* 275: 11291-11299, 2000.

138.   **Keith M, Geranmayegan A, Sole MJ, Kurian R, Robinson A, Omran AS, and Jeejeebhoy KN.** Increased oxidative stress in patients with congestive heart failure. *Journal of the American College of Cardiology* 31: 1352-1356, 1998.

139.   **Kelly VP, Ellis EM, Manson MM, Chanas SA, Moffat GJ, McLeod R, Judah DJ, Neal GE, and Hayes JD.** Chemoprevention of aflatoxin B1 hepatocarcinogenesis by coumarin, a natural benzopyrone that is a potent inducer of aflatoxin B1-aldehyde reductase, the glutathione S-transferase A5 and P1 subunits, and NAD(P)H:quinone oxidoreductase in rat liver. *Cancer Res* 60: 957-969, 2000.

140.   **Kerppola TK and Curran T.** A conserved region adjacent to the basic domain is required for recognition of an extended DNA binding site by Maf/Nrl family proteins. *Oncogene* 9: 3149-3158, 1994.

141.   **Keum YS, Han YH, Liew C, Kim JH, Xu C, Yuan X, Shakarjian MP, Chong S, and Kong AN.** Induction of heme oxygenase-1 (HO-1) and NAD[P]H: quinone oxidoreductase 1 (NQO1) by a phenolic antioxidant, butylated hydroxyanisole (BHA)

and its metabolite, tert-butylhydroquinone (tBHQ) in primary-cultured human and rat hepatocytes. *Pharmaceutical research* 23: 2586-2594, 2006.

142. **Kimes BW and Brandt BL.** Properties of a clonal muscle cell line from rat heart. *Experimental cell research* 98: 367-381, 1976.

143. **Kinugawa S, Tsutsui H, Hayashidani S, Ide T, Suematsu N, Satoh S, Utsumi H, and Takeshita A.** Treatment with dimethylthiourea prevents left ventricular remodeling and failure after experimental myocardial infarction in mice: role of oxidative stress. *Circ Res* 87: 392-398, 2000.

144. **Kirchhoff F, Dringen R, and Giaume C.** Pathways of neuron-astrocyte interactions and their possible role in neuroprotection. *European archives of psychiatry and clinical neuroscience* 251: 159-169, 2001.

145. **Kobayashi A, Ito E, Toki T, Kogame K, Takahashi S, Igarashi K, Hayashi N, and Yamamoto M.** Molecular cloning and functional characterization of a new Cap'n' collar family transcription factor Nrf3. *J Biol Chem* 274: 6443-6452, 1999.

146. **Kobayashi A, Kang MI, Okawa H, Ohtsuji M, Zenke Y, Chiba T, Igarashi K, and Yamamoto M.** Oxidative stress sensor Keap1 functions as an adaptor for Cul3-based E3 ligase to regulate proteasomal degradation of Nrf2. *Mol Cell Biol* 24: 7130-7139, 2004.

147. **Kobayashi A, Kang MI, Watai Y, Tong KI, Shibata T, Uchida K, and Yamamoto M.** Oxidative and electrophilic stresses activate Nrf2 through inhibition of ubiquitination activity of Keap1. *Mol Cell Biol* 26: 221-229, 2006.

148. **Kohgo Y, Ohtake T, Ikuta K, Suzuki Y, Hosoki Y, Saito H, and Kato J.** Iron accumulation in alcoholic liver diseases. *Alcoholism, clinical and experimental research* 29: 189S-193S, 2005.

149. **Kong AN, Owuor E, Yu R, Hebbar V, Chen C, Hu R, and Mandlekar S.** Induction of xenobiotic enzymes by the MAP kinase pathway and the antioxidant or electrophile response element (ARE/EpRE). *Drug Metab Rev* 33: 255-271, 2001.

150. **Kong L, Tanito M, Huang Z, Li F, Zhou X, Zaharia A, Yodoi J, McGinnis JF, and Cao W.** Delay of photoreceptor degeneration in tubby mouse by sulforaphane. *J Neurochem*, 2007.

151. **Kotkow KJ and Orkin SH.** Dependence of globin gene expression in mouse erythroleukemia cells on the NF-E2 heterodimer. *Mol Cell Biol* 15: 4640-4647, 1995.

152. **Kraft AD, Johnson DA, and Johnson JA.** Nuclear factor E2-related factor 2-dependent antioxidant response element activation by tert-butylhydroquinone and sulforaphane occurring preferentially in astrocytes conditions neurons against oxidative insult. *J Neurosci* 24: 1101-1112, 2004.

153. **Kris-Etherton PM, Hecker KD, and Binkoski AE.** Polyunsaturated fatty acids and cardiovascular health. *Nutrition reviews* 62: 414-426, 2004.

154. **Kris-Etherton PM, Lichtenstein AH, Howard BV, Steinberg D, and Witztum JL.** Antioxidant vitamin supplements and cardiovascular disease. *Circulation* 110: 637-641, 2004.

155. **Kritharides L and Stocker R.** The use of antioxidant supplements in coronary heart disease. *Atherosclerosis* 164: 211-219, 2002.

156.   **Kumaki K, Jensen NM, Shire JG, and Nebert DW.** Genetic differences in induction of cytosol reduced-NAD(P):menadione oxidoreductase and microsomal aryl hydrocarbon hydroxylase in the mouse. *J Biol Chem* 252: 157-165, 1977.

157.   **Kwak MK, Egner PA, Dolan PM, Ramos-Gomez M, Groopman JD, Itoh K, Yamamoto M, and Kensler TW.** Role of phase 2 enzyme induction in chemoprotection by dithiolethiones. *Mutation research* 480-481: 305-315, 2001.

158.   **Kwak MK, Itoh K, Yamamoto M, Sutter TR, and Kensler TW.** Role of transcription factor Nrf2 in the induction of hepatic phase 2 and antioxidative enzymes in vivo by the cancer chemoprotective agent, 3H-1, 2-dimethiole-3-thione. *Molecular medicine (Cambridge, Mass* 7: 135-145, 2001.

159.   **Kwak MK, Wakabayashi N, Greenlaw JL, Yamamoto M, and Kensler TW.** Antioxidants enhance mammalian proteasome expression through the Keap1-Nrf2 signaling pathway. *Mol Cell Biol* 23: 8786-8794, 2003.

160.   **Kwong M, Kan YW, and Chan JY.** The CNC basic leucine zipper factor, Nrf1, is essential for cell survival in response to oxidative stress-inducing agents. Role for Nrf1 in gamma-gcs(l) and gss expression in mouse fibroblasts. *J Biol Chem* 274: 37491-37498, 1999.

161.   **Lakka HM, Laaksonen DE, Lakka TA, Niskanen LK, Kumpusalo E, Tuomilehto J, and Salonen JT.** The metabolic syndrome and total and cardiovascular disease mortality in middle-aged men. *Jama* 288: 2709-2716, 2002.

162.   **Larson RA, Wang Y, Banerjee M, Wiemels J, Hartford C, Le Beau MM, and Smith MT.** Prevalence of the inactivating 609C-->T polymorphism in the NAD(P)H:quinone oxidoreductase (NQO1) gene in patients with primary and therapy-related myeloid leukemia. *Blood* 94: 803-807, 1999.

163.   **Le Good JA, Ziegler WH, Parekh DB, Alessi DR, Cohen P, and Parker PJ.** Protein kinase C isotypes controlled by phosphoinositide 3-kinase through the protein kinase PDK1. *Science (New York, NY* 281: 2042-2045, 1998.

164.   **Lee JM, Calkins MJ, Chan K, Kan YW, and Johnson JA.** Identification of the NF-E2-related factor-2-dependent genes conferring protection against oxidative stress in primary cortical astrocytes using oligonucleotide microarray analysis. *J Biol Chem* 278: 12029-12038, 2003.

165.   **Lee JM, Hanson JM, Chu WA, and Johnson JA.** Phosphatidylinositol 3-kinase, not extracellular signal-regulated kinase, regulates activation of the antioxidant-responsive element in IMR-32 human neuroblastoma cells. *J Biol Chem* 276: 20011-20016, 2001.

166.   **Lee JM, Li J, Johnson DA, Stein TD, Kraft AD, Calkins MJ, Jakel RJ, and Johnson JA.** Nrf2, a multi-organ protector? *Faseb J* 19: 1061-1066, 2005.

167.   **Lee JM, Moehlenkamp JD, Hanson JM, and Johnson JA.** Nrf2-dependent activation of the antioxidant responsive element by tert-butylhydroquinone is independent of oxidative stress in IMR-32 human neuroblastoma cells. *Biochem Biophys Res Commun* 280: 286-292, 2001.

168.   **Lee JM, Shih AY, Murphy TH, and Johnson JA.** NF-E2-related factor-2 mediates neuroprotection against mitochondrial complex I inhibitors and increased concentrations of intracellular calcium in primary cortical neurons. *J Biol Chem* 278: 37948-37956, 2003.

169.	**Lee Y, Ahn C, Han J, Choi H, Kim J, Yim J, Lee J, Provost P, Radmark O, Kim S, and Kim VN.** The nuclear RNase III Drosha initiates microRNA processing. *Nature* 425: 415-419, 2003.

170.	**Leitinger N.** Oxidized phospholipids as modulators of inflammation in atherosclerosis. *Current opinion in lipidology* 14: 421-430, 2003.

171.	**Leonard MO, Kieran NE, Howell K, Burne MJ, Varadarajan R, Dhakshinamoorthy S, Porter AG, O'Farrelly C, Rabb H, and Taylor CT.** Reoxygenation-specific activation of the antioxidant transcription factor Nrf2 mediates cytoprotective gene expression in ischemia-reperfusion injury. *Faseb J* 20: 2624-2626, 2006.

172.	**Levonen AL, Landar A, Ramachandran A, Ceaser EK, Dickinson DA, Zanoni G, Morrow JD, and Darley-Usmar VM.** Cellular mechanisms of redox cell signalling: role of cysteine modification in controlling antioxidant defences in response to electrophilic lipid oxidation products. *Biochem J* 378: 373-382, 2004.

173.	**Li J, Johnson D, Calkins M, Wright L, Svendsen C, and Johnson J.** Stabilization of Nrf2 by tBHQ Confers Protection against Oxidative Stress-Induced Cell Death in Human Neural Stem Cells. *Toxicol Sci*, 2004.

174.	**Li J and Johnson JA.** Time-dependent changes in ARE-driven gene expression by use of a noise-filtering process for microarray data. *Physiological genomics* 9: 137-144, 2002.

175.	**Li J, Lee JM, and Johnson JA.** Microarray analysis reveals an antioxidant responsive element-driven gene set involved in conferring protection from an oxidative stress-induced apoptosis in IMR-32 cells. *J Biol Chem* 277: 388-394, 2002.

176.	**Li J, Spletter ML, and Johnson JA.** Dissecting tBHQ induced ARE-driven gene expression through long and short oligonucleotide arrays. *Physiological genomics* 21: 43-58, 2005.

177.	**Li J, Stein TD, and Johnson JA.** Genetic dissection of systemic autoimmune disease in Nrf2-deficient mice. *Physiological genomics* 18: 261-272, 2004.

178.	**Li MH, Cha YN, and Surh YJ.** Peroxynitrite induces HO-1 expression via PI3K/Akt-dependent activation of NF-E2-related factor 2 in PC12 cells. *Free Radic Biol Med* 41: 1079-1091, 2006.

179.	**Li N, Alam J, Venkatesan MI, Eiguren-Fernandez A, Schmitz D, Di Stefano E, Slaughter N, Killeen E, Wang X, Huang A, Wang M, Miguel AH, Cho A, Sioutas C, and Nel AE.** Nrf2 is a key transcription factor that regulates antioxidant defense in macrophages and epithelial cells: protecting against the proinflammatory and oxidizing effects of diesel exhaust chemicals. *J Immunol* 173: 3467-3481, 2004.

180.	**Li N and Nel AE.** Role of the Nrf2-mediated signaling pathway as a negative regulator of inflammation: implications for the impact of particulate pollutants on asthma. *Antioxidants & redox signaling* 8: 88-98, 2006.

181.	**Li R, Chen W, Yanes R, Lee S, and Berliner JA.** OKL38 is an oxidative stress response gene stimulated by oxidized phospholipids. *Journal of lipid research* 48: 709-715, 2007.

182.	**Li W, Jain MR, Chen C, Yue X, Hebbar V, Zhou R, and Kong AN.** NRF2 possesses a Redox-insensitive nuclear export signal overlapping with the leucine zipper motif. *J Biol Chem*, 2005.

183.   **Li X, Blizzard KK, Zeng Z, DeVries AC, Hurn PD, and McCullough LD.** Chronic behavioral testing after focal ischemia in the mouse: functional recovery and the effects of gender. *Experimental neurology* 187: 94-104, 2004.

184.   **Li Y and Jaiswal AK.** Regulation of human NAD(P)H:quinone oxidoreductase gene. Role of AP1 binding site contained within human antioxidant response element. *J Biol Chem* 267: 15097-15104, 1992.

185.   **Lieber CS.** Cytochrome P-4502E1: its physiological and pathological role. *Physiological reviews* 77: 517-544, 1997.

186.   **Lin W, Shen G, Yuan X, Jain MR, Yu S, Zhang A, Chen JD, and Kong AN.** Regulation of Nrf2 transactivation domain activity by p160 RAC3/SRC3 and other nuclear co-regulators. *Journal of biochemistry and molecular biology* 39: 304-310, 2006.

187.   **Liu RM, Hu H, Robison TW, and Forman HJ.** Differential enhancement of gamma-glutamyl transpeptidase and gamma-glutamylcysteine synthetase by tert-butylhydroquinone in rat lung epithelial L2 cells. *Am J Respir Cell Mol Biol* 14: 186-191, 1996.

188.   **Liu X, Wei J, Peng DH, Layne MD, and Yet SF.** Absence of heme oxygenase-1 exacerbates myocardial ischemia/reperfusion injury in diabetic mice. *Diabetes* 54: 778-784, 2005.

189.   **Liu XM, Peyton KJ, Ensenat D, Wang H, Hannink M, Alam J, and Durante W.** Nitric oxide stimulates heme oxygenase-1 gene transcription via the Nrf2/ARE complex to promote vascular smooth muscle cell survival. *Cardiovascular research*, 2007.

190.   **Livak KJ and Schmittgen TD.** Analysis of relative gene expression data using real-time quantitative PCR and the 2(-Delta Delta C(T)) Method. *Methods (San Diego, Calif* 25: 402-408, 2001.

191.   **Liverman CS, Cui L, Yong C, Choudhuri R, Klein RM, Welch KM, and Berman NE.** Response of the brain to oligemia: gene expression, c-Fos, and Nrf2 localization. *Brain research* 126: 57-66, 2004.

192.   **Long DJ, 2nd, Gaikwad A, Multani A, Pathak S, Montgomery CA, Gonzalez FJ, and Jaiswal AK.** Disruption of the NAD(P)H:quinone oxidoreductase 1 (NQO1) gene in mice causes myelogenous hyperplasia. *Cancer Res* 62: 3030-3036, 2002.

193.   **Lorentzen RJ, Lesko SA, McDonald K, and Ts'o PO.** Toxicity of metabolic benzo(a)pyrenediones to cultured cells and the dependence upon molecular oxygen. *Cancer Res* 39: 3194-3198, 1979.

194.   **Louhelainen M, Merasto S, Finckenberg P, Lapatto R, Cheng ZJ, and Mervaala EM.** Lipoic acid supplementation prevents cyclosporine-induced hypertension and nephrotoxicity in spontaneously hypertensive rats. *Journal of hypertension* 24: 947-956, 2006.

195.   **Lubet RA, Connolly G, Kouri RE, Nebert DW, and Bigelow SW.** Biological effects of the Sudan dyes. Role of the Ah cytosolic receptor. *Biochemical pharmacology* 32: 3053-3058, 1983.

196.   **Ma Q, Kinneer K, Bi Y, Chan JY, and Kan YW.** Induction of murine NAD(P)H:quinone oxidoreductase by 2,3,7,8-tetrachlorodibenzo-p-dioxin requires the CNC (cap 'n' collar) basic leucine zipper transcription factor Nrf2 (nuclear factor

erythroid 2-related factor 2): cross-interaction between AhR (aryl hydrocarbon receptor) and Nrf2 signal transduction. *Biochem J* 377: 205-213, 2004.

197.   **Marini MG, Chan K, Casula L, Kan YW, Cao A, and Moi P.** hMAF, a small human transcription factor that heterodimerizes specifically with Nrf1 and Nrf2. *J Biol Chem* 272: 16490-16497, 1997.

198.   **Marzec JM, Christie JD, Reddy SP, Jedlicka AE, Vuong H, Lanken PN, Aplenc R, Yamamoto T, Yamamoto M, Cho HY, and Kleeberger SR.** Functional polymorphisms in the transcription factor NRF2 in humans increase the risk of acute lung injury. *Faseb J*, 2007.

199.   **Maulik N, Sharma HS, and Das DK.** Induction of the haem oxygenase gene expression during the reperfusion of ischemic rat myocardium. *J Mol Cell Cardiol* 28: 1261-1270, 1996.

200.   **Maurer BJ, Metelitsa LS, Seeger RC, Cabot MC, and Reynolds CP.** Increase of ceramide and induction of mixed apoptosis/necrosis by N-(4-hydroxyphenyl)-retinamide in neuroblastoma cell lines. *Journal of the National Cancer Institute* 91: 1138-1146, 1999.

201.   **McMahon M, Itoh K, Yamamoto M, Chanas SA, Henderson CJ, McLellan LI, Wolf CR, Cavin C, and Hayes JD.** The Cap'n'Collar basic leucine zipper transcription factor Nrf2 (NF-E2 p45-related factor 2) controls both constitutive and inducible expression of intestinal detoxification and glutathione biosynthetic enzymes. *Cancer Res* 61: 3299-3307, 2001.

202.   **McMahon M, Itoh K, Yamamoto M, and Hayes JD.** Keap1-dependent proteasomal degradation of transcription factor Nrf2 contributes to the negative regulation of antioxidant response element-driven gene expression. *J Biol Chem* 278: 21592-21600, 2003.

203.   **McMahon M, Thomas N, Itoh K, Yamamoto M, and Hayes JD.** Dimerization of substrate adaptors can facilitate cullin-mediated ubiquitylation of proteins by a "tethering" mechanism: a two-site interaction model for the Nrf2-Keap1 complex. *J Biol Chem* 281: 24756-24768, 2006.

204.   **McManus MT and Sharp PA.** Gene silencing in mammals by small interfering RNAs. *Nature reviews* 3: 737-747, 2002.

205.   **Menard C, Pupier S, Mornet D, Kitzmann M, Nargeot J, and Lory P.** Modulation of L-type calcium channel expression during retinoic acid-induced differentiation of H9C2 cardiac cells. *J Biol Chem* 274: 29063-29070, 1999.

206.   **Miller ER, 3rd, Pastor-Barriuso R, Dalal D, Riemersma RA, Appel LJ, and Guallar E.** Meta-analysis: high-dosage vitamin E supplementation may increase all-cause mortality. *Annals of internal medicine* 142: 37-46, 2005.

207.   **Min SK, Kim SY, Kim CH, Woo JS, Jung JS, and Kim YK.** Role of lipid peroxidation and poly(ADP-ribose) polymerase activation in oxidant-induced membrane transport dysfunction in opossum kidney cells. *Toxicology and applied pharmacology* 166: 196-202, 2000.

208.   **Moehlenkamp JD and Johnson JA.** Activation of antioxidant/electrophile-responsive elements in IMR-32 human neuroblastoma cells. *Archives of biochemistry and biophysics* 363: 98-106, 1999.

209.	**Moi P, Chan K, Asunis I, Cao A, and Kan YW.** Isolation of NF-E2-related factor 2 (Nrf2), a NF-E2-like basic leucine zipper transcriptional activator that binds to the tandem NF-E2/AP1 repeat of the beta-globin locus control region. *Proc Natl Acad Sci U S A* 91: 9926-9930, 1994.

210.	**Moi P and Kan YW.** Synergistic enhancement of globin gene expression by activator protein-1-like proteins. *Proc Natl Acad Sci U S A* 87: 9000-9004, 1990.

211.	**Moran JA, Dahl EL, and Mulcahy RT.** Differential induction of mafF, mafG and mafK expression by electrophile-response-element activators. *Biochem J* 361: 371-377, 2002.

212.	**Moran JL, Siegel D, and Ross D.** A potential mechanism underlying the increased susceptibility of individuals with a polymorphism in NAD(P)H:quinone oxidoreductase 1 (NQO1) to benzene toxicity. *Proc Natl Acad Sci U S A* 96: 8150-8155, 1999.

213.	**Motohashi H, Katsuoka F, Engel JD, and Yamamoto M.** Small Maf proteins serve as transcriptional cofactors for keratinocyte differentiation in the Keap1-Nrf2 regulatory pathway. *Proc Natl Acad Sci U S A* 101: 6379-6384, 2004.

214.	**Motohashi H, Shavit JA, Igarashi K, Yamamoto M, and Engel JD.** The world according to Maf. *Nucleic acids research* 25: 2953-2959, 1997.

215.	**Mourelatos Z, Dostie J, Paushkin S, Sharma A, Charroux B, Abel L, Rappsilber J, Mann M, and Dreyfuss G.** miRNPs: a novel class of ribonucleoproteins containing numerous microRNAs. *Genes Dev* 16: 720-728, 2002.

216.	**Nagai T, Igarashi K, Akasaka J, Furuyama K, Fujita H, Hayashi N, Yamamoto M, and Sassa S.** Regulation of NF-E2 activity in erythroleukemia cell differentiation. *J Biol Chem* 273: 5358-5365, 1998.

217.	**Naughton P, Hoque M, Green CJ, Foresti R, and Motterlini R.** Interaction of heme with nitroxyl or nitric oxide amplifies heme oxygenase-1 induction: involvement of the transcription factor Nrf2. *Cell Mol Biol (Noisy-le-grand)* 48: 885-894, 2002.

218.	**Nebert DW, Roe AL, Vandale SE, Bingham E, and Oakley GG.** NAD(P)H:quinone oxidoreductase (NQO1) polymorphism, exposure to benzene, and predisposition to disease: a HuGE review. *Genet Med* 4: 62-70, 2002.

219.	**Ney PA, Andrews NC, Jane SM, Safer B, Purucker ME, Weremowicz S, Morton CC, Goff SC, Orkin SH, and Nienhuis AW.** Purification of the human NF-E2 complex: cDNA cloning of the hematopoietic cell-specific subunit and evidence for an associated partner. *Mol Cell Biol* 13: 5604-5612, 1993.

220.	**Nguyen T, Huang HC, and Pickett CB.** Transcriptional regulation of the antioxidant response element. Activation by Nrf2 and repression by MafK. *J Biol Chem* 275: 15466-15473, 2000.

221.	**Nguyen T, Rushmore TH, and Pickett CB.** Transcriptional regulation of a rat liver glutathione S-transferase Ya subunit gene. Analysis of the antioxidant response element and its activation by the phorbol ester 12-O-tetradecanoylphorbol-13-acetate. *J Biol Chem* 269: 13656-13662, 1994.

222.	**Nguyen T, Sherratt PJ, Huang HC, Yang CS, and Pickett CB.** Increased protein stability as a mechanism that enhances Nrf2-mediated transcriptional activation of the antioxidant response element. Degradation of Nrf2 by the 26 S proteasome. *J Biol Chem* 278: 4536-4541, 2003.

223.   **Nguyen T, Sherratt PJ, and Pickett CB.** Regulatory mechanisms controlling gene expression mediated by the antioxidant response element. *Annu Rev Pharmacol Toxicol* 43: 233-260, 2003.

224.   **Novotny V, Prieschl EE, Csonga R, Fabjani G, and Baumruker T.** Nrf1 in a complex with fosB, c-jun, junD and ATF2 forms the AP1 component at the TNF alpha promoter in stimulated mast cells. *Nucleic acids research* 26: 5480-5485, 1998.

225.   **Nykanen A, Haley B, and Zamore PD.** ATP requirements and small interfering RNA structure in the RNA interference pathway. *Cell* 107: 309-321, 2001.

226.   **Ohlemiller KK, Hughes RM, Lett JM, Ogilvie JM, Speck JD, Wright JS, and Faddis BT.** Progression of cochlear and retinal degeneration in the tubby (rd5) mouse. *Audiology & neuro-otology* 2: 175-185, 1997.

227.   **Ohlemiller KK, Hughes RM, Mosinger-Ogilvie J, Speck JD, Grosof DH, and Silverman MS.** Cochlear and retinal degeneration in the tubby mouse. *Neuroreport* 6: 845-849, 1995.

228.   **Okawa H, Motohashi H, Kobayashi A, Aburatani H, Kensler TW, and Yamamoto M.** Hepatocyte-specific deletion of the keap1 gene activates Nrf2 and confers potent resistance against acute drug toxicity. *Biochem Biophys Res Commun* 339: 79-88, 2006.

229.   **Ossareh-Nazari B, Bachelerie F, and Dargemont C.** Evidence for a role of CRM1 in signal-mediated nuclear protein export. *Science (New York, NY* 278: 141-144, 1997.

230.   **Owens IS.** Genetic regulation of UDP-glucuronosyltransferase induction by polycyclic aromatic compounds in mice. Co-segregation with aryl hydrocarbon (benzo(alpha)pyrene) hydroxylase induction. *J Biol Chem* 252: 2827-2833, 1977.

231.   **Oyake T, Itoh K, Motohashi H, Hayashi N, Hoshino H, Nishizawa M, Yamamoto M, and Igarashi K.** Bach proteins belong to a novel family of BTB-basic leucine zipper transcription factors that interact with MafK and regulate transcription through the NF-E2 site. *Mol Cell Biol* 16: 6083-6095, 1996.

232.   **Padmanabhan B, Tong KI, Ohta T, Nakamura Y, Scharlock M, Ohtsuji M, Kang MI, Kobayashi A, Yokoyama S, and Yamamoto M.** Structural basis for defects of Keap1 activity provoked by its point mutations in lung cancer. *Molecular cell* 21: 689-700, 2006.

233.   **Pagano M, Naviglio S, Spina A, Chiosi E, Castoria G, Romano M, Sorrentino A, Illiano F, and Illiano G.** Differentiation of H9c2 cardiomyoblasts: The role of adenylate cyclase system. *J Cell Physiol* 198: 408-416, 2004.

234.   **Papaiahgari S, Kleeberger SR, Cho HY, Kalvakolanu DV, and Reddy SP.** NADPH oxidase and ERK signaling regulates hyperoxia-induced Nrf2-ARE transcriptional response in pulmonary epithelial cells. *J Biol Chem* 279: 42302-42312, 2004.

235.   **Papaiahgari S, Zhang Q, Kleeberger SR, Cho HY, and Reddy SP.** Hyperoxia stimulates an Nrf2-ARE transcriptional response via ROS-EGFR-PI3K-Akt/ERK MAP kinase signaling in pulmonary epithelial cells. *Antioxidants & redox signaling* 8: 43-52, 2006.

236.   **Park EY and Kim SG.** NO signaling in ARE-mediated gene expression. *Methods Enzymol* 396: 341-349, 2005.

237. **Pedersen TX, Leethanakul C, Patel V, Mitola D, Lund LR, Dano K, Johnsen M, Gutkind JS, and Bugge TH.** Laser capture microdissection-based in vivo genomic profiling of wound keratinocytes identifies similarities and differences to squamous cell carcinoma. *Oncogene* 22: 3964-3976, 2003.

238. **Pi J, Qu W, Reece JM, Kumagai Y, and Waalkes MP.** Transcription factor Nrf2 activation by inorganic arsenic in cultured keratinocytes: involvement of hydrogen peroxide. *Experimental cell research* 290: 234-245, 2003.

239. **Picciotto MR and Wickman K.** Using knockout and transgenic mice to study neurophysiology and behavior. *Physiological reviews* 78: 1131-1163, 1998.

240. **Piconi L, Quagliaro L, and Ceriello A.** Oxidative stress in diabetes. *Clin Chem Lab Med* 41: 1144-1149, 2003.

241. **Piret JP, Arnould T, Fuks B, Chatelain P, Remacle J, and Michiels C.** Mitochondria permeability transition-dependent tert-butyl hydroperoxide-induced apoptosis in hepatoma HepG2 cells. *Biochemical pharmacology* 67: 611-620, 2004.

242. **Pischke SE, Zhou Z, Song R, Ning W, Alam J, Ryter SW, and Choi AM.** Phosphatidylinositol 3-kinase/Akt pathway mediates heme oxygenase-1 regulation by lipopolysaccharide. *Cell Mol Biol (Noisy-le-grand)* 51: 461-470, 2005.

243. **Plum L, Wunderlich FT, Baudler S, Krone W, and Bruning JC.** Transgenic and knockout mice in diabetes research: novel insights into pathophysiology, limitations, and perspectives. *Physiology (Bethesda, Md* 20: 152-161, 2005.

244. **Prestera T, Holtzclaw WD, Zhang Y, and Talalay P.** Chemical and molecular regulation of enzymes that detoxify carcinogens. *Proc Natl Acad Sci U S A* 90: 2965-2969, 1993.

245. **Prieschl EE, Novotny V, Csonga R, Jaksche D, Elbe-Burger A, Thumb W, Auer M, Stingl G, and Baumruker T.** A novel splice variant of the transcription factor Nrf1 interacts with the TNFalpha promoter and stimulates transcription. *Nucleic acids research* 26: 2291-2297, 1998.

246. **Prochaska HJ, De Long MJ, and Talalay P.** On the mechanisms of induction of cancer-protective enzymes: a unifying proposal. *Proc Natl Acad Sci U S A* 82: 8232-8236, 1985.

247. **Prochaska HJ and Talalay P.** Regulatory mechanisms of monofunctional and bifunctional anticarcinogenic enzyme inducers in murine liver. *Cancer Res* 48: 4776-4782, 1988.

248. **Purdom-Dickinson SE, Lin Y, Dedek M, Morrissy S, Johnson J, and Chen QM.** Induction of antioxidant and detoxification response by oxidants in cardiomyocytes: evidence from gene expression profiling and activation of Nrf2 transcription factor. *J Mol Cell Cardiol* 42: 159-176, 2007.

249. **Ramos-Gomez M, Dolan PM, Itoh K, Yamamoto M, and Kensler TW.** Interactive effects of nrf2 genotype and oltipraz on benzo[a]pyrene-DNA adducts and tumor yield in mice. *Carcinogenesis* 24: 461-467, 2003.

250. **Ramos-Gomez M, Kwak MK, Dolan PM, Itoh K, Yamamoto M, Talalay P, and Kensler TW.** Sensitivity to carcinogenesis is increased and chemoprotective efficacy of enzyme inducers is lost in nrf2 transcription factor-deficient mice. *Proc Natl Acad Sci U S A* 98: 3410-3415, 2001.

251.	**Rangasamy T, Cho CY, Thimmulappa RK, Zhen L, Srisuma SS, Kensler TW, Yamamoto M, Petrache I, Tuder RM, and Biswal S.** Genetic ablation of Nrf2 enhances susceptibility to cigarette smoke-induced emphysema in mice. *The Journal of clinical investigation* 114: 1248-1259, 2004.

252.	**Reiners JJ, Jr., Lee JY, Clift RE, Dudley DT, and Myrand SP.** PD98059 is an equipotent antagonist of the aryl hydrocarbon receptor and inhibitor of mitogen-activated protein kinase kinase. *Mol Pharmacol* 53: 438-445, 1998.

253.	**Riley SJ and Stouffer GA.** Cardiology Grand Rounds from the University of North Carolina at Chapel Hill. The antioxidant vitamins and coronary heart disease: Part II. Randomized clinical trials. *The American journal of the medical sciences* 325: 15-19, 2003.

254.	**Rimm EB, Stampfer MJ, Ascherio A, Giovannucci E, Colditz GA, and Willett WC.** Vitamin E consumption and the risk of coronary heart disease in men. *The New England journal of medicine* 328: 1450-1456, 1993.

255.	**Rushmore TH, King RG, Paulson KE, and Pickett CB.** Regulation of glutathione S-transferase Ya subunit gene expression: identification of a unique xenobiotic-responsive element controlling inducible expression by planar aromatic compounds. *Proc Natl Acad Sci U S A* 87: 3826-3830, 1990.

256.	**Rushmore TH, Morton MR, and Pickett CB.** The antioxidant responsive element. Activation by oxidative stress and identification of the DNA consensus sequence required for functional activity. *J Biol Chem* 266: 11632-11639, 1991.

257.	**Rushmore TH and Pickett CB.** Transcriptional regulation of the rat glutathione S-transferase Ya subunit gene. Characterization of a xenobiotic-responsive element controlling inducible expression by phenolic antioxidants. *J Biol Chem* 265: 14648-14653, 1990.

258.	**Rushworth SA, Chen XL, Mackman N, Ogborne RM, and O'Connell MA.** Lipopolysaccharide-induced heme oxygenase-1 expression in human monocytic cells is mediated via Nrf2 and protein kinase C. *J Immunol* 175: 4408-4415, 2005.

259.	**Sankaranarayanan K and Jaiswal AK.** Nrf3 negatively regulates antioxidant-response element-mediated expression and antioxidant induction of NAD(P)H:quinone oxidoreductase1 gene. *J Biol Chem* 279: 50810-50817, 2004.

260.	**Seo YJ, Lee JW, Lee EH, Lee HK, Kim HW, and Kim YH.** Role of glutathione in the adaptive tolerance to H2O2. *Free Radic Biol Med* 37: 1272-1281, 2004.

261.	**Sharma HS, Maulik N, Gho BC, Das DK, and Verdouw PD.** Coordinated expression of heme oxygenase-1 and ubiquitin in the porcine heart subjected to ischemia and reperfusion. *Molecular and cellular biochemistry* 157: 111-116, 1996.

262.	**Sharp PA.** RNA interference--2001. *Genes Dev* 15: 485-490, 2001.

263.	**Sharples EJ, Thiemermann C, and Yaqoob MM.** Mechanisms of disease: Cell death in acute renal failure and emerging evidence for a protective role of erythropoietin. *Nat Clin Pract Nephrol* 1: 87-97, 2005.

264.	**Shih AY, Imbeault S, Barakauskas V, Erb H, Jiang L, Li P, and Murphy TH.** Induction of the Nrf2-driven antioxidant response confers neuroprotection during mitochondrial stress in vivo. *J Biol Chem* 280: 22925-22936, 2005.

265.	**Shih AY, Johnson DA, Wong G, Kraft AD, Jiang L, Erb H, Johnson JA, and Murphy TH.** Coordinate regulation of glutathione biosynthesis and release by Nrf2-expressing glia potently protects neurons from oxidative stress. *J Neurosci* 23: 3394-3406, 2003.

266.	**Shih AY, Li P, and Murphy TH.** A small-molecule-inducible Nrf2-mediated antioxidant response provides effective prophylaxis against cerebral ischemia in vivo. *J Neurosci* 25: 10321-10335, 2005.

267.	**Shinkai Y, Sumi D, Fukami I, Ishii T, and Kumagai Y.** Sulforaphane, an activator of Nrf2, suppresses cellular accumulation of arsenic and its cytotoxicity in primary mouse hepatocytes. *FEBS Lett* 580: 1771-1774, 2006.

268.	**Simon C, Simon M, Vucelic G, Hicks MJ, Plinkert PK, Koitschev A, and Zenner HP.** The p38 SAPK pathway regulates the expression of the MMP-9 collagenase via AP-1-dependent promoter activation. *Experimental cell research* 271: 344-355, 2001.

269.	**Singh A, Misra V, Thimmulappa RK, Lee H, Ames S, Hoque MO, Herman JG, Baylin SB, Sidransky D, Gabrielson E, Brock MV, and Biswal S.** Dysfunctional KEAP1-NRF2 interaction in non-small-cell lung cancer. *PLoS medicine* 3: e420, 2006.

270.	**Siow RC, Li FY, Rowlands DJ, de Winter P, and Mann GE.** Cardiovascular targets for estrogens and phytoestrogens: Transcriptional regulation of nitric oxide synthase and antioxidant defense genes. *Free Radic Biol Med* 42: 909-925, 2007.

271.	**Smith MT, Wang Y, Kane E, Rollinson S, Wiemels JL, Roman E, Roddam P, Cartwright R, and Morgan G.** Low NAD(P)H:quinone oxidoreductase 1 activity is associated with increased risk of acute leukemia in adults. *Blood* 97: 1422-1426, 2001.

272.	**Smith MT, Wang Y, Skibola CF, Slater DJ, Lo Nigro L, Nowell PC, Lange BJ, and Felix CA.** Low NAD(P)H:quinone oxidoreductase activity is associated with increased risk of leukemia with MLL translocations in infants and children. *Blood* 100: 4590-4593, 2002.

273.	**Soares MP, Lin Y, Anrather J, Csizmadia E, Takigami K, Sato K, Grey ST, Colvin RB, Choi AM, Poss KD, and Bach FH.** Expression of heme oxygenase-1 can determine cardiac xenograft survival. *Nat Med* 4: 1073-1077, 1998.

274.	**Srisook K and Cha YN.** Super-induction of HO-1 in macrophages stimulated with lipopolysaccharide by prior depletion of glutathione decreases iNOS expression and NO production. *Nitric Oxide* 12: 70-79, 2005.

275.	**Stade K, Ford CS, Guthrie C, and Weis K.** Exportin 1 (Crm1p) is an essential nuclear export factor. *Cell* 90: 1041-1050, 1997.

276.	**Stephens NG, Parsons A, Schofield PM, Kelly F, Cheeseman K, and Mitchinson MJ.** Randomised controlled trial of vitamin E in patients with coronary disease: Cambridge Heart Antioxidant Study (CHAOS). *Lancet* 347: 781-786, 1996.

277.	**Stewart D, Killeen E, Naquin R, Alam S, and Alam J.** Degradation of transcription factor Nrf2 via the ubiquitin-proteasome pathway and stabilization by cadmium. *J Biol Chem* 278: 2396-2402, 2003.

278.	**Subbanagounder G, Leitinger N, Shih PT, Faull KF, and Berliner JA.** Evidence that phospholipid oxidation products and/or platelet-activating factor play an important role in early atherogenesis : in vitro and In vivo inhibition by WEB 2086. *Circ Res* 85: 311-318, 1999.

279.   **Talalay P, Fahey JW, Holtzclaw WD, Prestera T, and Zhang Y.** Chemoprotection against cancer by phase 2 enzyme induction. *Toxicology letters* 82-83: 173-179, 1995.

280.   **Talalay P and Zhang Y.** Chemoprotection against cancer by isothiocyanates and glucosinolates. *Biochemical Society transactions* 24: 806-810, 1996.

281.   **Talman WT.** NO and central cardiovascular control: a simple molecule with a complex story. *Hypertension* 48: 552-554, 2006.

282.   **Taniyama Y and Griendling KK.** Reactive oxygen species in the vasculature: molecular and cellular mechanisms. *Hypertension* 42: 1075-1081, 2003.

283.   **Telakowski-Hopkins CA, King RG, and Pickett CB.** Glutathione S-transferase Ya subunit gene: identification of regulatory elements required for basal level and inducible expression. *Proc Natl Acad Sci U S A* 85: 1000-1004, 1988.

284.   **Thimmulappa RK, Scollick C, Traore K, Yates M, Trush MA, Liby KT, Sporn MB, Yamamoto M, Kensler TW, and Biswal S.** Nrf2-dependent protection from LPS induced inflammatory response and mortality by CDDO-Imidazolide. *Biochem Biophys Res Commun* 351: 883-889, 2006.

285.   **Todd S, Woodward M, and Bolton-Smith C.** An investigation of the relationship between antioxidant vitamin intake and coronary heart disease in men and women using logistic regression analysis. *Journal of clinical epidemiology* 48: 307-316, 1995.

286.   **Todd S, Woodward M, Bolton-Smith C, and Tunstall-Pedoe H.** An investigation of the relationship between antioxidant vitamin intake and coronary heart disease in men and women using discriminant analysis. *Journal of clinical epidemiology* 48: 297-305, 1995.

287.   **Tong KI, Katoh Y, Kusunoki H, Itoh K, Tanaka T, and Yamamoto M.** Keap1 recruits Neh2 through binding to ETGE and DLG motifs: characterization of the two-site molecular recognition model. *Mol Cell Biol* 26: 2887-2900, 2006.

288.   **Tong KI, Kobayashi A, Katsuoka F, and Yamamoto M.** Two-site substrate recognition model for the Keap1-Nrf2 system: a hinge and latch mechanism. *Biological chemistry* 387: 1311-1320, 2006.

289.   **Toufektsian MC, Boucher FR, Tanguy S, Morel S, and de Leiris JG.** Cardiac toxicity of singlet oxygen: implication in reperfusion injury. *Antioxidants & redox signaling* 3: 63-69, 2001.

290.   **Tuschl T.** RNA interference and small interfering RNAs. *Chembiochem* 2: 239-245, 2001.

291.   **Uhlig S.** Who tidies up the lung? Listen to Cox-2 and Nrf2. *American journal of respiratory and critical care medicine* 171: 1198-1199, 2005.

292.   **Vandesompele J, De Preter K, Pattyn F, Poppe B, Van Roy N, De Paepe A, and Speleman F.** Accurate normalization of real-time quantitative RT-PCR data by geometric averaging of multiple internal control genes. *Genome Biol* 3: RESEARCH0034, 2002.

293.   **Venugopal R and Jaiswal AK.** Nrf1 and Nrf2 positively and c-Fos and Fra1 negatively regulate the human antioxidant response element-mediated expression of NAD(P)H:quinone oxidoreductase1 gene. *Proc Natl Acad Sci U S A* 93: 14960-14965, 1996.

294.   **Venugopal R and Jaiswal AK.** Nrf2 and Nrf1 in association with Jun proteins regulate antioxidant response element-mediated expression and coordinated induction of genes encoding detoxifying enzymes. *Oncogene* 17: 3145-3156, 1998.

295.   **Wakabayashi N, Itoh K, Wakabayashi J, Motohashi H, Noda S, Takahashi S, Imakado S, Kotsuji T, Otsuka F, Roop DR, Harada T, Engel JD, and Yamamoto M.** Keap1-null mutation leads to postnatal lethality due to constitutive Nrf2 activation. *Nature genetics* 35: 238-245, 2003.

296.   **Wang W and Chan JY.** Nrf1 is targeted to the endoplasmic reticulum membrane by an N-terminal transmembrane domain. Inhibition of nuclear translocation and transacting function. *J Biol Chem* 281: 19676-19687, 2006.

297.   **Wild AC, Moinova HR, and Mulcahy RT.** Regulation of gamma-glutamylcysteine synthetase subunit gene expression by the transcription factor Nrf2. *J Biol Chem* 274: 33627-33636, 1999.

298.   **Xue F and Cooley L.** kelch encodes a component of intercellular bridges in Drosophila egg chambers. *Cell* 72: 681-693, 1993.

299.   **Yao P, Nussler A, Liu L, Hao L, Song F, Schirmeier A, and Nussler N.** Quercetin protects human hepatocytes from ethanol-derived oxidative stress by inducing heme oxygenase-1 via the MAPK/Nrf2 pathways. *J Hepatol*, 2007.

300.   **Yet SF, Layne MD, Liu X, Chen YH, Ith B, Sibinga NE, and Perrella MA.** Absence of heme oxygenase-1 exacerbates atherosclerotic lesion formation and vascular remodeling. *Faseb J* 17: 1759-1761, 2003.

301.   **Yet SF, Melo LG, Layne MD, and Perrella MA.** Heme oxygenase 1 in regulation of inflammation and oxidative damage. *Methods Enzymol* 353: 163-176, 2002.

302.   **Yet SF, Tian R, Layne MD, Wang ZY, Maemura K, Solovyeva M, Ith B, Melo LG, Zhang L, Ingwall JS, Dzau VJ, Lee ME, and Perrella MA.** Cardiac-specific expression of heme oxygenase-1 protects against ischemia and reperfusion injury in transgenic mice. *Circ Res* 89: 168-173, 2001.

303.   **Yoshida T, Maulik N, Ho YS, Alam J, and Das DK.** H(mox-1) constitutes an adaptive response to effect antioxidant cardioprotection: A study with transgenic mice heterozygous for targeted disruption of the Heme oxygenase-1 gene. *Circulation* 103: 1695-1701, 2001.

304.   **Yu R, Chen C, Mo YY, Hebbar V, Owuor ED, Tan TH, and Kong AN.** Activation of mitogen-activated protein kinase pathways induces antioxidant response element-mediated gene expression via a Nrf2-dependent mechanism. *J Biol Chem* 275: 39907-39913, 2000.

305.   **Yu R, Lei W, Mandlekar S, Weber MJ, Der CJ, Wu J, and Kong AT.** Role of a mitogen-activated protein kinase pathway in the induction of phase II detoxifying enzymes by chemicals. *J Biol Chem* 274: 27545-27552, 1999.

306.   **Yu R, Mandlekar S, Lei W, Fahl WE, Tan TH, and Kong AT.** p38 mitogen-activated protein kinase negatively regulates the induction of phase II drug-metabolizing enzymes that detoxify carcinogens. *J Biol Chem* 275: 2322-2327, 2000.

307.   **Zamore PD.** RNA interference: listening to the sound of silence. *Nature structural biology* 8: 746-750, 2001.

308.   **Zhang DD and Hannink M.** Distinct cysteine residues in Keap1 are required for Keap1-dependent ubiquitination of Nrf2 and for stabilization of Nrf2 by chemopreventive agents and oxidative stress. *Mol Cell Biol* 23: 8137-8151, 2003.

309.   **Zhang Y and Gordon GB.** A strategy for cancer prevention: stimulation of the Nrf2-ARE signaling pathway. *Molecular cancer therapeutics* 3: 885-893, 2004.

310.   **Zhang Z, Ferraris JD, Brooks HL, Brisc I, and Burg MB.** Expression of osmotic stress-related genes in tissues of normal and hyposmotic rats. *American journal of physiology* 285: F688-693, 2003.

311.   **Zhao J, Kobori N, Aronowski J, and Dash PK.** Sulforaphane reduces infarct volume following focal cerebral ischemia in rodents. *Neuroscience letters* 393: 108-112, 2006.

312.   **Zhao K, Luo G, Giannelli S, and Szeto HH.** Mitochondria-targeted peptide prevents mitochondrial depolarization and apoptosis induced by tert-butyl hydroperoxide in neuronal cell lines. *Biochemical pharmacology* 70: 1796-1806, 2005.

313.   **Zhu H, Itoh K, Yamamoto M, Zweier JL, and Li Y.** Role of Nrf2 signaling in regulation of antioxidants and phase 2 enzymes in cardiac fibroblasts: protection against reactive oxygen and nitrogen species-induced cell injury. *FEBS Lett* 579: 3029-3036, 2005.

314.   **Zimmet JM and Hare JM.** Nitroso-redox interactions in the cardiovascular system. *Circulation* 114: 1531-1544, 2006.

315.   **Zipper LM and Mulcahy RT.** Erk activation is required for Nrf2 nuclear localization during pyrrolidine dithiocarbamate induction of glutamate cysteine ligase modulatory gene expression in HepG2 cells. *Toxicol Sci* 73: 124-134, 2003.

316.   **Zipper LM and Mulcahy RT.** Inhibition of ERK and p38 MAP kinases inhibits binding of Nrf2 and induction of GCS genes. *Biochem Biophys Res Commun* 278: 484-492, 2000.

APPENDICES

Appendix A. A list of compounds reported to activate the ARE.

ARE-Inducers		
1-[2-cyano-3-1,2-dioxooleana-1,9(11)-dien-28-oyl] imdazole	carnosol	lippopolysaccaride
12346 penta O-gallo D-glucose	caroteniods	Low density lipoprotein
17 beta estradiol	chromium IV	mercury
2,3,7,8-tetrachlorodibenzo-p-dioxin	cisplatin	N-3-fatty acid
2,7-dichlorodihydrofluoresceine diacetate	cobalt	Nickel II
3 H-1,2-dimethiole-3-thione	cobalt protophorphyrin	nitric oxide
3-hydroxyanthanilic acid	copper	oltipraz
3-methylcholanthrene	curcumin	organosulfur
3-O-caffeoyl acid	diethylnitrosamine	PD98059
4-hydroxynonenal	deprenyl	pentacholorphenol
acetominophen	diallyl sulfide	peroxynitrate
acetylcarnitine	diesel exhaust	phenolic acid
acrolein	dithiolethiones	phorbol ester
allyl sulfide	ethoxyquin	phytochemicals
alpha lipoic acid	fibroblast growth factor	piperine
antirheumatic gold	flavonoids	polyphenols
apomorphine	garlic	quercetin-glycosides
arsenic	ginkgo biloba	resveratrol
arsenite	hemin	sulforaphane
bis(2-hydroxybenzylidene)acetone	indole-3-carbinol	*tert*-butyl hydroquinone
bucillamine	Insulin	trans-stibene oxide
butylated hydroxyanisol	isothiocyanates	triterpenoids
cadmium	kainic acid	UV radiation
cadmium chloride	Keratinocyte growth factor	valporic acid
carbon monoxide	lead	xanthohumol

Appendix B. Genes reported to be ARE-driven. List generated from Lee et al. 2003. (164)

Detoxification
      NQO1
      GST A4
      GST Pi2
      GST Mu1
      GST Mu2
      GST Mu3
      Aldehyde dehydrogenase-1
      Aldehyde dehydrogenase-2
      Cytochrome P450 1B1

Antioxidant/reducing Potential
      GCLM
      GCLC
      HO1
      TXNRD 1
      Ferritin light chain
      Type I peroxiredoxin
      1-Cys peroxiredoxin protein-2
      G6PD, X-linked
      G6PD-2 gene
      Transketolase
      Malic enzyme, supernatant

Transcription
      Nrf2
      Homeo box, MSH-like 2
      Prolactin regulatory element binding
      CCAAT/enhancer-binding protein-
      Zinc finger protein of cerebellum 3

Growth
      Colony-stimulating factor-1 receptor
      Ecotropic viral integration site-2
      Insulin-like growth factor-1
      Nerve growth factor-

Defense/immune/inflammation
      Macrophage C-type lectin
      Cathepsin E
      Cathepsin S
      P lysozyme structural
      Matrix metalloproteinase-12
      Cytotoxic T lymphocyte-associated protein-2
      Cytotoxic T lymphocyte-associated protein-2
      Chemokine (C-C) receptor-5
      Complement component-1q
      Complement component-1q
      Complement component-1qc
      Small inducible cytokine A9
      Small inducible cytokine A27
      Small inducible cytokine subfamily D1
      Integrin   2
      Lysosomal-associated protein transmembrane-5
      Prostaglandin-endoperoxide synthase-2
      Lipopolysaccharide-binding protein
      PAF acetylhydrolase

Signaling

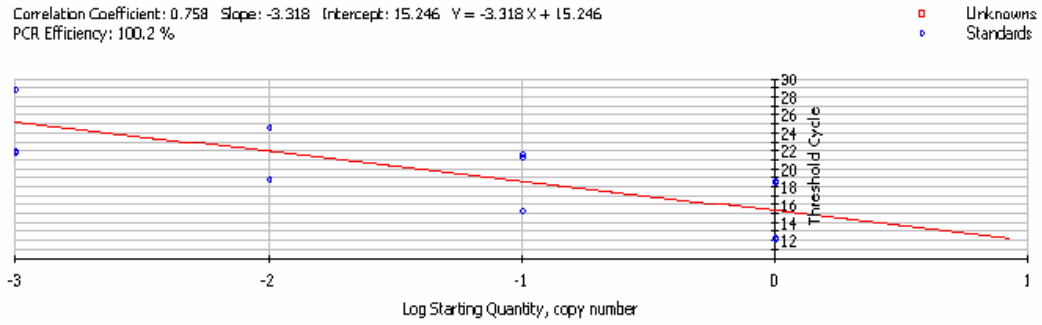Protein kinase C

Thyroid-stimulating hormone receptor

Others

Retinoid-inducible serine caroboxypetidase

Lipoprotein lipase

Neoplastic progression-3

Retinoic acid inducible E3 protein

Plastin-2L

Adenylosuccinate synthetase-1

Esterase-10

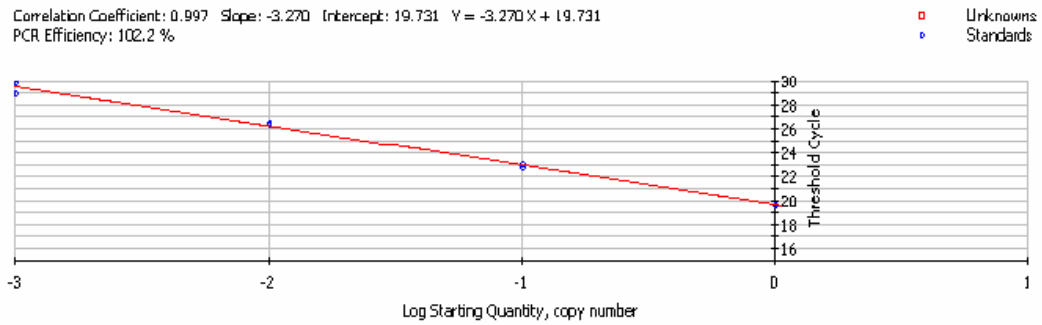Low density lipoprotein receptor-related protein 2

Appendix C. Real-time PCR standard curves for each primer set (HO1, NQO1, GAP, rat Nrf2, human Nrf2, Keap1, 36B4). Standard curves are generated using a 10 fold dilution series of cDNA with primer concentration constant. Each standard curve has a PCR efficiency used by the gene expression macro, and is calculated from the standard curve.
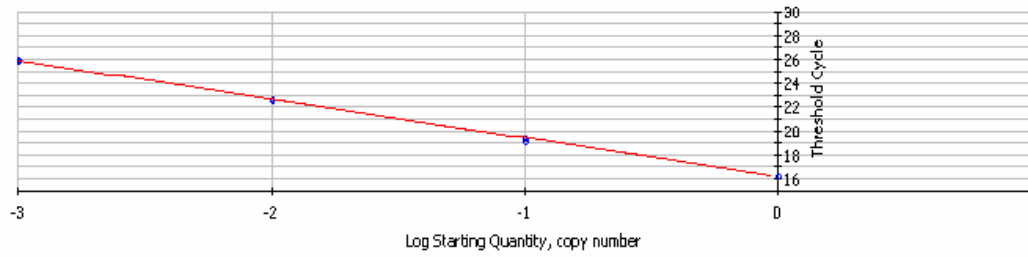
HO1

Correlation Coefficient: 0.758   Slope: -3.318   Intercept: 15.246   Y = -3.318 X + 15.246
PCR Efficiency: 100.2 %

NQO1

Correlation Coefficient: 0.997   Slope: -3.270   Intercept: 19.731   Y = -3.270 X + 19.731
PCR Efficiency: 102.2 %

GAP

Correlation Coefficient: 0.999   Slope: -3.245   Intercept: 16.163   Y = -3.245 X + 16.163
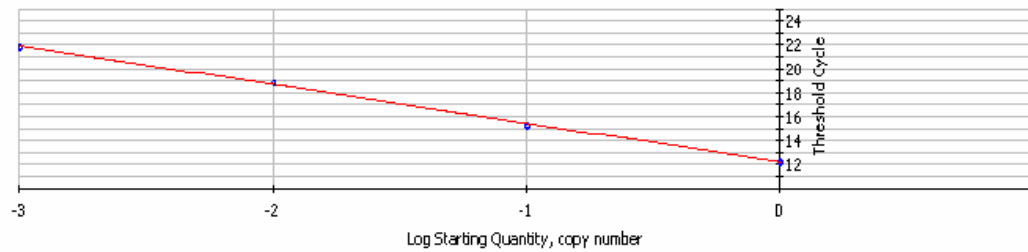PCR Efficiency: 103.3 %

□ Unknowns
○ Standards

Log Starting Quantity, copy number

Rat Nrf2

Correlation Coefficient: 0.999   Slope: -3.227   Intercept: 12.223   Y = -3.227 X + 12.223
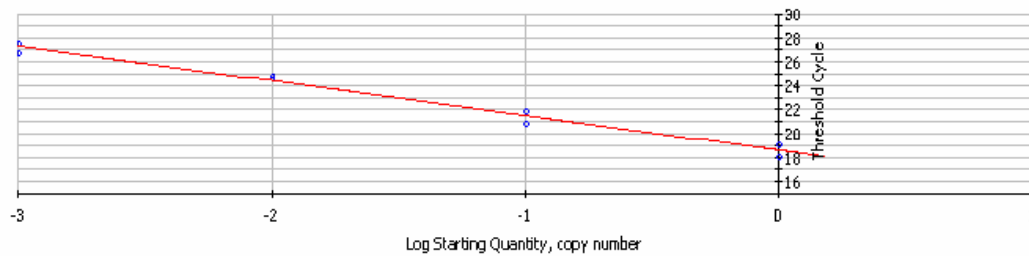PCR Efficiency: 104.1 %

□ Unknowns
○ Standards

Log Starting Quantity, copy number

Human Nrf2

Correlation Coefficient: 0.990   Slope: -2.921   Intercept: 18.606   Y = -2.921 X + 18.606
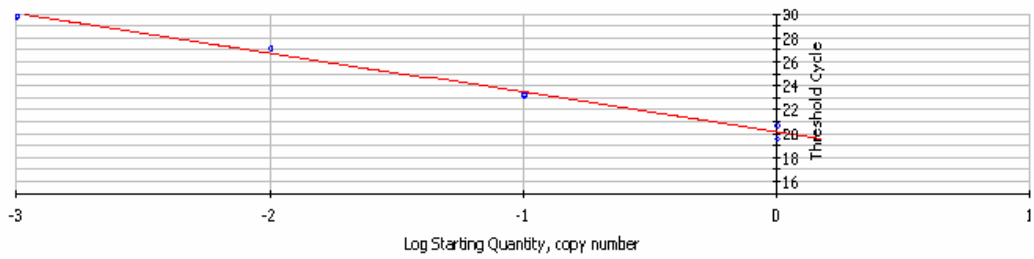PCR Efficiency: 120.0 %

□ Unknowns
○ Standards

Log Starting Quantity, copy number

142

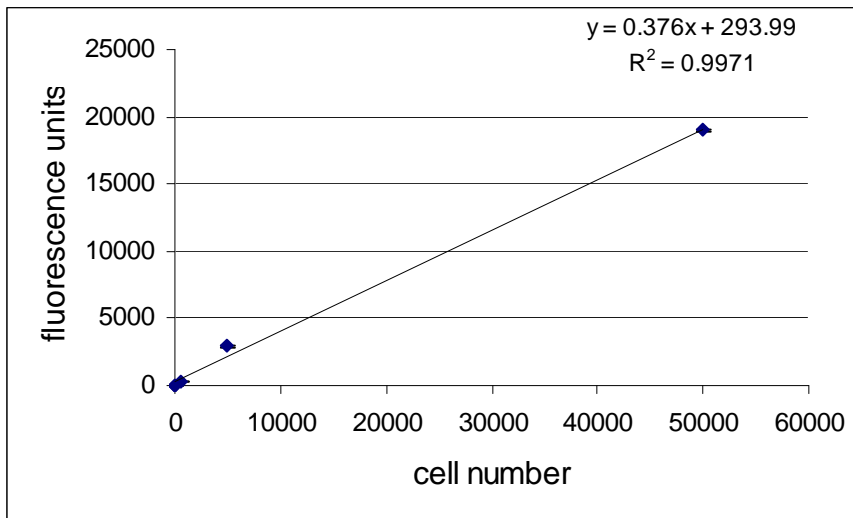## Rat Keap1

Correlation Coefficient: 0.994   Slope: -3.265   Intercept: 20.214   Y = -3.265 X + 20.214
PCR Efficiency: 102.4 %

□ Unknowns
▫ Standards

Log Starting Quantity, copy number

Appendix D: Cell proliferation assay standard curve. The fit is linear with a correlation coefficient of no less than 0.95.

$y = 0.376x + 293.99$
$R^2 = 0.9971$

143

Appendix E: List of Abbreviations

15dPGJ2	15-deoxy-delta(12,14)-prostaglandin J(2)
6-OHDA	6-hydroxydopamine
Abrp	acidic ribophosphoprotein
AhR	ayrl-hydrocarbon receptor
AP1	Activator Protein 1
ARE	Antioxidant Response Element
ATF2	activating transcription factor 2
ATF4	activating transcription factor 4
BACH	BTB and CNC homology 1
BHA	Butylated hydroxyanisole
BLAST	Basic Local Alignment Search Tool
β-NF	b-naphthoflavone
bp	base pairs
cAMP	cyclic adenine monophosphate
Carboxy-H2DCFDA	5-(and 6)-carboxy-2',7'-dichlorodihydrofluorescein diacetate
CAT	chloramphenicol acetyltransferase
cDNA	complementary DNA
CNC	CAP N Collar
CoIP	Co-immunoprecipitation
Cox-2	cyclooxygenase 2
C^{P450}	cytochrome P 450
CREB	cAMP Responsive Element Binding protein
CVD	cardiovascular disease
CYP1A1	cytochrome P 450 gene
CYP2E1	Cytochrome P450 2E1
D3T	1,2-dithiole-3-thione
$\Delta\Delta$CT	delta delta cycle threshold
DEM	diethylmalate
DEPC	diethyl pyrocarbonate
DGR	double glycine repeat
DMEM	Dulbecco's Modified Eagle's Medium
dsRNA	double stranded RNA
EpRE	electrophile response element
ER	endoplasmic reticulum
ERK	Extracellular signal regulated kinase
EtOH	ethanol
FBS	Fetal Bovine Serum
GFP	green fluorescent protein

γ-GCS	g-glutamylcysteine synthetase
γ-GCS$_{h\&l}$	g-glutamylcysteine synthetase heavy and light subunits
GPX	glutathione peroxidase
GR	glutathione reductase
GSH	glutathione
GST	glutathione transferase
H_2O_2	hydrogen peroxide
HBSS	Hank's balanced salt solution
HO1	Heme oxygenase 1
hPAP	human placental alkaline phosphatase
HRP	horseradish peroxidase
IgG	immunoglobulin G
JNK	c-Jun N-terminal kinase
Keap1	Kelch-like associated protein-1
LDL	low density lipoprotein
MAPK	mitogen-activated protein kinase
MARE	Maf recognition elements
MOPS	3-(N-morpholino)propanesulfonic acid
MPTP	1-methyl-4-phenyl-1,2,3,6-tetrahydropyridine
NES	nuclear export signal
NF-E2	nuclear factor (erythroid-derived 2)
NLS	nuclear localization sequence
NO	nitric oxide
NOS	nitric oxide synthase
NQO1	NADPH quinone oxidoreductase 1
Nrf1	NF-E2 related factor 1
Nrf2	NF-E2 related factor 2
Nrf3	NF-E2 related factor 3
OAS2	2'-5'-oligoadelylate synthetase
PAH	polycyclic aromatic hydrocarbons
PBS	phosphate buffered saline
PCR	polymerase chain reaction
PD	Parkinson's disease
PDTC	pyrrolidin-edithiocarbamate
PI3K	phosphatidylinositol 3-kinase
PEITC	ethyl isothiocyanate
PKC	protein kinase C
Prot 26s	proteosome 26s
RAC3	Nuclear receptor-associated coactivator-3
RISC	RNA-Induced Silencing Complex
ROS	reactive oxygen species
RT	reverse transcriptase

SDS PAGE	sodium dodecyl sulfate poly acrylamide gel electrophoresis
SIN-1	3-morpholinosydnonimine-N-ethylcarbamide
siRNA	small inhibitory RNA
SOD	superoxide dismutase
TAE	tris acetate EDTA
tBHP	tert-butyl hydroperoxide
tBHQ	tert-butyl hydroquinone
TBS-T	Tris borate sodium tween 20
TE	Tris EDTA
TNFα	tumor necrosis factor alpha
TPA	12-O-tetradecanoylphorbol-13-acetate
UV	ultra violet
XRE	xenobiotic response element